1994

Application of normal forms of vector fields to stressed power systems

Shelli Kay Starrett
Iowa State University

Order Number 9503596

Application of normal forms of vector fields to stressed power systems

Starrett, Shelli Kay, Ph.D.

Iowa State University, 1994

U·M·I
300 N. Zeeb Rd.
Ann Arbor, MI 48106

Application of normal forms of vector fields to stressed power systems

by

Shelli Kay Starrett

A Dissertation Submitted to the

Graduate Faculty in Partial Fulfillment of the

Requirements for the Degree of

DOCTOR OF PHILOSOPHY

Department: Electrical Engineering and Computer Engineering
Major: Electrical Engineering (Electric Power Systems)

Approved:

Signature was redacted for privacy.

In Charge of Major Work

Signature was redacted for privacy.

For the Major Department

Signature was redacted for privacy.

For the Graduate College

Iowa State University
Ames, Iowa

1994

TABLE OF CONTENTS

LIST OF FIGURES

LIST OF TABLES

NOMENCLATURE

A	Plant matrix (m by m) of the system in state space (corresponds to the state vector x)
α_i	Real part of the eigenvalue λ_i (also has another use in Appendix A)
B	Input matrix (m by *ninputs*) for the system with states x
β, β_{ij}	β is the matrix VB (m by *ninputs*), from the transformation of the system of equations including inputs to the Jordan form. β_{ij} are the elements of β.
C	Output matrix (*noutputs* by m) for the system with states x
C_{ij}	$= \lvert V_i \rvert \lvert V_j \rvert \lvert Y_{ij} \rvert sin(\theta_{ij})$ and is used to develop the Taylor series
D_{ij}	$= \lvert V_i \rvert \lvert V_j \rvert \lvert Y_{ij} \rvert cos(\theta_{ij})$ and is used to develop the Taylor series
D_k	Linear mode dominance measure for mode k (corresponds to λ_k)
D_{2k}	Second-order mode dominance measure for single eigenvalue mode k (corresponds to λ_k)
D_{22k}	Second-order mode dominance measure for two-eigenvalue mode kl (corresponds to $\lambda_k + \lambda_l$)
δ, δ_i	δ is the vector (n by 1) of absolute internal generator angles. δ_i is the i^{th} element of δ.
δ_o, δ_{io}	δ_o is the initial condition (condition at end of disturbance) of vector δ. δ_{io} is the i^{th} element of δ_o.
e_k	k^{th} Natural basis vector. The k^{th} element is one, rest of the elements are zero.
γ_{ij}	Angle of the linear contribution factor, σ_{ij}

γ_{2ij}	Angle of the second-order contribution factor for single eigenvalue modes, σ_{2ij}
γ_{22ijk}	Angle of the second-order contribution factor for two-eigenvalue modes, σ_{2ijk}
h_r	Normal-form-transformation vector (m by 1) containing functions of polynomial order r
h_2, h_{2i}, h_{2ijk}	h_2 is the second-order, normal-form-transformation vector (m by 1) containing second-order polynomial functions. The function h_{2i} is the i^{th} element of h_2, and h_{2ijk} is the coefficient of the jk product in the function h_{2i}.
J	Plant matrix (m by m) for the Jordan form. It is diagonal and complex with the eigenvalues on the diagonal.
k	Factor used in the Newton-Raphson iteration of the initial conditions to slow changes between iterations
λ_i	i^{th} eigenvalue of the system plant matrix A. $\lambda_i = \alpha_i + j\varpi_i$
m	Number of states in the system in state space, Jordan and normal forms, equal to 2([number of generators] - 1)
M_i	Inertia constant for generator i
μ, μ_{ij}	μ is the matrix CU (m by $ninputs$), from the transformation of the system of equations including inputs to the Jordan form. μ_{ij} are the elements of μ.
n	Number of generators modeled in the system
O_i	Linear machine state perturbation factor for the i^{th} machine state
O_{2i}	Second-order machine state perturbation factor for the i^{th} machine state
p_{ki}	Linear participation factor for the k^{th} machine and the i^{th} mode

p_{2ki}	Second-order participation factor for the k^{th} machine and the i^{th} single-eigenvalue mode
p_{2kij}	Second-order participation factor for the k^{th} machine and the two-eigenvalue mode ij
P_{mi}	Mechanical power output by generator i
P_i	Constant power for generator i. $P_i = P_{mi} - \|V_i\|^2 \|Y_{ij}\| cos(\theta_{ii})$
r, r_j	r is the vector ($ninputs$ by 1) of inputs for the system with states x. r_j is an element of r.
σ_{ij}	Linear contribution factor for machine state i and mode j. $\sigma_{ij} = \|\sigma_{ij}\| \angle\gamma_{ij}$
σ_{2ij}	Second-order contribution factor for machine state i and single-eigenvalue mode j. $\sigma_{2ij} = \|\sigma_{2ij}\| \angle\gamma_{2ij}$
σ_{22ijk}	Second-order contribution factor for machine state i and two-eigenvalue mode jk. $\sigma_{22ijk} = \|\sigma_{22ij}\| \angle\gamma_{22ijk}$
θ_{ij}	Angle of Y_{ij}
U, u_{ij}	U is the complex matrix (m by m) with the right eigenvectors of A as its columns. u_{ij} is an element of U.
u_{2ijk}	Second-order term resulting from right eigenvector elements for machine state i and two-eigenvalue mode jk
V, v_{ki}	V is the complex matrix (m by m) with the left eigenvectors of A as its rows. v_{ij} is an element of V.
v_{2kij}	Second-order term resulting from left eigenvector elements for mode k and machine states i and j
V_i	Internal voltage for generator i
w, w_k	w is the output vector ($noutputs$ by 1) for the system with states x. w_k is an element of w.
$\omega, \omega_i,$	ω is the vector (n by 1) of absolute internal generator speeds. ω_i is the i^{th} element of ω

ω_o, ω_{io}	ω_o is the initial condition (condition at end of disturbance) of vector ω. ω_{io} is the i^{th} element of ω_o.
ϖ_i	Imaginary part of the eigenvalue λ_i
x, x_i	x is the vector (m by 1) of machine states. The system of equations is linearly independent (a reference was chosen), and the equilibrium of the system has been moved to the origin (via a variable transformation or series expansion). x_i is an element of x.
x_o, x_{io}	x_o is the initial condition (condition at end of disturbance) of vector x. x_{io} is the i^{th} element of x_o.
X_2, X_3	X_2 is a vector (m by 1) containing all second-order terms of the Taylor series expansion of the system's equations. X_3 is a similar vector containing all the third-order terms.
y, y_i	y is the vector (m by 1) of Jordan form states. y_i is an element of y.
y_o, y_{io}	y_o is the initial condition (condition at end of disturbance) of vector y. y_{io} is an element of y_o.
Y_{ij}	Element of the Y_{bus} admittance matrix for the system. $Y_{ij} = \lvert Y_{ij} \rvert \angle\theta_{ij}$
z, z_i	z is the vector (m by 1) of normal-form states. z_i is an element of z.
z_o, z_{io}	z_o is the initial condition (condition at end of disturbance) of vector z. z_{io} is an element of z_o.
T*	Denotes complex conjugate of T
$D_x[\cdot]$	Denotes the Jacobian of $\cdot$ with respect to the vector x

† Some of the notation used in the appendices is not included here.

CHAPTER 1. INTRODUCTION

1.1 Transient Analysis

The transient analysis of today's electric power systems is a challenging and computationally intensive problem that exhibits many interesting and yet to be explained phenomena. This is due in part to the fact that individual electric utilities are no longer islands of independent generation and control. The interconnections of large regions and the heavy use of these interconnections present the power system engineer with a large, stressed, nonlinear system to analyze and operate. The physical indicators of stress include the heavy loading of transmission lines, generators near real or reactive power limits, and the separation generation and loads by long distances.

Power-system transient analysis is primarily related to the synchronous operation of the generators within the system after a disturbance occurs. The swings of generator torque angles as well as voltage swings are of concern in transient studies. Stability requirements are becoming an increasingly important factor for determining limiting conditions for system operation. Whereas in the past transient analysis was done at the planning stages of system operation, it is now becoming necessary for transient studies to be done much closer to "real time."

When a disturbance occurs in an unstressed system, a few machines (often only one) exhibit large oscillations an may become unstable if the disturbance is large enough. This type of response, in which only a single plant is usually affected, is often referred to as a plant-mode or local-mode response. The increased stress on modern power systems has brought a phenomenon to the surface that was not previously seen in the more moderately loaded power systems of the past. This phenomenon, sometimes referred to as the "interarea mode," is an interaction of groups of machines within the power system that is quite complex in nature [1-5]. In response to a small disturbance (small enough so that nonlinearities are negligible), interarea oscillations occur as two groups of generators, in different regions, oscillating with respect to each other. A large-disturbance (nonlinearities cannot be ignored) interarea-mode response can be described as follows: initially following a large disturbance, generators local to the

disturbance are accelerated; as the transient continues, other generators, which may be far from the disturbance, also become adversely affected. This system wide response involving a large number of generators is in contrast to the more local response, involving only a few generators, typical of unstressed power systems. In addition, these interarea-mode oscillations may cause instabilities to occur at some time after the initial swing caused by the fault. Interarea oscillations are typically in the frequency range of 0.1 to 0.8 Hz.

1.2 Linear Analysis

Linear analysis involves the linearization (about an operating point) of the non-linear differential equations describing the dynamics of a power system. The linearized system's response approximates the nonlinear system's response for small changes within the system and can provide quantitative answers concerning the stability of the system. The eigenvalues of the system, which correspond to modes or natural frequencies, represent frequencies that may be observed in the oscillations of system variables. For a given initial condition, the linearized system's response can be expressed in closed form using the eigenvalues and eigenvectors of the system. Thus linear analysis completely describes the linearized system's response.

Linear modal analysis has been extensively applied to the power system oscillation control problem [6-9]. Mode-machine relationships, such as participation factors and measures of modal dominance, are used extensively to characterize linearized power system behavior. Interarea oscillations have been studied using linear system techniques [1,2]. Other linear system techniques, such as observability and controllability, utilize the system eigenvectors to aid in the location and design of controls. The eigenvectors themselves have been used to aid in location of controls [6], and various forms of participation factors [7-9] (which are derived using the eigenvectors) have been used to determine the effectiveness of controls on the system modes. Applications, such as modal analysis and some energy methods, also take advantage of linear system approximations [6-12].

The general power-system response (linear or nonlinear) is often considered to be a combination of the many natural modes of oscillation present in the

system. The linear modes (eigenvalues) represent these basic frequencies that appear in the motions of the machines of the system. Even for large disturbances when nonlinearities are significant, the linear modes play an important role in determining the dynamic response of the machine variables. The nonlinear effects should be considered as additions to the linear-modal picture, not as replacements for it.

1.3 Motivation for Including Higher Order Terms

The analysis of the response of stressed power systems represents a challenging problem in power-system, transient-stability analysis. Although the number of inertial modes is equal to the number of system states ($2[n-1]$), typically only a few modes dominate the system response. Under stressed conditions, modes related to groups of machines from different regions begin to dominate. There is also evidence that the nonlinear interactions of the inertial modes increase under stressed conditions [3]. Thus, the transient analysis of stressed systems requires analysis techniques that do not ignore the nonlinearities present in a power system's dynamics.

How important are the nonlinearities in the system response? Linear analysis is accurate in the neighborhood of the equilibrium, but the size of this neighborhood is not well defined. With the emergence of the interarea mode and other problems not explained by linear analysis, there is a need to extend the analysis to include at least some of the effects of the nonlinearities. A natural way to extend the analysis to nonlinearities is by including higher-order terms in the Taylor series expansion of the system's vector field (differential equations). In a preliminary study [13], the question of what is gained by including higher-order terms was addressed. The findings show that significant information regarding oscillations within the system is gained by including second-order terms. The inclusion of third-order terms provides improved stability information. This work is described in more detail in Chapter 3.

1.4 Normal Forms

Poincaré introduced a mathematical technique for studying systems of nonlinear, differential equations using their normal forms [14,15]. The method provides the means by which a differential equation may be transformed into a simpler form (higher-order terms are eliminated). It also provides the conditions under which the transformation is possible. Although the normal form of a vector field or differential equation may be expressed using a number of forms, the polynomial form is selected because of its natural relationship to the Taylor-series expansion. The polynomial normal form of a system of equations contains a limited number of nonlinear terms, which are present due to resonances of system eigenvalues. This normal form is obtained via a nonlinear, variable transformation performed on the series expansion of the power system's nonlinear, differential equations. The nonlinear transformation is derived by requiring that higher-order terms in the system of differential equations be set to zero (one order at a time). In this work second-order terms and thus a second-order normal-form variable transformation are studied. Through the application of the normal-form method to the second-order system, an approximate solution can be determined in closed form. Using the transformation and the approximate second-order solutions, quantitative measures of the system response are developed.

1.5 Problem Statement

Increased system stress has brought about the need for a better understanding of nonlinearities in power-system dynamic behavior. The second-order terms of the series expansion have been shown to contain significantly more information than the traditionally-used, linear approximation. There is a need for a systematic approach to study the effects of second-order terms in stressed power systems. Information related to machine oscillations (modal behavior), groupings of machines, and boundaries of separation between machines is of interest. Quantitative measures of interactions and nonlinear effects within the system are needed. The relationship between system stress and the nonlinearity of the differential

equations should be quantified. Normal-form analysis has the potential to simplify nonlinear analysis of a stressed systems' response and will be applied to this problem.

1.6 Explanation of Dissertation Format

The format of this dissertation follows. This introduction gives a motivation and general summary of the techniques used in this research work. It also provides the reader a preview of the problem studied in this dissertation. Following is a literature review that provides a concise record of the source material for this work as well as for related topics and background information. A summary of publications resulting from this work and closely related work here at Iowa State University is also included. Chapter 3 presents the power system model used and describes the Taylor series expansion of the system's differential equations. Motivation for the main study, in the form of an investigation of the significance of the second-order and third-order terms of the Taylor series expansion, is also a part of Chapter 3. In Chapter 4, the general theory of normal forms is applied to the second-order, power system approximation described in Chapter 3. First the procedure, including important equations, is presented. The procedure is followed by a description of the methods used to determine the initial conditions for the various systems. Chapter 5 describes the utilization of the normal-form results to develop measures of system performance. Modal interactions, modal dominance, machine perturbation, and mode-machine relationships are addressed. Numerical results of the application of these techniques to a stressed power system (the 50-generator IEEE test system) are found in Chapters 6-9. Observations regarding the data are also included in these chapters. Chapter 10 presents conclusions, summarizes this work, and suggests future work. Finally the Acknowledgments and Bibliography are followed by the appendices described in the following paragraph.

The details of the expansion of the classical, power-system model are given in Appendix A. Some of the details of the Jordan form transformation of Chapter 4 are left for Appendix B. An example using a 3-generator system is

presented in Appendix C to illustrate some of the measures introduced in Chapter 5.

CHAPTER 2. LITERATURE REVIEW

Much work exists in the treatment of power system analysis. The classical texts by Kimbark [16], as well as texts by Anderson and Fouad [17], Pai [16], and Fouad and Vittal [11] explain many concepts for the modeling, simulation, stability analysis, and transient analysis of power systems. During recent years, the effect of stress on system performance has received much attention. One characteristic of stressed systems, interarea oscillations or interarea modes, has been studied by a number of authors. Kundur, et. al. [1,2] have analyzed interarea oscillations in the systems of the western United States using linear analysis techniques. Vittal, Bahtia, and Fouad [3] reported on the correlation between interarea modes and the size of the second-order terms in the series approximation of system's differential equations. Berggen, et. al. [4] studied stress in a 126-generator equivalent of the western system by increasing load levels and observing the behavior of equilibrium points. Bifurcation, changes in the character of a system's equilibria and invariant manifolds, has also been studied by a number of authors [19,20] and is thought to be related to system stress.

Linear analysis is widely used for control and system analysis. Many texts are available on the topic [21,22]. Concepts such as controllability and observability exist for determining which variables should be controlled, which should be input, and how controllers should be designed. In power-system analysis, linear system theory has been applied to unstressed and stressed systems. DeMello, et. al. [6] used the linear system's eigenvectors to determine optimum locations for power system stabilizers. Kundur, et. al. [23] also use eigenvectors to determine "mode shapes" for use in determining which machines are affected by a given mode. Participation factors, measures of the participation of a machine in a mode's oscillations, were applied to power system analysis by Perrez-Arriaga, et. al. [7]. A group of papers published by the IEEE summarizes much of the work in applying "Eigenanalysis and Frequency Domain Methods for System Dynamic Performance" [24].

A wide variety of measures and methods based on linear system theory have been applied to power system analysis. Martins, et. al. use observability and controllability indices and residues in determining suitable locations for power system stabilizers and static VAR compensators. Pagola, et. al. [8] described power

system stabilizer siting and design using sensitivities, residues, and generalized participations (related to participation factors). Hauer, et. al. [25] and McCalley [5] have applied Prony analysis to quantify power-system characteristics using linear measures that are determined using nonlinear system responses.

Time simulation is a well-known and widely-accepted means for studying the nonlinear transient behavior of power systems [17]. Simulation provides a detailed picture of the system's performance for specific conditions within the system. Many computer programs, such as EPRI's ETMSP [26], are available for simulating power systems and are well documented.

Direct methods, such as the transient energy function (TEF) method [11] are increasingly being used and further developed to analyze system performance and stability quantitatively. Some work, utilizing modal analysis, has also been done [10,12,27,28] to improve the TEF method's analysis of stressed systems.

Tamura, Yorino, and Yoo, et. al. [29-31] discussed auto-parametric resonance in the study of power-system dynamic behavior. They described conditions for this type of resonance in the system's nonlinear oscillations and consider stressed system conditions.

The use of normal forms of vector fields is a well known mathematical tool for dynamical-system analysis. It was presented by Poincaré in his dissertation. Arrowsmith and Place [14], Arnold [15], and Ruelle [32] gave basic introductions to the Lie derivative-based method. Normal forms have a number of uses, one of which is the classification of families of equations by the reduction of their vector fields to a simple form. Normal-form theory has also been applied to control design [33]. In this work, nonlinear (quadratic) controllers were applied to nonlinear (quadratic) systems to produce linearized system performance. Normal forms have also been applied to study small mechanical systems with slowly varying parameters [34]. Chua described the application of normal forms to a number of small systems [35,36]. Closely related methods have been used to study center manifolds for use in voltage stability analysis of power systems [37].

In the work of the power system dynamics groups at Iowa State University, normal-form theory is presently being applied to understand, characterize and quantify the stressed system's transient response to a disturbance. A preliminary study, conducted to help determine the number of higher order terms to be included in the analysis was presented in [13]. In [38] the method was applied to a

small system, and in [39] normal forms were utilized to identify second-order effects in a stressed power system. Second-order measures of mode dominance and machine perturbation, derived using normal forms were presented in [40]. The second-order relationship between modes and machine states was addressed in [41]. Additional work, utilizing normal-form theory to determine the affects of controls on second-order interactions is also under way [42].

CHAPTER 3. POWER SYSTEM MODELS

3.1 Power System Dynamics

Power-system, dynamic analysis using classical machine models is based on nonlinear, differential equations known as the swing equations. The swing equations describe the motions of the rotor of each generator within the system. They are derived using Newton's second law of motion in rotational form (torque equals inertial times rotational acceleration). For the classical-power-system model, the swing equation in per unit is [17 section 2.9]:

$$M_i\ddot{\delta}_i = P_i - \sum_{\substack{j=1 \\ j\neq i}}^{n} |V_i||V_j||Y_{ij}|cos(\theta_{ij} - \delta_i + \delta_j) \qquad i = 1,2,\ldots n \qquad (3.1)$$

Y_{ij} is an element of Y_{bus} the system admittance matrix, M_i is the generator inertia constant, $V_i\angle\delta_i$, and $V_j\angle\delta_j$ are internal generator voltages. In the classical model the angles δ_i and δ_j represent the rotor angles for machines i and j respectively. P_i represents the portions of the machine power not dependent on rotor angle (i.e., the mechanical power and the term containing the self admittance of bus i). The classical power system model can be written in state space form as

$$\dot{\delta}_i = \omega_i$$

$$M_i\dot{\omega}_i = P_i - \sum_{\substack{j=1 \\ j\neq i}}^{n} |V_i||V_j||Y_{ij}|cos(\theta_{ij} - \delta_i + \delta_j) \qquad i = 1,2,\ldots n \qquad (3.2)$$

A number of assumptions are made in the classical-machine-model analysis of this dissertation:

1. Constant mechanical power
2. Constant impedance loads
3. Y_{bus} is reduced to generator terminals
4. Damping is zero (unless otherwise stated)

To obtain an independent set of equations, the n^{th} generator is chosen to be the reference generator (without loss of generality). The system variables become the generator angles and speeds *relative* to the n^{th} angle and the n^{th} speed, respectively (e.g., $\delta_{in} = \delta_i - \delta_n = i^{th}$ system variable).

3.2 Linear Analysis

Eigenanalysis involves the linearization (about an operating point) of the non-linear differential equations describing the dynamics of a power system. The linearized system's response approximates the nonlinear system's response for small changes within the system and can provide quantitative answers concerning the stability of the system. The eigenvalues of the system, which correspond to modes or natural frequencies, represent the frequencies that may be observed in the oscillations of the system variables. The linearized system's response can be expressed in closed form in terms of the eigenvalues and eigenvectors for a given initial condition of the system [43,44]. Because it completely describes the linearized system's response, eigenanalysis also gives a measure of the linear system's stability.

The linear system is the system obtained by including only the first-order terms in the Taylor series expansion (about an equilibrium point) of the system's dynamical equations (3.2). The linear system is given by

$$\dot{x} = Ax \tag{3.3}$$

where x is the vector of difference variables (angles and speeds) that make states of the system. A is the Jacobian (plant) matrix. The eigenvalues of A characterize the stability of the linear system, and they are given by λ_i, $i = 1, \ldots, n$. The eigenvectors of A make up columns of the transformation matrix U. The variable transformation $x = Uy$ is applied to the system of equations (3.3) to obtain the Jordan form. y is the vector of Jordan-form state variables.

The Jordan form is obtained as follows. Differentiating the transformation equation yields $\dot{x} = U\dot{y}$, and substituting into (3.3) yields

$$U\dot{y} = AUy \tag{3.4}$$

The matrix with the left eigenvectors as rows, V, is the inverse of the right eigenvector matrix U. Pre-multiplying both sides of (3.4) by $V = U^{-1}$ results in

$$\dot{y} = Jy \tag{3.5}$$

where $J = VAU$ is a diagonal matrix with the eigenvalues on the diagonal. This means that the equations of linear Jordan-form system given by (3.5) are decoupled (because the eigenvalues are distinct).

Thus, the solution for the i^{th} Jordan-form variable is

$$y_j(t) = y_{jo} e^{\lambda_j t} \tag{3.6}$$

where y_{jo} is the j^{th} initial condition in the Jordan-form coordinate system. The linear solution in the original machine states is obtained by using the variable transformation $x = Uy$ and is given by

$$x_i(t) = \sum_{j=1}^{n} u_{ij} y_{jo} e^{\lambda_j t} \qquad i = 1,2,...,n \tag{3.7}$$

where u_{ij} is the element in the i^{th} row and j^{th} column of the right eigenvector matrix U.

Thus, the solution to the linear equation has been obtained in closed form. It is also evident that the signs of the real parts of the eigenvalues λ_i, determine whether the system's oscillations will grow, shrink, or remain constant with time (system stability). The initial condition vector in the Jordan form, y_o, is obtained using the inverse transformation, i.e., $y_o = Vx_o$, where x_o is the initial condition (post-fault condition) in terms of the original machine states.

Using the above linear, modal analysis, this system's response has been shown to be a linear combination of oscillatory modes corresponding to the system eigenvalues. In general, the stability of the nonlinear system is closely related to that of the linear system (within a neighborhood of the equilibrium). The Hartman-Grobman Theorem [14 section 2.2] states that if the eigenvalues of the system at the equilibrium are hyperbolic (the real part is not equal to zero), there exists a neighborhood of the equilibrium in which the linear and nonlinear systems are topologically conjugate (i.e., have the same stability and solution characteristics). This same result is the basis of Lyapunov's indirect method [45 section 5.4], which classifies the stability of the nonlinear system (under certain conditions) based on the eigenvalues of the linear system.

The expansion is done about a stable equilibrium point, and the linearized, classically-modeled system (without damping) is *marginally* stable. This is because the eigenvalues of the linear system are distinct and lie on the imaginary axis for the classical machine model with zero damping. If damping is included, the linear system becomes stable.

3.3 Higher Order Equations

The Taylor series expansion of the swing equations can be expressed as in (3.8). The expansion is done about a stable equilibrium point of the system and terms up to third order are included. As in the linear analysis given above, the equilibrium has been shifted to the origin so that the vector of state variables x represents perturbations from the equilibrium. The details of the derivation of (3.8) from (3.2) are given in Appendix A.

$$\dot{x} = Ax + X_2 + X_3 + \ldots \tag{3.8}$$

In (3.8) A is the linear plant matrix, X_2 contains only second-order terms, and X_3 contains only third-order terms.

3.4 Approximate Systems

This analysis considers systems that are approximations to the full nonlinear system. These systems are determined by including a given order of terms of the series expansion. Each approximation behaves in the same manner as the full system within a region of the state space. As more terms are included, the approximate system's response becomes the same as the original system's response in a wider range of the state space. In stressed systems the region of validity for the linear system may become quite limited. Thus for larger disturbances or even small disturbances in stressed systems, higher order analysis may be necessary.

3.4.1 Linear System

$$\dot{x} = Ax \tag{3.9}$$

This linear system can be completely described by eigenanalysis. The eigenvalues of the linear system are distinct and lie on the imaginary axis for the classical machine model with zero damping. For small disturbances, the linear system's behavior is the same as the full system's behavior.

3.4.2 Second-Order System

$$\dot{x} = Ax + X_2 \tag{3.10}$$

This system contains first and second-order polynomial nonlinearities. Normal-form theory indicates that, if certain conditions are satisfied (see section 4.1), second-order dynamics can be eliminated from the second-order normal form. Thus, the second-order normal-form system has the same stability properties as the linear system, within the range of validity of the second-order transformation. Second-order effects may influence system response and machine groupings, and thus second-order terms are of interest. The second-order system's behavior is the same as that of the full-nonlinear system in a more extended range of the state space than is the linear system.

3.4.3 Third-Order System

$$\dot{x} = Ax + X_2 + X_3 \tag{3.11}$$

Third-order polynomial nonlinearities are added in this system. Normal forms indicate that the third-order system will retain some third-order dynamics because of certain properties of the classically modeled power system (see section 4.1). Thus the stability properties of the third-order system need not be the same as those of the linear system. The third-order system should contain more information concerning stability. Again, the third-order system is equivalent to the full-nonlinear system in a larger range of the state space than the previous equivalents.

3.5 Simulations of Approximate Systems

The system tested is the 50 generator IEEE test system [46]. This system is known to exhibit the interarea mode behavior in response to certain disturbance locations. The interarea mode is seen as the instability in the positive direction of a large number of generators. In some cases, one machine is perturbed in the negative direction. The generators were modeled classically, and constant

impedance load models and zero damping were used. The base case loading of 700 MW at each of the generators at plant A was considered. Numerical integration for varying clearing times was performed to obtain the time solutions for the three approximate systems and the full nonlinear system. The conditions at fault clearing were determined using the full system and the same initial condition was applied to each of the four systems. The approximate systems are simulated using the truncated Taylor series expansions given in (3.9), (3.10), and (3.11).

3.5.1 Cases

Fault locations were chosen so that system response could be studied for both plant and interarea modes of disturbance. The faults were applied and cleared with no lines removed. The cases studied are summarized in Table 3.1.

Table 3.1 Summary of fault cases

Fault bus	Perturbed Generators	Description
100	16	Plant mode
112	27	Plant mode
1	1-17, 19-27, 33-35, 43	Interarea mode
7	1-17, 19-27, 33-35, 43	Interarea and plant modes

3.5.2 Fault at Bus 100

In this plant mode case, only generator 16 becomes unstable. Dominant frequencies of oscillation are relatively high (approximately 1.6 Hz), in agreement with expectations of a plant mode.

Figure 3.1 shows how generator 16 responds in time to various faults in

each of the four systems. The linear and second-order systems remain stable for all clearing times. As the clearing time is increased, the second-order and linear systems' oscillations grow. The second-order system's oscillations also become lower in frequency with increased clearing time, making them more comparable to the full and third-order systems' oscillations. The third-order system appears unstable for all but the shortest clearing time of 0.22 seconds.

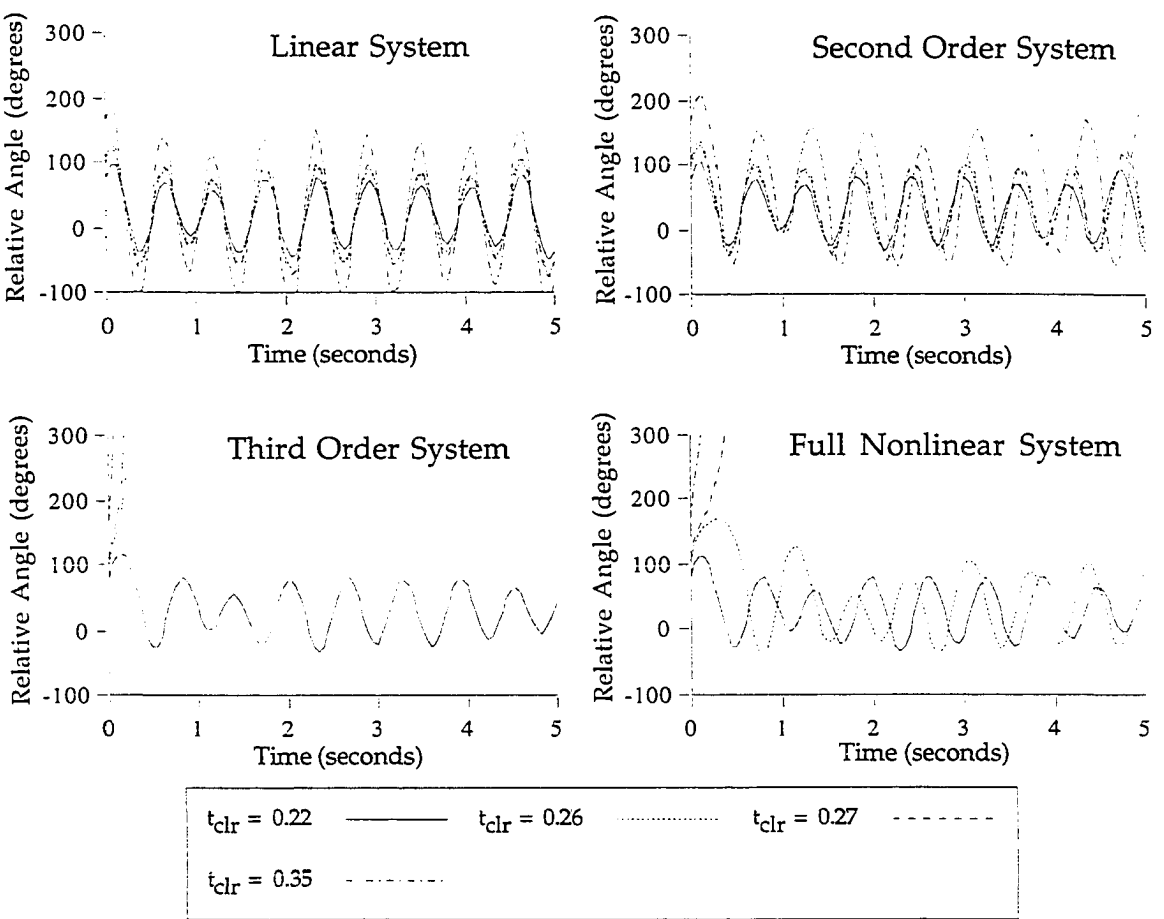

Figure 3.1 Generator 16's response to a fault at bus 100

3.5.3 Fault at Bus 7

Table 3.1 provides a list of the perturbed generators for this interarea mode case. Figures 3.2 and 3.3 show how generators 20 and 43 respond in each of the four systems. The linear system remains stable for all clearing times. The third-order system appears unstable for all clearing times shown. The second-order system's oscillations grow with increased fault clearing time, and machine 43's angle appears unstable for the 0.22 second clearing time. In this case, the group of machines represented by generator 20 shows unbounded angles at the 0.22 second clearing time as well.

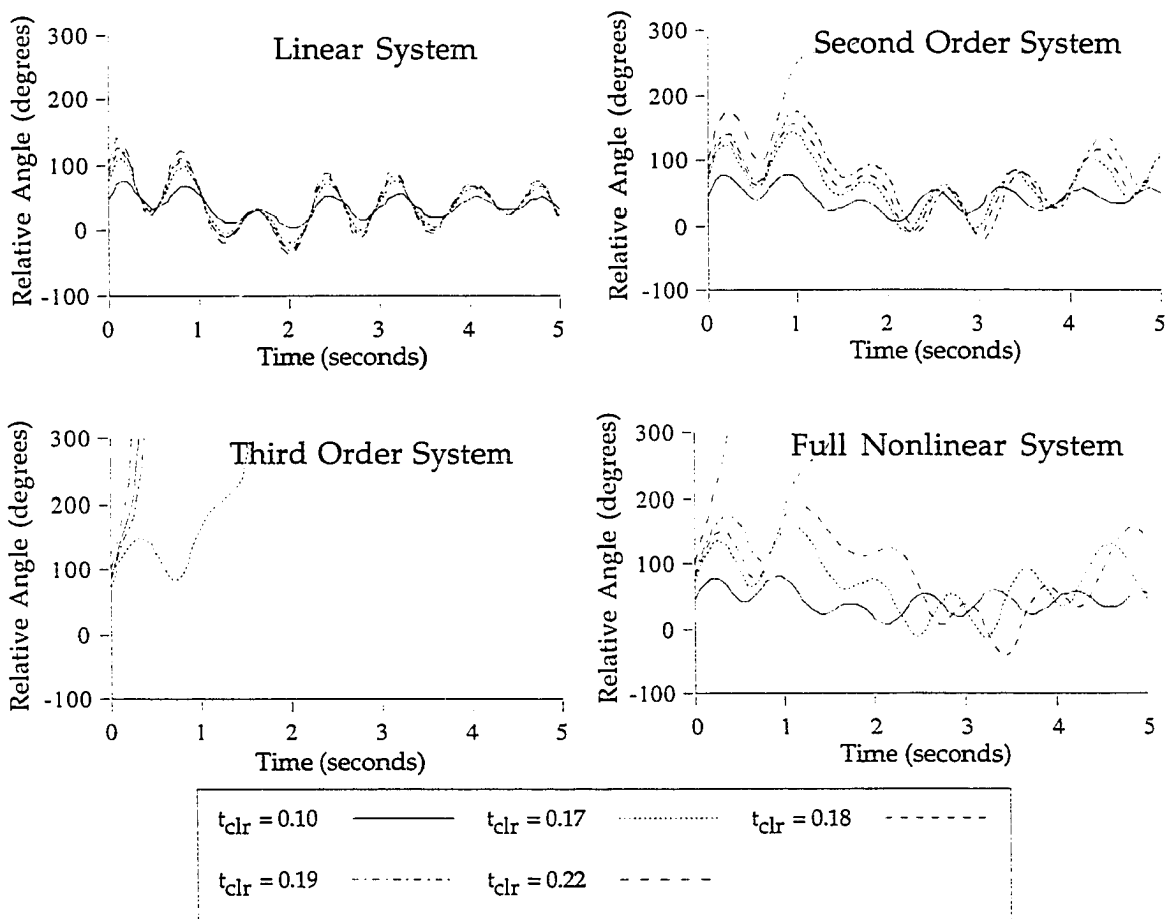

Figure 3.2 Generator 20's response to a fault at bus 7

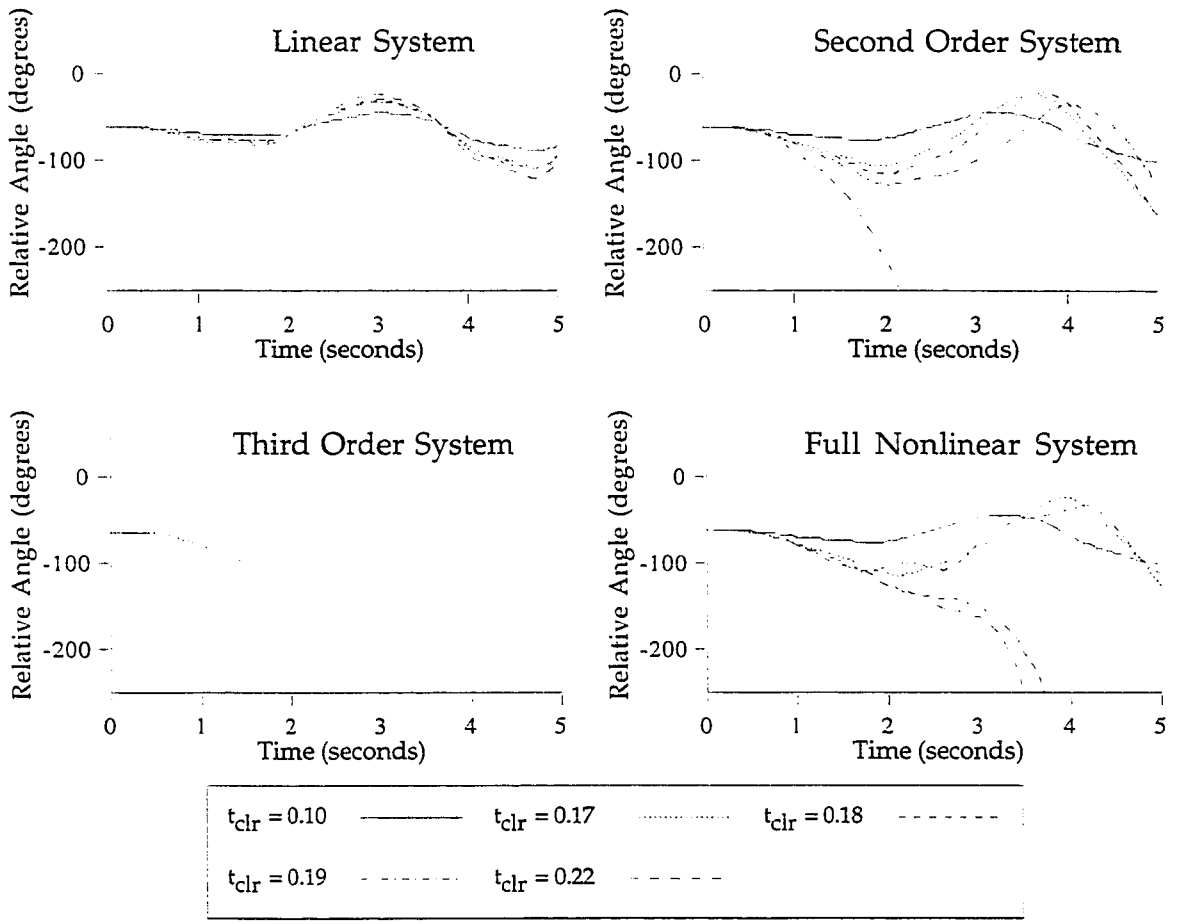

Figure 3.3 Generator 43's response to a fault at bus 7

Comparing the linear and second-order systems' approximations to the full system's response clearly indicates that the second-order system gives a more accurate indication of the shape of the generators' oscillations. For this fault case, both high and low frequency oscillations appear to dominate the full system's response. As the length of the fault increases, the low frequency mode becomes much more dominant and appears to go unstable. As is seen in Figure 3.3, this trend is more clearly evident in the second-order system approximation than in the linear one. The integration processes are stopped when any angle magnitude exceeds a pre-set level. This is why many of the third-order curves end before the five second point. (For example, the third-order curves of Figure 3.2 end because of the instability seen in Figure 3.3)

3.5.4 Fault at Bus 112

In this plant mode case, only generator 27 becomes unstable. Figure 3.4 shows how generator 27 responds in each of the four systems. The linear and second-order systems remain stable for all clearing times. Again the second-order and linear systems' oscillations grow with increased fault clearing time, and the second-order system's oscillations also become lower in frequency more like the full and third-order systems' oscillations. The third-order system appears unstable for all but the shortest clearing time of 0.22 seconds. Dominant frequencies are again relatively high.

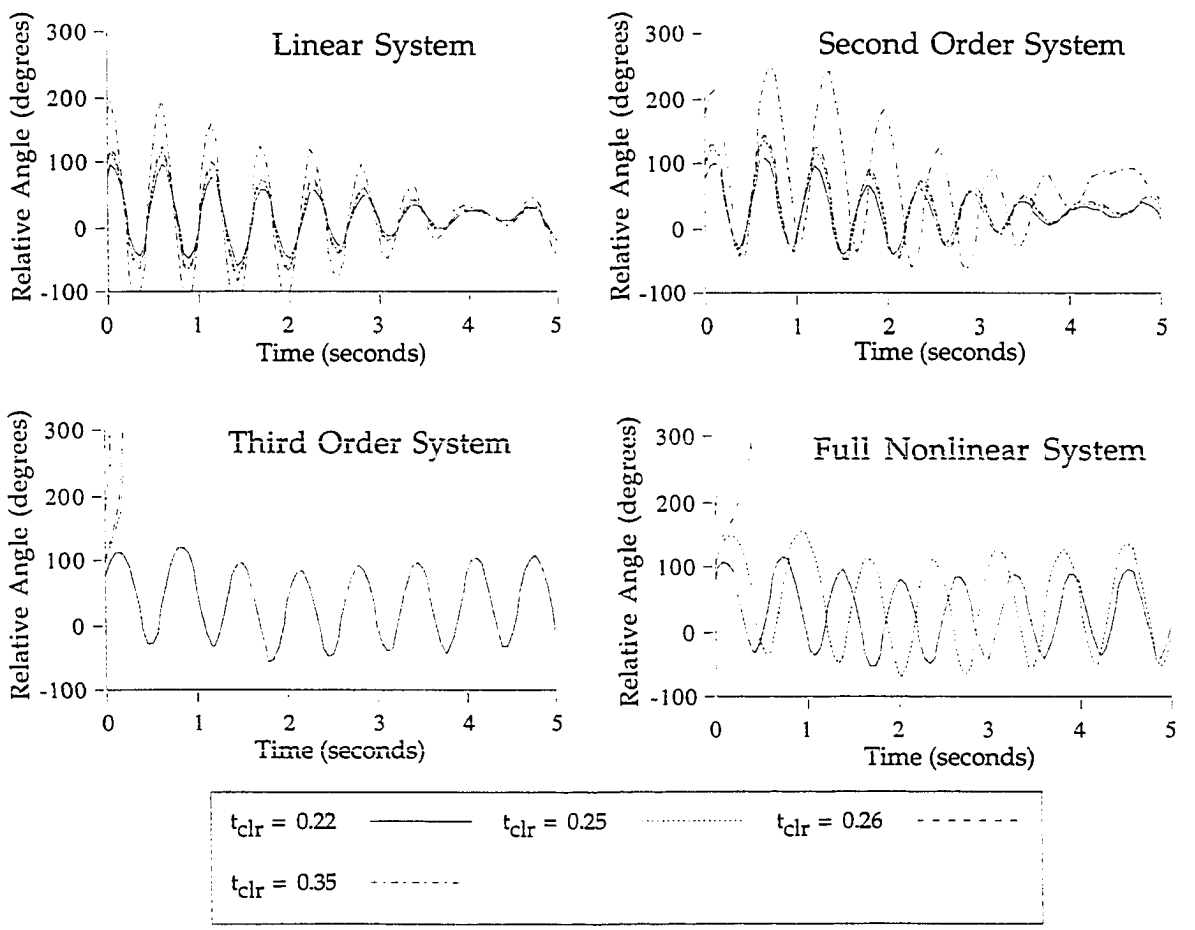

Figure 3.4 Generator 27's response to a fault at bus 112

3.5.5 Fault at Bus 1

In this interarea mode case, a number of generators become unstable (see Table 3.1). Figure 3.5 shows how generators 20 and 43 respond in each of the four systems. Generator 20's response is indicative of a group of generators becoming unstable in the positive angular direction. Generator 43 is the first to become unstable and does so in the negative direction. The linear system remains stable for all clearing times.

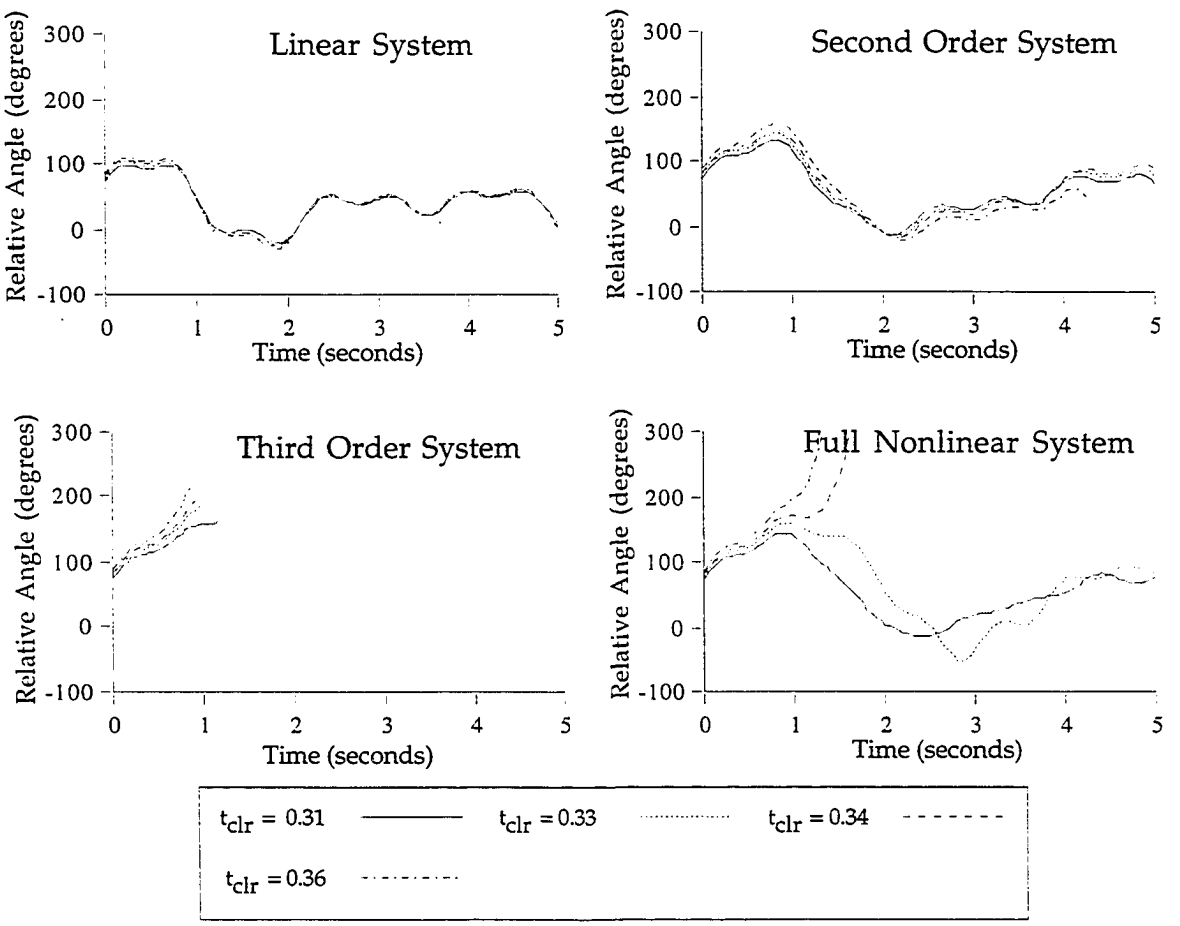

Figure 3.5 Generator 20's response to a fault at bus 1

The third-order system appears unstable for all clearing times shown. The second-order system's oscillations grow with increased fault clearing time, and machine 43's angle appears unstable for the 0.36 second clearing time. In the second-order system, the group of machines represented by generator 20 does not show unbounded angles in the positive direction but does exhibit large, low frequency swings. Comparing the linear and second-order systems' approximations to the full system's response indicates that the second-order system gives a more accurate indication of the shape of generator 20's oscillations. The dominant frequencies in this case are quite low as is expected of the interarea mode. Higher order frequencies are present but generally have smaller magnitudes.

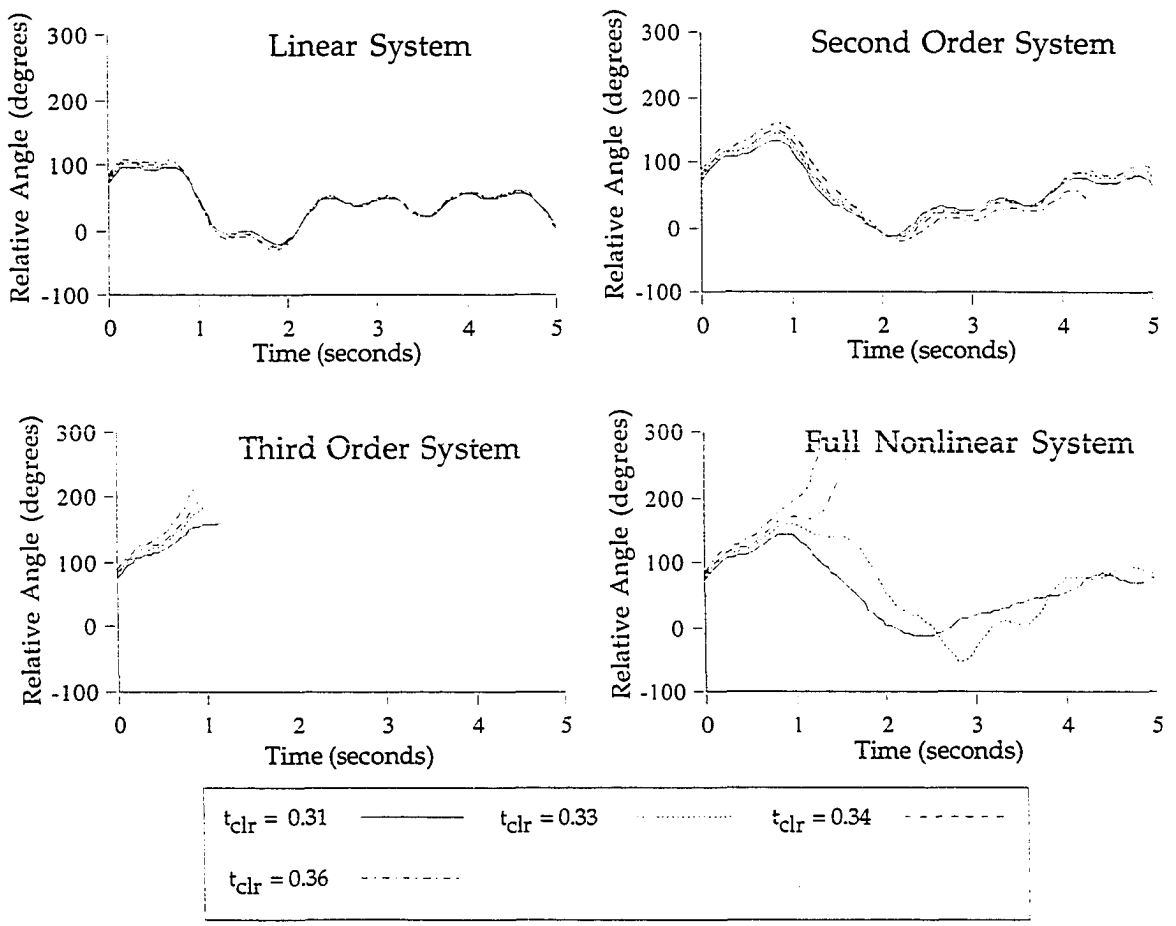

Figure 3.6 Generator 43's response to a fault at bus 1

3.5.6 Summary

The linear system approximation appears to provide basic oscillation information in the unstressed or plant mode cases for the large disturbances presented here. Even under stressed conditions, the linear modes are detectable in the system response. However, in the interarea mode cases the linear system underestimates the low frequency oscillations characteristic of the interarea mode. Nonlinear system stability information is not expected from the linear system because of its limited range of applicability.

The second-order system indicates oscillation size and frequency (modal behavior) nearly the same as the linear system in the plant mode cases. In the interarea mode cases the second-order approximations detect the low frequency oscillations significantly better than the linear approximation does. The size of the oscillations and/or apparent instabilities, in the interarea mode cases indicate that second-order terms capture the key oscillations leading to system instability. Thus, the second-order terms contain significant information concerning critical system oscillations.

The third-order system contains additional stability information. In many cases, this system was unstable at clearing times well below the critical clearing time of the full-nonlinear system. These terms contain significant information about system stability, giving a good indication of which machines become unstable, although critical clearing times are not accurate. This agrees with the fact that the third-order system contains addition information about the nonlinear systems dynamics.

These results indicate the significance of higher order terms in a power system's modal behavior. The second-order system response is significantly more accurate than the linear system and more clearly indicates the troublesome oscillations within the system's response in the interarea mode cases. Third-order terms also show promise as indicators of potentially unstable modes of oscillation. In conclusion, this work clearly indicates that the analysis of these nonlinear terms using normal forms merits further research work in the study of power system modal behavior. We do not expect, however, that the second-order normal form system will contain all of the effects seen in the second-order Taylor series system. This is because some of the second-order terms present in

the Taylor series are converted to third-order and fourth-order terms (which are truncated) in the normal form.

CHAPTER 4. NORMAL FORMS OF VECTOR FIELDS

Mathematical techniques based on Lie theory exist for studying systems of nonlinear differential equations using their normal forms [14]. The normal form is obtained via a nonlinear variable transformation performed on the series expansion of the power system's nonlinear differential equations. The nonlinear variable transformation is derived based on the requirement that terms of higher order in the system of differential equations are to be eliminated. Normal-form analysis may be used to analyze power system modal behavior by including nonlinearities one order at a time. Poincaré's normal-form theorem [14 section 2.3,15] states that if there is no resonance of a given order, then the series expansion of the system equations may be reduced to a linear equation by a polynomial change of variable.

The application of normal-form analysis requires the determination of the series expansion of the nonlinear differential equations describing the system's dynamics. For a classically-modeled power system, the starting point is the set of swing equations. This set is reduced to an independent set by choosing a reference generator, and the equilibrium is shifted to the origin.

The series expansion in terms of relative generator angle and speed differences was discussed in Chapter 3 and is

$$\dot{x} = Ax + X_2 + X_3 + \ldots \tag{4.1}$$

where x is the vector of machine states, A is the plant matrix, and X_i contains only polynomial terms of order i.

4.1 Jordan-Form Transformation

Next the system of equations is transformed to the Jordan-form basis using the similarity transformation $x = Uy$, where y is the vector of Jordan-form variables. The variable transformation $x = Uy$ is applied to the system of equations (4.1) to obtain the Jordan form. y is the vector of Jordan-form state variables. Differentiating the transformation equation yields $\dot{x} = U\dot{y}$, and substituting into (4.1) yields

$$U\dot{y} = AUy + X_2(Uy) + X_3(Uy) + \ldots \tag{4.2}$$

The matrix with the left eigenvectors as rows, V, is the inverse of the right eigenvector matrix U. Pre-multiplying both sides of (4.2) by $V = U^{-1}$ results in

$$\dot{y} = VAUy + VX_2(Uy) + VX_3(Uy) + \ldots \tag{4.3}$$

Let $J = VAU$, which is a diagonal matrix with the eigenvalues on the diagonal, and $Y_2(y) = VX_2(Uy)$, etc. The system is now expressed in terms of the Jordan coordinate system as given by (4.4).

$$\dot{y} = Jy + Y_2(y) + Y_3(y) + \ldots \tag{4.4}$$

In this form the transformed plant matrix J is diagonalized with the eigenvalues on the diagonal. The details of the transformation of the Taylor-series expansion of (4.1) are given in Appendix B.

4.2 Normal-Form Transformation

The next step is to determine the desired nonlinear transformations, one polynomial order at a time, to remove as many higher order terms as possible. The second-order normal-form transformation is defined as

$$y = z + h_2(z) \tag{4.5}$$

where h_2 contains only second-order polynomial terms and z is the vector of normal-form state variables. The transformation [14 section 2.3], is derived by requiring that the Lie bracket $\{D_z[h_2(z)]\, Jz - Jh_2(z)\} \equiv L_J(h_2(z))$ be equal to $Y_2(z)$. This means that the second-order terms in the normal form resulting from the transformation will cancel out the second-order terms from the Jordan form. The result is that all second-order terms are eliminated from the normal form equations (if certain conditions are met).

Rearranging (4.5) to solve for the vector of normal-form variables

$$z = y - h_2(z) \tag{4.6}$$

Differentiating (applying the chain rule to the h_2 term) gives

$$\dot{z} = \dot{y} - \left\{D_z\left[h_2(z)\right]\right\}\dot{z} \tag{4.7}$$

Substituting for $\dot{y}$ and including up to second-order terms, we get

$$\dot{z} = Jy + Y_2(y) - \left\{D_z\left[h_2(z)\right]\right\}\dot{z} \tag{4.8}$$

and substituting for y using (4.5)

$$\begin{aligned}\dot{z} &= J[z+h_2(z)]+Y_2(z+h_2(z))-\{D_z[h_2(z)]\}\dot{z}\\ \dot{z} &= Jz+Jh_2(z)+Y_2(z+h_2(z))-\{D_z[h_2(z)]\}\dot{z}\end{aligned} \tag{4.9}$$

Y_2 is a second-order polynomial function; thus $Y_2(z + h_2(z))$ is made up of products of the form $Y_{2kij}(z_i + h_{2i}(z))(z_j + h_{2j}(z))$. Here the h_{2i}'s are the second-order polynomials that are the elements of h_2, and Y_{2kij} is the coefficient in an element function of Y_2 corresponding to the k^{th} equation and the i times j variable product (e.g., z_iz_j). Thus, $Y_2(z + h_2(z))$ contains second-order, third-order and fourth-order terms. The second-order terms are given by $Y_2(z)$.

In analyzing (4.9), it is evident that the only linear terms are given by Jz. Because h_2 contains only second-order terms, $D[h_2]$ will contain only first-order terms. Thus the second-order terms contained in the last terms can be expressed by replacing $\dot{z}$ with it's linear part Jz. Including up to second-order terms in z (4.9) becomes

$$\dot{z} = Jz+Jh_2(z)+Y_2(z)-\{D_z[h_2(z)]\}Jz \tag{4.10}$$

Thus, setting the second-order terms to zero results in the equation

$$0 = Jh_2(z)+Y_2(z)-\{D_z[h_2(z)]\}Jz \tag{4.11}$$

which is precisely the Lie bracket condition given above. The application of this requirement to the system of differential equations results in a straight-forward definition for the transformation function h_2. This can be done by considering one row of the matrix-vector equation (4.11). The i^{th} equation is given by:

$$0 = \lambda_i h_{2i}(z)+Y_{2i}(z)-\sum_{j=1}^{m}\left[\frac{\partial}{\partial z_j}\{h_{2i}(z)\}\right]\lambda_j z_j \tag{4.12}$$

where $m = 2(n-1)$ is the number of system states.

The second-order function $h_{2i}(z)$ in expanded form is

$$h_{2i}(z) = \sum_{a=1}^{m}\sum_{b=a}^{m} h_{2iab}z_a z_b \tag{4.13}$$

Similarly, $Y_{2i}(z)$ is given by

$$Y_{2i}(z) = \sum_{a=1}^{m}\sum_{b=a}^{m} Y_{2iab}z_a z_b \tag{4.14}$$

Evaluating the partial derivative term in (4.12) yields

$$\frac{\partial}{\partial z_j}\{h_{2i}(z)\} = \sum_{a=1}^{m}\sum_{b=a}^{m}\frac{\partial}{\partial z_j}\{h_{2iab}z_a z_b\} = h_{2ijj}2z_j + \sum_{\substack{d=1\\d\neq j}}^{m} h_{2ijd}z_d \tag{4.15}$$

and the desired equation (4.12) in expanded form is

$$\begin{aligned} 0 &= \lambda_i \sum_{a=1}^{m}\sum_{b=a}^{m} h_{2iab}z_a z_b + \sum_{a=1}^{m}\sum_{b=a}^{m} Y_{2iab}z_a z_b - \sum_{j=1}^{m}\left[h_{2ijj}2z_j + \sum_{\substack{d=1\\d\neq j}}^{m} h_{2ijd}z_d \right]\lambda_j z_j \\ &= \sum_{a=1}^{m}\sum_{b=a}^{m}\{\lambda_i h_{2iab}z_a z_b + Y_{2iab}z_a z_b\} - \sum_{j=1}^{m}\sum_{\substack{d=1\\d\neq j}}^{m}\lambda_j h_{2ijd}z_d z_j - \sum_{j=1}^{m} 2\lambda_j h_{2ijj}z_j z_j \end{aligned} \tag{4.16}$$

The last two terms of (4.16) may be re-written as

$$\sum_{j=1}^{m}\sum_{\substack{d=1\\d\neq j}}^{m}\lambda_j h_{2ijd}z_d z_j + \sum_{j=1}^{m} 2\lambda_j h_{2ijj}z_j z_j = \sum_{a=1}^{m}\sum_{b=a}^{m}(\lambda_a + \lambda_b)h_{2iab}z_a z_b \tag{4.17}$$

so that the equation defining the variable transformation becomes

$$\begin{aligned} 0 &= \sum_{a=1}^{m}\sum_{b=a}^{m}\{\lambda_i h_{2iab}z_a z_b + Y_{2iab}z_a z_b\} - \sum_{a=1}^{m}\sum_{b=a}^{m}(\lambda_a + \lambda_b)h_{2iab}z_a z_b \\ &= \sum_{a=1}^{m}\sum_{b=a}^{m}\{\lambda_i h_{2iab} + Y_{2iab} - (\lambda_a + \lambda_b)h_{2iab}\}z_a z_b \end{aligned}$$

This must hold for all values of z, thus each coefficient in the double sum must be zero individually. In equation form

$$0 = \lambda_i h_{2iab} + Y_{2iab} - (\lambda_a + \lambda_b)h_{2iab} \tag{4.18}$$

Rearranging, the elements of the second-order transformation for the power network are given by

$$h_{2iab} = \frac{Y_{2iab}}{\lambda_a + \lambda_b - \lambda_i} \qquad \text{i, a, b = 1, 2, ... m} \tag{4.19}$$

Thus, h_{2iab} is defined provided (4.20) does *not* hold.

$$\lambda_a + \lambda_b = \lambda_i \tag{4.20}$$

The condition given in (4.20) is referred to as a second-order resonance. According to normal-form theory, if no resonances of second-order occur, all second-order terms may be removed from the normal form using the second-order transformation. In other words, a system consisting of first and second-

order terms is equivalent to a purely linear system in the normal form (including terms to second-order). The second-order, normal-form system is given by

$$\begin{aligned} \dot{z} &= Jz \\ \dot{z}_j &= \lambda_j z_j \end{aligned} \tag{4.21}$$

where z_j is an element of the normal-form variable vector z.

The second-order, normal-form system has now been separated into two parts; its dynamics that are described by a set of purely-linear decoupled differential equations, and a second-order, polynomial variable transformation.

4.3 Solution of Second-Order System using Normal Form

The solution to the normal-form differential equation is

$$z_j(t) = z_{jo} e^{\lambda_j t} \tag{4.22}$$

where z_{jo} is the initial condition of the normal-form variable z_j.

This solution can be transformed back to the Jordan-form coordinate system using the transformation $y=z+h_2(z)$. The solution in terms of the Jordan form is given by

$$\begin{aligned} y_j(t) &= z_j(t) + h_{2_j}(z(t)) \\ y_j(t) &= z_{jo} e^{\lambda_j t} + \sum_{k=1}^{n} \sum_{l=k}^{n} h_{2jkl} z_{ko} z_{lo} e^{(\lambda_k + \lambda_l)t} \end{aligned} \tag{4.23}$$

Finally, the solution to the original differential equation (including up to second-order terms of the normal form) can be found by applying the similarity transformation $x=Uy$ to (4.23) to obtain $x_i(t)$ as

$$x_i(t) = \sum_{j=1}^{n} u_{ij} z_{jo} e^{\lambda_j t} + \sum_{j=1}^{n} u_{ij} \left[\sum_{k=1}^{n} \sum_{l=k}^{n} h_{2jkl} z_{ko} z_{lo} e^{(\lambda_k + \lambda_l)t} \right] \tag{4.24}$$

Here x_i is the i^{th} element of the machine state vector x, and the u_{ij} are elements of the right eigenvector matrix U.

Thus, the approximate second-order solutions are obtained in closed form. In (4.24) the contributions of particular modes of oscillation to the machine state oscillations are given explicitly. An overview of the obtaining a the approximate second-order solution (4.24) is given in Figure 4.1.

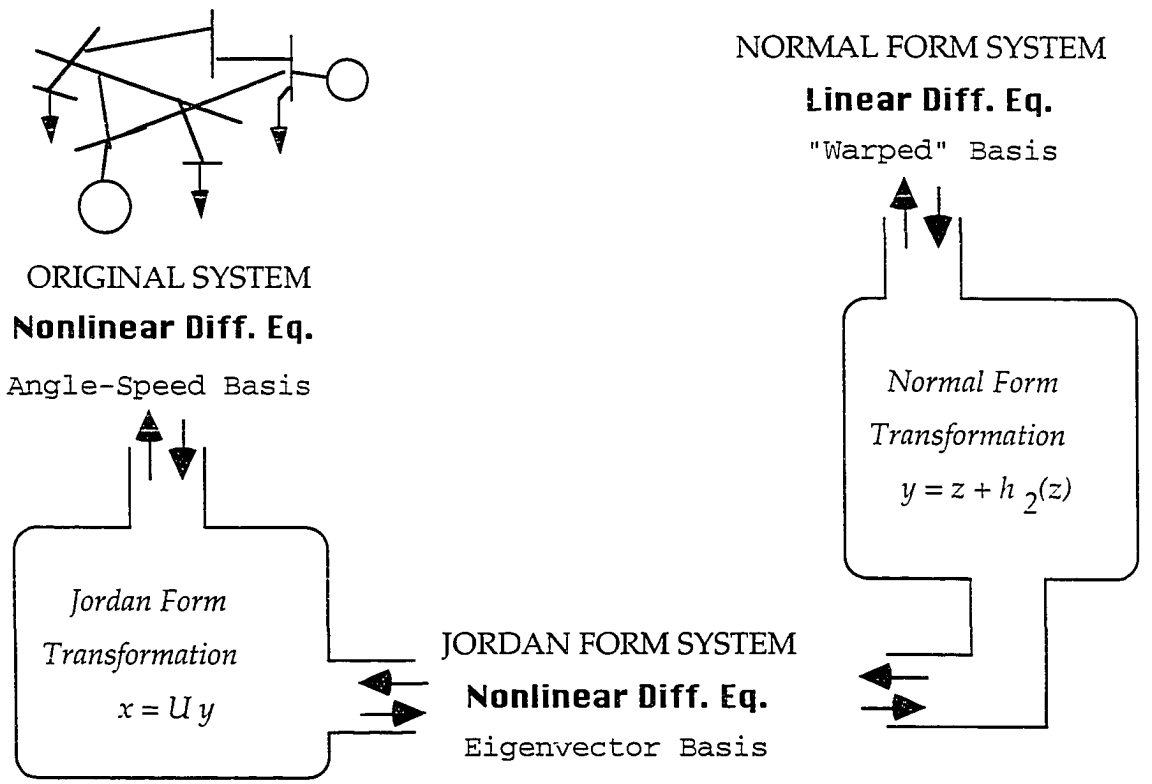

Figure 4.1 Overview of approximate second-order solution

4.4 Initial Condition Considerations

The initial conditions for the original (ω_o, δ_o, x_o), Jordan (y_o), and normal-form (z_o) systems are required in much of this analysis. Because we are working with the post-disturbance system, the initial conditions are the conditions at fault clearing. Thus the vectors of speeds and angles at the time of clearing must be determined and transformed to the appropriate forms. Time simulation of the differential equations describing the pre-disturbance and disturbance-on periods is used to determine the initial angles and speeds.

The angles and speeds at the instant of disturbance clearing are then converted to relative variables by subtracting the values for the reference machine from the values for each of the other machines. The initial conditions of the Jordan form are found using the inverse transformation $y = V x$ (i.e., $y_o = V x_o$). The calculation is obtained by a linear summation.

It is more difficult to transform the initial conditions to the normal form. This is because the inverse of the nonlinear, normal-form transformation is needed. For approximate purposes, the series expression for the inverse transformation of (4.25) can be used.

$$z = y - h_2(y) + \textit{higher order terms} \tag{4.25}$$

If only second-order terms are included the approximation is simply $z = y - h_2(y)$. This approximation will be used when an expression for the inverse transformation is needed. Numerical results indicate that this approximate expression may contain significant errors when the disturbance is of "normal" size. Thus a more accurate means of obtaining the z_{j0}'s is desired. When an analytical expression is not needed, numerical iteration can be used to solve the equation $0 = -y_0 + z_0 + h_2(z_0)$ for z_0 given y_0. In this work, a Newton-Raphson [47 section 4.3] type iterative technique is applied to this problem. The initial condition vector z_0 is iterated using the vector/matrix equations:

$$\begin{aligned} f(z_o) &= z_o - y_o + h_2(z_o) = 0 \\ z_o^{new} &= z_o^{old} - \frac{1}{k}\left\{D_{zo}[f(z_o)]\right\}^{-1}\Big|_{z_o = z_o^{old}} f(z_o^{old}) \end{aligned} \tag{4.26}$$

Here $D_{zo}[\ ]$ indicates the Jacobian matrix of the function inside the brackets. The factor $1/k$ is added to the equation to keep the process from producing very large changes between iteration steps. k is set to one once the changes between the steps becomes small. When the iterative process reaches a given tolerance level, the iterations are stopped and the last value of z_0 is used in the calculations. This procedure is illustrated in the computation described in the next chapter (i.e., those not requiring an analytical expression).

CHAPTER 5. APPLICATION OF NORMAL FORMS TO POWER SYSTEMS

The second-order normal-form system has been separated into two parts: 1) its dynamics, which are described by a set of purely linear, decoupled equations, and 2) a second-order, polynomial variable transformation. The linear part of the normal-form system approximates the second-order original system. The approximation is due to neglecting the higher-order terms in the normal-form differential equations and in the inverse transformation used to obtain the initial conditions. In this chapter, normal-form theory is used to develop measures of system performance. Both linear and second-order systems are considered for comparison purposes.

5.1 Normal-Form Transformation Coefficients

The transformation coefficients indicate the extent of the curvature of the normal-form state space with respect to the Jordan form state space. Thus, the larger the size of these coefficients, the more curved are the invariant manifolds of the system. (If the system were purely linear, the manifolds would be linear.) Thus, the size of the normal-form transformation coefficients indicates the significance of the higher-order terms in the system's dynamics. However, these coefficients are very closely related to the resonance condition. Referring to (4.19), note that if any three modes are nearly resonant (e.g., $\lambda_k + \lambda_l \approx \lambda_j$), not only will the size of h_{2jkl} be larger, indicating a potentially large interaction between modes k, l and j, but also the frequency of the second-order oscillation will be near the frequency of the "linear mode." Two types of modal variables are related by an individual transformation coefficient: those of the Jordan form and those of the normal form. Because they relate the Jordan and normal-form systems, the transformation coefficients do not give information with respect to the machine states.

5.2 Fault-Dependent Measures of System Performance

The measures of system performance presented in this section are dependent on the initial conditions (x_{io}, y_{io}, and z_{io}). This means that they are

dependent on the location and duration of the disturbance as well as the system's structure and loading.

5.2.1 Linear Contribution Factors

In the linear case, the Jordan form solution is $y_j(t) = y_{j0}e^{\lambda_j t}$ where y_{j0} is the j^{th} initial condition in the Jordan form coordinate system. The linear solution in time for the i^{th} state variable is

$$x_i(t) = \sum_{j=1}^{n} u_{ij} y_{j0} e^{\lambda_j t} = \sum_{j=1}^{n} \sigma_{ij} e^{\lambda_j t} \tag{5.1}$$

The $\sigma_{ij} = u_{ij}\, y_{j0}$ are referred to as "contribution factors" [39,40]. Zadeh and Desoer referred to them as the "excitation" of a mode [48 section 5.4]. They indicate the size of mode j's contribution to the oscillations of machine state i for a given disturbance. The solution (5.1) is made up of a sum of weighted exponential oscillations. The "weights" are the contribution factors. The frequencies of oscillation are given by the imaginary parts of the eigenvalues (λ_j's).

The eigenvalues for a classically modeled power system appear in complex conjugate pairs, and the contribution factors corresponding to a complex conjugate pair of eigenvalues are also complex conjugates. Using these observations, (5.1) can be rewritten as in (5.2). Here the role of the contribution factors is seen clearly. The magnitude of the contribution factor σ_{ij} indicates the magnitude of the λ_j oscillation in the i^{th} state-variable solution. The angle of σ_{ij} indicates the phase shift of the oscillation associated with $\lambda_j = \alpha_j + j\varpi_j$. Note that in the case of zero damping, $\alpha_j = 0$ for all j. Here γ_{ij} is the phase of the contribution factor σ_{ij}.

$$x_i(t) = \sum_{\substack{j=1 \\ j\ odd}}^{n} \left[\sigma_{ij}^{*} e^{\lambda_j^{*} t} + \sigma_{ij} e^{\lambda_j t} \right] = \sum_{\substack{j=1 \\ j\ odd}}^{n} e^{\alpha_j t} \left[|\sigma_{ij}| e^{-j\gamma_{ij}} e^{-j\varpi_j t} + |\sigma_{ij}| e^{j\gamma_{ij}} e^{j\varpi_j t} \right]$$

$$= \sum_{\substack{j=1 \\ j\ odd}}^{n} e^{\alpha_j t} \left[|\sigma_{ij}| e^{-j(\varpi_j t + \gamma_{ij})} + |\sigma_{ij}| e^{j(\varpi_j t + \gamma_{ij})} \right]$$

$$x_i(t) = \sum_{\substack{j=1 \\ j\ odd}}^{n} e^{\alpha_j t}\left|\sigma_{ij}\right|\left[cos\left(\varpi_j t + \gamma_{ij}\right) - j\,sin\left(\varpi_j t + \gamma_{ij}\right) + cos\left(\varpi_j t + \gamma_{ij}\right) + j\,sin\left(\varpi_j t + \gamma_{ij}\right)\right]$$
$$= \sum_{\substack{j=1 \\ j\ odd}}^{n} 2e^{\alpha_j t}\left|\sigma_{ij}\right| cos\left(\varpi_j t + \gamma_{ij}\right) \tag{5.2}$$

The solution of (5.2) does not depend on how the eigenvectors are scaled or normalized. Thus, the contribution factors are *independent* of eigenvector scaling. The units of the contribution factors are the units of the state variables themselves (usually radians and rad/sec).

5.2.2 Linear Machine-State Perturbation Factors

It is also useful to know which machine states will have the largest oscillations. An indicator of the size of machine variable i's perturbation [39,40] is proposed as

$$O_i = \sum_{\substack{j=1 \\ j=odd}}^{n} 2\left|\sigma_{ij}\right| e^{j\gamma_{ij}} \tag{5.3}$$

O_i is the sum of all the oscillations given in (5.2) for a single state. By adding the effects of all the modes as complex numbers, a rough approximation is obtained. (If all modes had the same frequency, it would be correct.) Because of the complex conjugate nature of the system eigenvalues, the contribution factors are also complex conjugates, and the complex conjugate pairs combine as indicated in (5.2). (5.3) takes advantage of this property to determine the overall size and phase of machine i's oscillations. As will be seen in the next chapter, this does provide reasonable results in most cases.

5.2.3 Linear Mode Dominance Measures

The question of which modes dominate the system response is very important for the tuning and design of controls. A measure of the size of mode j in the overall system response is needed. Adding the magnitudes of mode j's contributions to the oscillations of all the machine states results in the linear

mode dominance measure given in (5.4). I.e., D_j is obtained by summing the magnitudes of the contribution factors for mode j over all machine states.

$$D_j = \sum_{i=1}^{n} |\sigma_{ij}| \tag{5.4}$$

Thus, D_j is a linear measure of the dominance of mode j in the *whole* system. The dominance is in terms of the machine states rather than in terms of the Jordan form variables $y(t)$ as was done in [3].

5.2.4 Second-Order Contribution Factors

The comparison of the linear and second-order solutions, expressed in equations (5.1) and (4.24) respectively, shows that the second-order solution contains many more potential frequencies of oscillation. These combinations of frequencies are passed to the machine states as the "linear modes" are, via the right eigenvectors (as in (5.1)). The bracketed term in (4.24) represents the second-order effects related to these combinations of frequencies from the Jordan form (4.23). As shown in (4.24), these effects are transformed to the machine states using the right eigenvectors (u_{ij}'s).

The second-order solutions given in (4.24) for the original system may be re-written as

$$x_i(t) = \sum_{j=1}^{n} \sigma_{2ij} e^{\lambda_j t} + \sum_{k=1}^{n} \sum_{l=k}^{n} \sigma_{22ikl} e^{(\lambda_k + \lambda_l)t} \tag{5.5}$$

Here $\sigma_{2ij} = u_{ij}\, z_{jo}$, and $\sigma_{22ikl} = z_{ko} z_{lo} \sum_{j=1}^{n} u_{ij} h_{2jkl}$. Thus, these second-order contribution factors are defined in a manner very similar to the linear contribution factors described earlier. They are measures of the size and phase of the oscillations that make up the approximate second-order solution for the machine states. σ_{2ij} gives the contribution of the single-eigenvalue mode (λ_j) to the response of machine state i. Similarly σ_{22ikl} gives the contribution of the two-eigenvalue mode ($\lambda_k + \lambda_l$) to the response of machine state i. (Note that the linear contribution factor σ_{ij} makes up part of the second order contribution factor σ_{2ij}.)

5.2.5 Second-Order Machine-State Perturbation Factors

Second-order modal dominance and machine perturbation are defined in a manner similar to the linear analysis described in the previous section. Equation (5.6) gives the second-order machine perturbation factors. Here both types of second-order contribution factors are summed over all of the modes (both single-eigenvalue and two-eigenvalue type modes) to get a measure of the size of machine state i's oscillations.

$$O_{2i} = \sum_{\substack{j=1 \\ j=odd}}^{n} 2\left|\sigma_{2ij}\right| e^{j\gamma_{2ij}} + \sum_{\lambda_k+\lambda_l>0} \sum 2\left|\sigma_{22ikl}\right| e^{j\gamma_{22ikl}} \tag{5.6}$$

5.2.6 Second-Order Mode Dominance Measures

Equations (5.7) and (5.8) give equations for the second-order modal dominance measures for single eigenvalue modes (D_{2j}) and for "second-order modes" (D_{22jk}) respectively. Again, modal dominance is determined in terms of the machine states and is found by summing over all machine states.

$$D_{2j} = \sum_{i=1}^{n} \left|\sigma_{2ij}\right| \tag{5.7}$$

$$D_{22jk} = \sum_{i=1}^{n} \left|\sigma_{22ijk}\right| \tag{5.8}$$

Thus, linear and second-order measures of system performance in the same form have been defined, and numerical results are presented in Chapter 6.

5.3 Relationships Between Modes and Machine States

Whereas the above analysis provides detailed answers for the specific fault cases chosen, it may also be beneficial to study measures of system performance that depend only on system structure and loading (not on the disturbance location or duration). In this section, second-order analysis independent of disturbance conditions is developed to characterize:

i. the presence of a certain mode in a given state, i.e., a second-order mode shape or second-order terms resulting from right eigenvector elements. (referred to here as "observability of modes")

ii. the presence of a certain machine state in a given mode, i.e., a second-order term resulting from left eigenvector elements. (referred to here as "controllability of modes")

5.3.1 Observability and Controllability

In control theory [21,22], the concepts of controllability and observability are used determine how a given system will respond to the application of controls. A system is said to be controllable for a given input if the initial state of the system may be transferred to any given state in a finite amount of time. Likewise, a system is said to be observable for a given output if the initial state of the system can be determined by observing the output for a finite time interval. In many texts, the controllability and observability of systems is determined by testing the rank of specially formed matrices that depend on the plant, input and output matrices of the system [21 chapter 5]. Controllability matrix depends on the plant matrix A and the input matrix B, whereas the observability matrix depends on A and the output matrix C. The controllability and observability of a system may also be determined using Gilbert's criteria [22].

Gilbert's criterion for controllability can be developed starting with the general control system of (5.9). The input is given by the vector r, x is the vector of system states, and the output is the vector w. A is the plant matrix, and B and C are the input and output matrices, respectively.

$$\begin{aligned} \dot{x} &= Ax + Br \\ w &= Cx \end{aligned} \tag{5.9}$$

Gilbert's method requires that the eigenvalues of the plant matrix be distinct. Thus, there exists a nonsingular transformation matrix that diagonalizes A. This transformation matrix is a matrix of right eigenvectors, which is denoted as U. It follows that the inverse transformation matrix is V, a matrix of left eigenvectors. Applying the transformation $x = U\,y$ to (5.9) results in

$$\begin{aligned} \dot{Uy} &= AUy + Br \\ w &= CUy \end{aligned} \tag{5.10}$$

And utilizing the inverse transformation $y = V\,x$, yields

$$\begin{aligned} \dot{y} &= VAUy + VBr = Jy + \beta r \\ w &= CUy = \mu y \end{aligned} \tag{5.11}$$

Gilbert's criterion states that the system of (5.9) is controllable if the matrix $\beta = VB$ has no zero rows. Writing the equation for the i^{th} Jordan form variable, including the inputs yields

$$\dot{y}_i = \lambda_i y_i + \sum_{j=1}^{ninputs} \beta_{ij} r_j \tag{5.12}$$

where the β_{ij}'s are elements of the matrix β, $ninputs$ is the number of inputs, and r_j is the j^{th} input variable. Equation (5.12) shows that the size of the elements of β indicate the influence of the j^{th} input (r_j) on the i^{th} Jordan form variable (y_i). If β_{ij} is large, then input j "controls" the i^{th} modal variable, but if β_{ij} is small, input j's effect on mode i is small. If all of the elements of the i^{th} row of β are zero, then the i^{th} Jordan variable is independent of the control and its response depends only on the initial conditions. Thus, the left eigenvectors of the system are important for determining controllability because V is part of β.

Gilbert's criterion for observability can also be developed using (5.11). The expression the k^{th} output variable is

$$w_k = \sum_{i=1}^{noutputs} \mu_{ik} y_i \tag{5.13}$$

where the μ_{ki}'s are the elements of $\mu = CU$, and $noutputs$ is the number of system outputs. The system is said to be observable if no column of μ is zero. The size of μ_{ki} indicates the extent to which the i^{th} Jordan variable (y_i) can be observed in the k^{th} output variable (w_k). If μ_{ik} is large, the effects of modal variable y_i are "observed in output k. If μ_{ik} is small, y_i's motions are not seen in the output w_k. Thus the right eigenvectors of the system are important for determining observability because U is part of μ.

The problem can be approached from a different direction to see the role of the eigenvectors more clearly. Consider the Jordan form system as the "original" system. Then the Jordan form variables (y_i) are the system states, the outputs of

the system can be defined as the machine states (x_i), and the set of equations (without inputs) can be written as

$$\begin{aligned} \dot{y} &= Jy \\ x &= Uy \end{aligned} \tag{5.14}$$

U (the matrix of right eigenvectors of A) is the output matrix for this system. The system eigenvalues are the eigenvalues of J, which are the eigenvalues of A. The eigenvectors of J are simply the natural basis vectors, e^k's (since J is diagonal, $J\ e^k = \lambda_k\ e^k$). The matrix of J's right eigenvectors is just the identity matrix I. Thus, the μ matrix for this system is $\mu = UI = U$. This means that the columns of the right eigenvector matrix tell the observability of a modal state (i.e., Jordan form variable) in the machines states (here thought of as outputs). The element u_{ij}, indicates the degree to which mode j can be observed in machine state i.

Next consider a special form for the input matrix B in (5.9). If $B = I$ then the k^{th} input (r_k) will affect only the k^{th} machine state (x_k); in addition r_k will be the *only* input that affects x_k (i.e., there is a one-to-one correspondence of inputs to states). The controllability matrix $\beta = VB$ is then equal to V. The rows of V indicate how the modal variables (y_j) can be controlled through a single machine state. The element v_{jk} indicates the effectiveness of controlling mode j by controlling machine state k.

Using Gilbert's criterion for controllability and observability, the system eigenvectors have been shown to contain useful information regarding the relationships between the modal (or Jordan form) variables and the machine variables. In the next section, second-order measures that are closely related to these linear eigenvectors are introduced.

5.3.2 Terms Associated with Right Eigenvectors

The approximate second-order solution can be written as

$$x_i(t) = \sum_{j=1}^{n} u_{ij} z_{jo} e^{\lambda_j t} + \sum_{k=1}^{n} \sum_{l=k}^{n} u_{2ikl} z_{ko} z_{lo} e^{(\lambda_k + \lambda_l)t} \tag{5.15}$$

where u_{ij} is an element of the i^{th} right eigenvector, and

$$u_{2ikl} = \sum_{j=1}^{n} u_{ij} h_{2jkl} \tag{5.16}$$

Here h_{2jkl} is the second-order normal-form transformation coefficient of the kl product in the j^{th} equation.

As shown in the expression for the second-order solution (5.15), u_{2ikl} performs the same function for the second-order mode $\lambda_k + \lambda_l$, as u_{ij} does for the linear mode j (i.e., it is the coefficient of the initial condition-exponential product). Thus, u_{2ikl} can be thought of as a second-order term resulting from right-eigenvector elements. In linear analysis, right eigenvectors are an important factor in the determination of the observability. As (5.15) shows, right eigenvector terms (linear and second-order) indicate how the modal oscillations are translated to the machine states. Thus, by looking at the relative size of the u_{ij}'s and u_{2ikl}'s one can determine the extent to which a given mode (assuming it has been perturbed) will be exhibited by a given system state. This perturbation-type information is closely linked to open-loop control of the system and may be useful for determining which states should be used as inputs for controllers assigned to damp a given mode.

5.3.3 Terms Associated with Left Eigenvectors

As described in Chapter 4, the initial conditions, y_{jo}'s and z_{jo}'s are determined using the inverse Jordan-form and normal-form transformations. In the linear case, this consists of multiplication by the left eigenvector matrix, i.e.,

$$y_{jo} = \sum_{i=1}^{n} v_{ji} x_{io} \tag{5.17}$$

For the second-order case, an approximate (accurate to second-order) inverse transformation is given by $z_i = y_i - h_{2i}(y)$. This can be used to develop approximate second-order terms resulting from left eigenvector elements. The approximate expression for z_{jo} is

$$z_{jo} = y_{jo} - \sum_{k=1}^{n} \sum_{l=k}^{n} h_{2jkl} y_{ko} y_{lo} \tag{5.18}$$

substituting (5.17) for $y_{?o}$, yields

$$z_{jo} = \sum_{i=1}^{n} v_{ji} x_{io} + \sum_{p=1}^{n} \sum_{q=p}^{n} v_{2jpq} x_{po} x_{qo} \tag{5.19}$$

where v_{ij} is an element of the j^{th} left eigenvector, and

$$v_{2jpq} = -2\sum_{k=1}^{n}\sum_{l=k}^{n} h_{2jkl} v_{kp} v_{lq} \qquad \text{for } p \neq q \qquad (5.20a)$$

$$v_{2jpp} = -\sum_{k=1}^{n}\sum_{l=k}^{n} h_{2jkl} v_{kp} v_{lp} \qquad \text{for } p = q \qquad (5.20b)$$

In linear control analysis, the left eigenvectors are an important part of the determination of state controllability. As evident in (5.19), the left eigenvectors elements determine how perturbation of the machine states is translated into perturbation of the system modes. The size of these elements can be thought of as indicating the amount of influence a machine state has on the oscillations of a given system mode. Again, this open-loop perturbation-type information may be useful in control applications to help determine which states should be controlled in order to most effectively damp a certain mode.

One problem with using eigenvectors in this manner is the issue of scaling or normalization. In this work, the right eigenvectors are normalized so that each right eigenvector has a Euclidean norm equal to one. Normalization is needed to ensure that the transformation is uniquely defined. The use of other forms of normalization may also need to be further investigated. The left eigenvectors are determined through the inversion of the right eigenvector matrix, and thus they are not scaled individually because this process (right eigenvector scaling and inversion) results in a unique solution.

5.3.4 Participation Factors

Linear participation factors, which are defined in [7], are a commonly used measure of mode-machine interactions. The participation factor p_{ki} represents a measure of the participation of the k^{th} machine state in the trajectory of the i^{th} mode. One advantage of using participation factors is that they measure mode-machine relationships independent of eigenvector scaling. This is because they are functions of both the left and right eigenvectors. In [7] it is observed that the participation factors represent the size of the modal oscillations in a machine state when only that machine state is perturbed. This means that the initial condition vector is $x_0 = e_k$ (all elements of e_k are zero except the k^{th}, which is one). In equation form, this means that when $x_0 = e_k$, the time solution for the k^{th} state variable x_k is

$$x_k(t) = \sum_{i=1}^{n} p_{ki} e^{\lambda_i t} \tag{5.21}$$

In this type of analysis, the responses for each of the perturbed machines (found using the participation factors for that machine) are assumed to combine to give the full response.

Using normal-form theory one can extend this concept to include second-order terms. The approximate second-order, normal-form inverse transformation for any initial condition is given in (5.17). When the initial condition vector $x_o = e_k$ is applied, the Jordan form initial conditions (using (5.16)) become

$$y_{jo} = v_{jk} \tag{5.22}$$

The normal-form initial conditions, using the second-order approximation of the inverse transformation (5.18), are

$$z_{jo} = v_{jk} - \sum_{p=1}^{n}\sum_{q=p}^{n} h_{2jpq} v_{pk} v_{qk} = v_{jk} + v_{2jkk} \tag{5.23}$$

The solution for the k^{th} machine state variable (when $x_{io} = 0$, for all $i \neq k$) can be written as

$$\begin{aligned} x_k(t) = &\sum_{i=1}^{n} u_{ki}(v_{ik} + v_{2ikk}) e^{\lambda_i t} + \\ &\sum_{p=1}^{n}\sum_{q=p}^{n} u_{2kpq}(v_{pk} + v_{2pkk})(v_{qk} + v_{2qkk}) e^{(\lambda_p + \lambda_q)t} \end{aligned} \tag{5.24}$$

Using the same approach as in the linear case, one can define second-order participation factors according to

$$x_k(t) = \sum_{i=1}^{n} p_{2ki} e^{\lambda_i t} + \sum_{p=1}^{n}\sum_{q=p}^{n} p_{2kpq} e^{(\lambda_p + \lambda_q)t} \tag{5.25}$$

(when $x_{io} = 0$ for all $i \neq k$.) Note that there are two types of second-order participation factors. p_{2ki} represents the second-order participation of the k^{th} machine state in the i^{th} single-eigenvalue mode. These factors can be thought of as providing second-order corrections to the linear participation factor information. In fact, viewing (5.24) reveals that the linear participation factor ($p_{ki} = u_{ki}\, v_{ik}$) is one term in the expression for p_{2ki}. The second type of second-order participation factor p_{2kpq}, represents the second-order participation of the k^{th} machine state in the "mode" formed by the combination of the eigenvalues

λ_p and λ_q, e.g., by $(\lambda_p + \lambda_q)$. As in the linear case, these second order factors are independent of eigenvector scaling.

As mentioned above, the inverse transformation is approximate. To obtain more accurate values for the normal-form initial conditions, an iterative procedure has been incorporated to find the z_{j0}'s numerically (described in Chapter 2). This numerical method does not provide an expression for the inverse normal-form transformation. However, it does provide a method for more accurately determining numerical values for the initial conditions of the normal form.

Because the participation factors are found by applying a specific initial condition ($x_0 = e^k$), the participation factors may also be determined numerically using the iterative approach. When the initial condition vector x_0 is set equal to e_k, the contribution factors become the participation factors. In this manner, both the linear and second-order participation factors (independent of disturbance) can be found using the same computer program used to find the disturbance-dependent contribution factors described earlier in this chapter. This method allows one to take advantage of the numerical iteration technique for determining z_0 in finding the participation factors.

5.4 Applying the Method to a Power System

These measures of system performance can be applied in a systematic way to obtain a quantitative picture of the system's modal response. The method can be described as follows:

1. Determine which modes dominate the system response.

    a. Apply a number contingencies to the system. These contingencies may be chosen to bring out a certain type of response (e.g., an interarea mode), or an existing list of "critical" contingencies could be used.

    b. Calculate and compare modal dominance measures. The relative size of the dominance measures indicates the relative strength of the modes for a given case. The sizes and

frequencies of the dominance measures indicate the type of system response (i.e., plant mode or interarea mode) as well as the severity of the disturbance. The size of the second-order dominance measures also indicates the influence of nonlinearities within the system.

c. Compile a list of "problem modes" to study further.

2. Determine and characterize severely affected machines.

   a. Calculate and compare machine perturbation factors. The size of these measures gives a rough indication of which machine states will oscillation the most. This can be used to reduce the number of machines to be studied in detail. The number of machine states with large perturbation factors also gives a good indication of the mode type (i.e., plant mode or interarea mode).

   b. Calculate the contribution factors. Now that the number of modes and machines to consider have been limited, the corresponding contribution factors can give a detailed map of which modes influence which machine states. Ranking the contribution factors for a given machine state provides a quantitative picture of that state's oscillatory response.

3. Characterize mode-machine state relationships (independent of fault location).

   a. Calculate linear and second-order terms resulting from the left eigenvector elements. These measures indicate which machines strongly influence the different modes including the "problem modes." This information may be used to determine which machine states should be controlled.

   b. Calculate linear and second-order terms related to right eigenvector elements. These measures tell which machines

are strongly influenced by the different modes including the "problem modes." This information may be used to determine which machine states are the strongest indicators of the problem mode. Knowledge of these machines can be useful in many control strategies. For example, they may be used to determine which states are candidates for control inputs or which machines may need added protection.

c. Calculate linear and second-order participation factors. Participation factors combine specific right-left eigenvector information to produce a single, scaling independent measure of the relationship between one mode and one machine state. They may be used to place controllers with limited choices for input and output variables.

CHAPTER 6. MODE-MACHINE RELATIONSHIP RESULTS: MODAL INTERACTIONS

6.1 The Test System

The second-order normal form method described in Chapter 5 was applied to the 50-generator IEEE test system, part of which is shown in Figure 6.1 Four load levels of plant A (700, 900, 1100, and 1300 MW for each generator) are considered. In each case, the slack bus adjusts its generation so that the total system load is constant. The generation is shifted from one area of the system to another causing changes in power flow on many lines. This shift in loading represents a commonly used means of stressing this system for operations-planning studies. Stub faults are presented; thus allowing for the direct comparison of modes between cases at the same loading. The faults located at bus 1 and bus 7 and are known to result in an interarea-type system responses. For these faults, machine 43 (not shown in Figure 6.1) and a large group of other machines become unstable with sufficiently long clearing times (Tables 6.1-6.2). The other fault is located at bus 112 and results in a plant mode in which one generator (number 27) becomes unstable in response to a large disturbance (Table 6.3). For the 1100 MW case, machine 43 also eventually becomes unstable in the negative direction.

Table 6.1 ETMSP critical clearing times for faults at bus 1

Plant A Load (MW each gen.)	Gen 43 Critical Clr. Time (Seconds)	Group Critical Clr. Time (Seconds)
700	$0.16 < t_{cc} < 0.17$	$0.33 < t_{cc} < 0.34$
900	$0.13 < t_{cc} < 0.14$	$0.28 < t_{cc} < 0.29$
1100	$0.10 < t_{cc} < 0.11$	$0.19 < t_{cc} < 0.20$

Table 6.2 ETMSP critical clearing times for faults at bus 7

Plant A Load (MW each gen.)	Gen 43 Critical Clr. Time (Seconds)	Group Critical Clr. Time (Seconds)
700	$0.12 < t_{cc} < 0.13$	$0.18 < t_{cc} < 0.19$
900	$0.11 < t_{cc} < 0.12$	$0.17 < t_{cc} < 0.18$
1100	$0.09 < t_{cc} < 0.10$	$0.14 < t_{cc} < 0.15$

Table 6.3 ETMSP critical clearing times for faults at bus 112

Plant A Load (MW each gen.)	Gen 43 Critical Clr. Time (Seconds)	Gen 27 Critical Clr. Time (Seconds)
700	N.A.	$0.25 < t_{cc} < 0.26$
900	N.A.	$0.25 < t_{cc} < 0.26$
1100	$0.23 < t_{cc} < 0.24$	$0.25 < t_{cc} < 0.26$

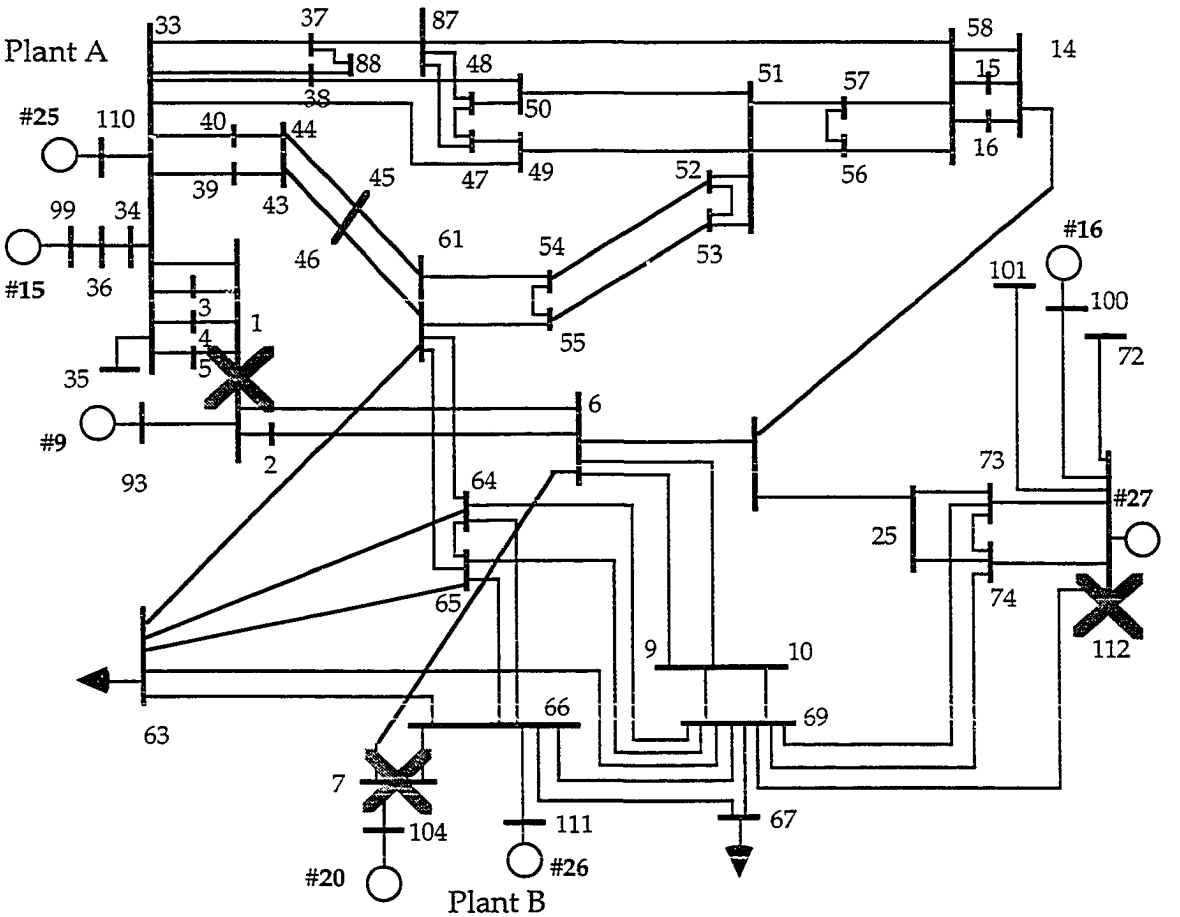

Figure 6.1 50-generator IEEE system - Plants A and B area

As the tables show, increasing the load levels on the generators of plant A decreases the critical clearing times for each of the fault cases. This is one indicator of stress on the system. The instability of generator 43 also seems to correlate with system stress. When plant A picks up generation, the swing generator must decrease it's output by approximately the same amount. This

machine is near the swing generator, and seems to be adversely affected by the decrease in generation in this area.

6.2 Normal-Form Transformation Coefficients

The second order coefficients are closely related to nonlinear resonance between the dominant fundamental modes of oscillation. The equation defining the normal-form transformation $y = z + h_2(z)$ written for the i^{th} Jordan-form variable is

$$y_j = z_j + \sum_{i=1}^{m} h_{2jkl} z_k z_l \tag{6.1}$$

The size of h_{2jkl} determines the relationship between second order mode k l, and Jordan mode j. As indicated by the equation for the coefficients (4.19), near resonance ($|\lambda_k + \lambda_l| \approx |\lambda_j|$) can result in a large value for h_{2jkl}. Thus second-order terms corresponding to λ_k and λ_l have a large component in the solution for the mode j given by (4.23). The large size of the normal-form a transformation coefficient (h_{2jkl}) indicates the *potential* for large second-order interactions between modes j, k, and l. Tables 6.4 and 6.5 present the largest transformation coefficients for four load levels at plant A. The modes with the largest h_2's for each case are included, along with the imaginary parts (frequencies) of the eigenvalues or eigenvalue sums. The modes (j's) chosen are those that have a maximum h_2 greater than 0.1 times the largest h_2 in the system.

Tables 6.4 and 6.5 show that the size of the largest h_2 is not a direct indicator of stress due to changes in generation levels within the system. From time simulations, we know that stress in this system increases with increasing load on plant A; however, no such trend appears in the size of the h_2's. For example the largest h_2 for the base case is 62.1, but as the load at plant A increases to 900 MW the largest h_2 is only 7.7. The size of these factors is closely related to resonance of the system eigenvalues. As the tables indicate, the frequency of the mode pair ($\mathrm{Im}[\lambda_k+\lambda_l]$) is very close to the frequency of the single mode j ($\mathrm{Im}[\lambda_j]$) for each of the large h_{2jkl}'s.

Tables 6.6 and 6.7 give similar transformation coefficient data for the same cases with damping added. A uniform damping to inertia ratio of 0.2 is used for

each machine. When this damping is included, all eigenvalues (at the stable equilibrium point) have real parts equal to -0.1. Thus, the resonance condition ($\lambda_j + \lambda_k - \lambda_i$) cannot be satisfied. (The smallest (in magnitude) the sum can be is -0.1.) These tables illustrate that, in the absence of second-order "near resonances," the normal-form transformation coefficients are much smaller and less sensitive to load changes.

Table 6.4 Largest transformation coefficients, 700 and 900 MW load levels

700 MW at Plant A					900 MW at Plant A				
j	$\mathrm{Im}[\lambda_j]$	$\lvert h_{2jkl} \rvert$	k,l	$\mathrm{Im}[\lambda_k+\lambda_l]$	j	$\mathrm{Im}[\lambda_j]$	$\lvert h_{2jkl} \rvert$	k,l	$\mathrm{Im}[\lambda_k+\lambda_l]$
45	10.9510	62.09	1,78	10.9591	69	9.2982	7.67	23,75	9.2984
29	4.0092	49.42	19,21	4.0076	25	2.0653	4.80	30,37	2.0649
1	18.1535	32.88	45,77	18.1535	75	7.3916	2.57	24,69	7.3914
21	2.0940	29.92	20,29	2.0956	23	1.9068	2.51	69,76	1.9066
19	1.9136	11.22	22,29	1.9152	33	4.0115	2.05	23,25	3.9721
77	7.1944	9.81	1,46	7.1944	39	5.2801	1.49	24,81	5.2786
					37	5.1132	1.31	25,29	5.1136
					81	7.1854	1.18	23,39	7.8169

Table 6.5 Largest transformation coefficients, 1100 and 1300 MW load levels

1100 MW at Plant A					1300 MW at Plant A				
j	$\mathrm{Im}[\lambda_j]$	$\lvert h_{2jkl} \rvert$	k,l	$\mathrm{Im}[\lambda_k+\lambda_l]$	j	$\mathrm{Im}[\lambda_j]$	$\lvert h_{2jkl} \rvert$	k,l	$\mathrm{Im}[\lambda_k+\lambda_l]$
45	11.0145	5.61	23,89	11.0150	91	7.9958	44.29	23,35	7.9957
21	2.0137	4.91	22,33	1.9989	35	5.2628	7.33	24,91	5.2629
33	4.0125	2.92	21,21	4.0273	21	1.9975	4.78	22,29	2.0146
57	10.5823	2.15	19,85	10.5811					
39	5.2688	1.05	20,77	5.2724					
19	1.8796	1.00	40,77	1.8831					
71	9.0726	0.92	25,43	9.0973					
49	10.7204	0.78	21,85	10.7152					
69	6.7021	0.76	19,35	6.7084					
35	4.8288	0.67	36,67	4.8283					
43	6.0801	0.60	25,25	6.0346					

Table 6.6 Largest transformation coefficients, 700 and 900 MW load levels with damping (D/M = 0.2)

700 MW at Plant A					900 MW at Plant A				
j	Im[λ_j]	$\lvert h_{2jkl} \rvert$	k,l	Im[$\lambda_k+\lambda_l$]	j	Im[λ_j]	$\lvert h_{2jkl} \rvert$	k,l	Im[$\lambda_k+\lambda_l$]
35	4.0079	0.76	23,25	4.0026	35	4.0102	0.74	25,27	3.9670
25	2.0916	0.46	24,35	2.0969	27	2.0628	0.45	26,35	2.1061
39	5.1082	0.33	34,83	4.9773	39	5.1123	0.32	34,83	4.9832
61	10.0290	0.28	37,41	10.0971	61	10.0183	0.25	37,41	10.1008
23	1.9110	0.22	24,35	2.0969	47	6.1597	0.21	31,31	6.0934
47	6.1841	0.21	31,31	6.1544	25	1.9042	0.19	26,35	2.1061
33	3.7104	0.16	23,23	3.8220	33	3.7109	0.15	25,25	3.8083
81	7.3982	0.15	33,33	7.4209	17	12.3487	0.15	31,71	12.1579
41	5.2811	0.15	34,83	4.9773	41	5.2792	0.14	34,83	4.9832
71	9.1313	0.15	17,32	9.2927	79	7.3909	0.14	33,33	7.4218
17	12.3698	0.14	31,71	12.2084	71	9.1112	0.14	17,32	9.3021
57	10.4823	0.13	31,81	10.4754	53	10.6061	0.12	41,41	10.5584
79	7.3251	0.13	33,33	7.4209	81	7.3199	0.12	23,36	7.3846
53	10.6071	0.12	41,41	10.5622	37	4.8216	0.11	25,27	3.9670
55	10.5804	0.12	31,81	10.4754	57	10.4790	0.11	31,79	10.4376
37	4.8160	0.11	23,25	4.0026	55	10.5808	0.10	31,81	10.3665
51	10.6385	0.09	3,90	10.7811	73	7.1258	0.10	31,35	7.0569
					51	10.6367	0.09	3,90	10.7841
					77	7.1847	0.09	31,35	7.0569
					65	9.6674	0.08	3,66	9.3856

Table 6.7 Largest transformation coefficients, 1100 and 1300 MW load levels with damping (D/M = 0.2)

1100 MW at Plant A					1300 MW at Plant A				
j	Im[λ_j]	$\lvert h_{2jkl} \rvert$	k,l	Im[$\lambda_k+\lambda_l$]	j	Im[λ_j]	$\lvert h_{2jkl} \rvert$	k,l	Im[$\lambda_k+\lambda_l$]
25	2.0112	0.72	26,33	2.0001	25	1.9950	0.80	26,33	2.0159
33	4.0113	0.53	23,25	3.8881	33	4.0109	0.50	25,25	3.9900
37	5.1088	0.31	32,83	4.9912	37	5.1048	0.30	32,83	4.9935
43	6.0792	0.24	29,29	6.0313	43	6.0520	0.25	29,29	6.0168
63	10.0084	0.23	35,37	9.9366	71	9.0560	0.24	29,43	9.0604
69	9.0720	0.22	29,43	9.0949	61	10.0076	0.24	35,37	9.9341
73	7.1081	0.18	29,33	7.0269	73	7.0961	0.21	29,33	7.0193
31	3.7097	0.14	32,81	3.5998	69	6.6945	0.17	27,33	6.7419
17	12.3140	0.14	29,69	12.0876	49	10.7205	0.16	27,91	10.7262
39	5.2679	0.14	32,83	4.9912	31	3.7088	0.15	32,81	3.5967
71	6.7014	0.13	27,33	6.7720	39	5.2618	0.13	32,83	4.9935
49	10.7200	0.12	27,93	10.7648	17	12.3013	0.13	29,71	12.0644
35	4.8278	0.12	25,27	4.7719	35	4.8293	0.11	25,27	4.7261
79	7.3773	0.12	31,31	7.4195	51	10.6314	0.11	3,90	10.7923
53	10.6061	0.11	37,39	10.3767	79	7.3722	0.11	31,31	7.4175
23	1.8769	0.11	24,33	2.1344	53	10.6065	0.11	37,39	10.3666
51	10.6330	0.11	3,90	10.7900	81	7.3055	0.10	34,41	7.3898
81	7.3095	0.11	34,41	7.3882	57	10.5821	0.10	3,90	10.7923
55	10.5819	0.09	3,90	10.7900	77	7.1581	0.08	29,33	7.0193
77	7.1666	0.08	29,33	7.0269	65	9.6520	0.08	3,66	9.3853
27	2.7608	0.08	26,35	2.8166					
65	9.6566	0.08	3,66	9.3852					

The h_2's only indicate potential interaction between modes because they are a characteristic of the system and are not dependent on the disturbance. It is the disturbance that determines the direction the system moves in state space, and thus it is the disturbance which determines which modes are perturbed. For this reason, the h_2's alone cannot predict the system response. In order to use this h_2 information to determine interactions, the effects of the disturbance must be take into account. Faults at bus 112 and bus 7 (plant and interarea mode respectively), for two plant A load levels (700 and 1300 MW), are discussed here. The data, shown in Tables 6.8-6.11, was obtained as follows:

- The initial conditions are determined and transformed to the Jordan form as discussed in Chapter 4
- The modes are then ranked according to $|y_{jo}|$. Those modes which have $|y_{jo}|$ within 22% of the maximum $|y_{jo}|$ are displayed
- The normal-form transformation coefficients are calculated as discussed in Chapter 4
- For each ranked mode j, the largest normal-form transformation coefficients h_{2jkl} are determined
- Large oscillations are expected when h_{2jkl} is large and y_{ko} and y_{lo} are of significant size

One way of judging modal dominance is using the size of $|y_{jo}|$ [3]. y_o is obtained (as all forms of the initial conditions are) using time simulation of the nonlinear differential equations. Determining y_o from x_o does not require knowledge of second-order terms, and thus finding y_o is simpler than calculating the dominance measures described in Chapter 5.

For the perturbed modes, the potential second-order interactions are indicated by the size of h_{2jkl}. The machines affected by the interaction are indicated by the corresponding elements of the right eigenvectors. In these tables (6.8-6.11) the modes are ranked according to y_{jo}. The size of the largest h_2 indicates second-order interactions in the modal variables, and the eigenvalue

sums give the frequency of these oscillations. The $h_{2jkl}\, z_{ko}\, z_{lo}$ product terms indicate the size of the second-order two eigenvalue terms in the Jordan form (see (4.23)). The affected generators are determined using the elements of the right eigenvectors. If a given mode has a $|u_{ij}|$ above the cutoff value of 0.7 times the maximum element for a given state, the perturbed machine state is taken to be affected by that mode. This cut-off value is selected by experience with the system analyzed and can be easily adjusted by the analyst.

Tables 6.8 and 6.10 present data for the faults at bus 7. This fault is known to represent the onset of the interarea mode. Although the low frequency (2.09 rad/sec) mode may not have the largest y_{jo},, the large size of h_2 and the significant size of the related modes indicate the presence of nonlinear interaction among the modes. For this fault, the 8.0 rad/sec mode has a large y_{jo}, but small h_2 for the first loading. This indicates that a local, higher-frequency, non-interacting mode is present along with the interarea modes. For the 1300 MW case (Table 6.10) this local mode begins to interact with lower-frequency modes, as indicated by the larger size of the related h_2's. At 1300 MW, both low-frequency and high-frequency modes show large interactions, resulting in a large group of machines being affected. In most cases (because of conditions of near resonance) the single eigenvalue mode i has nearly the same frequency as the second-order combination of frequencies $(\lambda_k + \lambda_j)$ that it interacts with.

Table 6.8 Interaction data, fault bus 7, 700 MW load level

$\lvert y_{jo} \rvert$	Freq. (r/s)	$\lvert h_2 \rvert$ max	$\lvert \lambda_k+\lambda_l \rvert$	h_{2jkl} $z_{ko}z_{lo}$	Gens. Affected
1.06	8.02	0.04	7.90	0.01	6, 15, 20, 23, 25, 26, 34, 39, 45, 46
0.90	8.07	0.11	8.08	0.01	15, 20, 26, 45
0.65	8.37	0.21	8.36	0.01	6, 14, 16, 19
0.64	2.09	29.92	2.10	0.01	1-10, 12-27, 29-39, 43-47, 49
0.59	10.48	2.63	10.48	0.57	5, 12, 26

Table 6.9 Interaction data, fault bus 112, 700 MW load level

$\lvert y_{jo} \rvert$	Freq. (r/s)	$\lvert h_2 \rvert$ max	$\lvert \lambda_k+\lambda_l \rvert$	$\frac{h_{2jkl}}{z_{ko}z_{lo}}$	Gens. Affected
0.89	11.00	0.15	10.99	0.00	16, 17, 27
0.61	11.74	0.02	11.73	0.00	17, 27
0.48	10.96	62.09	10.96	0.00	3, 16, 19, 27
0.28	10.48	2.63	10.48	0.11	5, 12, 26
0.20	2.09	29.92	2.10	0.00	1-10, 12-27, 29-39, 43-47, 49

Tables 6.9 and 6.11 present data for a fault at bus 112, which is known to be a plant mode case. In time simulations of this fault, machine number 27 becomes unstable for large disturbances. Machine number 17 shows significant oscillations at the same frequency, but does not become unstable. The tables indicate that the 11.0 rad/sec mode is dominant for both loading cases (as indicated by the size of y_{io}). This mode has low h_2's indicating low potential for modal interactions. Although some of the listed modes (with lower y_{io}'s) do show potential interactions (because of larger h_2's) the related modes have low values of y_{io} and thus the interactions are not significant.

Table 6.10 Interaction data, fault bus 7, 1300 MW load level

$\lvert y_{jo} \rvert$	Freq. (r/s)	$\lvert h_2 \rvert$ max	$\lvert \lambda_k+\lambda_l \rvert$	$\frac{h_{2jkl}}{z_{ko}z_{lo}}$	Gens. Affected
1.03	8.00	54.22	7.99	3.20	5, 6, 9, 20, 22-26, 33, 39, 45, 46
0.86	1.86	1.18	1.87	0.47	1-10, 12-27, 29-39, 43-46, 49
0.72	2.00	4.77	2.01	1.04	1-9, 12-27, 30, 31, 33-35, 39, 43, 46
0.63	2.73	0.72	2.74	0.00	1-27, 33-35, 37, 38, 44, 45, 47, 49
0.52	9.06	3.77	9.06	0.47	2, 5, 13, 20, 23, 24, 33

Table 6.11 Interaction data, fault bus 112, 1300 MW load level

$\lvert y_{jo} \rvert$	Freq. (r/s)	$\lvert h_2 \rvert$ max	$\lvert \lambda_k+\lambda_l \rvert$	$h_{2jkl} z_{ko} z_{lo}$	Gens. Affected
0.91	11.02	0.22	11.02	0.01	16, 17, 27
0.61	11.79	0.27	11.79	0.02	17, 27
0.37	10.97	0.37	10.98	0.01	3, 16, 19
0.26	1.86	1.18	1.87	0.03	1-10, 12-27, 29-39, 43-46, 49
0.22	2.00	4.77	2.01	0.23	1-9, 12-27, 30, 31, 33-35, 39, 43, 46

6.3 Summary

The following observations may be made concerning the results presented in this chapter:

- The h_2 coefficients alone cannot predict system response, the effects of the disturbance must be included.
- The h_2 coefficients can tell us which of the perturbed modes have potential for second-order interaction.
- The $\lvert y_{io} \rvert$ indicate which modes dominate the oscillations of the Jordan form system, thus indicating which of the potential modal interactions actually appear in the system response.
- The linear right eigenvectors are used to link the modes to the machine states. This allows us to determine whether a mode exhibits plant and interarea mode type behavior by determining how many machines are perturbed by that mode.
- The $h_{2jkl} z_{ko} z_{lo}$ products show the importance of including initial conditions. These products are consistently larger for the 1300 MW case; thus these products provide a better indication of system stress than the h_2's alone.

CHAPTER 7. MODE-MACHINE RELATIONSHIP RESULTS: MEASURES OF SYSTEM PERFORMANCE BASED ON SYSTEM TRAJECTORY

This chapter covers the fault-dependent measures of system performance introduced in Section 5.2. Three fault locations (buses 1, 7 and 112) at three plant A load levels (700, 900, and 1100 MW) are considered. The fault clearing time is 0.108 seconds for each case. The modal dominance measures are presented first. They indicate which frequencies will dominate the system response to a given fault, and whether these frequencies are because of linear or second-order effects. The machine perturbation factors are presented in the next section. These measures predict which machines are most severely affected by each fault. Linear and second-order measures are presented for comparison. The third set of fault-dependent measures presented in this chapter is the contribution factors. These factors link each machine state to each of the individual modes (both linear and second order). This information links the dominant modes with the most perturbed machines.

7.1 Modal Dominance

The new mode dominance measures D_k (5.4), D_{2k} (5.7) and D_{22kl} (5.8) were introduced in Chapter 5. They use the initial conditions and the system structure (including h_2's for second order) to quantify modal dominance in terms of oscillations of the machine states x (not the modal variables y). The number of linear dominance measures corresponds to the number of eigenvalues. For the classical machine model used here, the purely-imaginary, complex-conjugate pairs of eigenvalues will have equal linear dominance measures. Thus, only half of the total number of linear dominance measures need be studied. Tables 7.1-7.13 contain the linear dominance measures (D_k) for three load levels and three fault locations. Each table contains data for three faults at one load level, and the eigenvalues (that are the same for all three fault cases) are in the second column.

Second-order modes are of two types: 1) single eigenvalue modes corresponding to those of linear analysis, and 2) combinations of the eigenvalues two at a time, i.e., oscillations corresponding to second-order interactions. Tables

7.1-7.3 also contain the second-order dominance measures for the single-eigenvalue modes (D_{2k}'s). Again these measures appear in pairs, so only the odd numbered modes are presented. The second-order dominance measures for the two-eigenvalue modes are given in Tables 7.6-7.8. Due to the large number of this type of second-order modes, only those modes with dominance measures greater than 0.3 times the maximum second-order dominance measure are shown.

The dominance measures tell which frequencies dominate the system response. Comparing the size of the dominance measures between fault cases or between load levels gives a relative measure of fault severity and system stress. The relative size of the linear and second-order dominance measures, D_k and D_{2k}, is one indicator of the size of the nonlinearity in the system response. For the faults at bus 112, the 11 rad/sec mode is clearly dominant for the linear case. This relatively high frequency is typical of a plant mode. The corresponding linear and second-order measures are not much different for the higher frequency modes. This indicates that the second order effects are small for this fault location.

For the faults at bus 7, the interarea mode cases, the most dominant modes have significantly higher D_j's, indicative of increased fault severity. In the interarea mode case, a mixture of low and higher frequency modes dominate, and their size is comparable to the size of the linear modes.

It is important to keep in mind the size of the fault being used here. The 0.108 second clearing time is short compared to the critical clearing time of the group. A shorter clearing time was chosen to help insure the convergence of the numerical inverse transformation for determining the normal-form initial conditions. As the actual clearing time increases, the size of second-order effects increases due to the increased distance from the stable equilibrium point. Thus, the size of the second-order dominance measures would be expected to increase with longer clearing times.

Table 7.1 Single-eigenvalue-mode dominance measures for linear and second order, 700 MW load level

		Fault at Bus 7		Fault at Bus 1		Fault at Bus 112	
k	Eigenvalue (rad/sec)	D_k	D_{2k}	D_k	D_{2k}	D_k	D_{2k}
1	0.00000+j18.15345	0.18969	0.01938	0.28897	0.02723	0.07222	0.03283
3	0.00000+j19.05825	0.17448	0.17056	0.03520	0.03488	0.00359	0.00774
5	0.00000+j15.87950	0.03579	0.05012	0.01491	0.01702	0.00302	0.00308
7	0.00000+j15.24575	0.44941	3.13004	0.09661	1.73052	0.03134	0.39488
9	0.00000+j14.42371	0.08399	0.07984	0.14310	0.13937	0.02949	0.02907
11	0.00000+j14.34385	0.14585	0.22706	0.76765	0.74938	0.15459	0.15566
13	0.00000+j13.45857	0.30004	0.41373	0.15014	0.16667	0.03976	0.06309
15	0.00000+j12.97830	0.49571	0.46342	0.38676	0.37257	0.17451	0.17207
17	0.00000+j12.37023	0.15206	4.52075	0.35412	1.25315	0.01946	0.73795
19	0.00000+j1.91361	5.69412	0.03969	5.31962	0.02361	1.78824	0.01715
21	0.00000+j2.09403	22.23370	27.38169	20.80469	19.04232	6.97230	6.67694
23	0.00000+j2.87607	17.40377	7.30789	16.49347	15.00231	5.39434	5.17093
25	0.00000+j3.07881	14.71491	16.68390	14.03718	15.81372	4.51087	4.63059
27	0.00000+j3.71177	0.77964	1.26134	0.70816	0.83154	0.20826	0.21920
29	0.00000+j4.00918	1.19591	0.60857	1.22426	0.70917	0.39098	0.64814
31	0.00000+j11.83703	0.97486	0.87705	0.01818	0.19046	0.34021	0.33810
33	0.00000+j11.74426	0.01631	0.02644	0.09736	0.09937	4.89593	4.87294
35	0.00000+j4.81706	0.67942	1.78668	0.89025	1.47732	0.24100	0.28659
37	0.00000+j5.10917	1.38785	3.45224	0.99454	1.76898	0.25989	0.25151
39	0.00000+j5.28205	2.66232	3.29400	3.68824	3.68649	0.95135	0.95292
41	0.00000+j11.39134	0.04419	0.61254	0.00972	0.61072	0.11195	0.12127
43	0.00000+j6.18485	15.59200	8.25624	0.91788	7.09907	3.73791	2.85965
45	0.00000+j10.95910	1.12811	0.03210	1.18416	0.06963	6.56886	6.54108
47	0.00000+j10.99520	1.23255	1.31690	2.30744	2.30351	11.87600	11.81991
49	0.00000+j6.71699	7.13781	7.13139	4.94165	4.97081	2.83343	2.82643
51	0.00000+j10.72172	0.37313	1.02907	0.32157	0.32113	0.79187	0.78075
53	0.00000+j10.63898	0.60280	0.53342	0.08378	0.06928	0.35692	0.35889
55	0.00000+j10.60751	0.28738	0.19835	1.69290	1.62687	1.48744	1.47957
57	0.00000+j10.48274	7.62041	6.55610	1.96318	2.24111	3.02492	3.07938
59	0.00000+j10.58086	1.24989	0.90927	0.78637	0.54776	0.54752	0.47347
61	0.00000+j10.51380	4.71739	4.80770	0.22559	0.19769	0.16135	0.15866
63	0.00000+j10.02946	0.50904	0.45689	0.70286	0.82718	0.38439	0.38493
65	0.00000+j10.03632	2.51934	2.66152	0.40916	0.40937	0.25771	0.25745
67	0.00000+j9.67293	1.88495	1.89698	0.10363	0.09829	0.06368	0.06237
69	0.00000+j9.29742	0.18004	0.86749	1.40978	1.42393	0.50016	0.49858
71	0.00000+j9.13179	9.04887	9.84026	1.00715	1.55841	0.33364	0.28864
73	0.00000+j7.13053	1.61144	1.36474	2.00650	1.94094	0.88168	0.90263
75	0.00000+j7.17261	0.17444	1.15928	1.81775	1.88230	0.26323	0.25701
77	0.00000+j7.19436	4.02972	4.40787	3.39707	3.44016	1.70648	0.01055
79	0.00000+j7.39890	2.02900	1.87489	0.43826	0.29666	1.36265	1.32752
81	0.00000+j7.32574	0.35801	0.24304	1.63109	1.53188	0.28147	0.27593
83	0.00000+j8.68829	5.30377	5.25456	0.97932	0.92748	0.24542	0.24509
85	0.00000+j8.41316	1.18862	1.01047	0.02128	0.23259	0.03331	0.03628
87	0.00000+j8.36814	9.11653	8.99546	1.30099	1.18669	0.10604	0.09749
89	0.00000+j8.27749	13.19986	6.83943	3.39982	0.94497	1.01847	1.03348
91	0.00000+j7.81531	0.53825	0.53496	0.12865	0.08869	0.03645	0.03466
93	0.00000+j7.92166	1.76858	1.79681	0.49897	0.51276	0.20732	0.21310
95	0.00000+j8.02357	21.12117	20.86660	6.28521	6.19309	1.35907	1.36318
97	0.00000+j8.06592	12.38334	12.45415	0.94528	0.96514	0.72927	0.73158

Table 7.2 Single-eigenvalue-mode dominance measures for linear and second order, 900 MW load level

		Fault at Bus 7		Fault at Bus 1		Fault at Bus 112*	
k	Eigenvalue (rad/sec)	D_k	D_{2k}	D_k	D_{2k}	D_k	D_{2k}
1	0.00000+j18.09484	0.15556	0.14682	0.23570	0.16162	*0.06364*	*0.06120*
3	0.00000+j19.05325	0.22914	0.22773	0.10129	0.06675	*0.00599*	*0.00750*
5	0.00000+j15.88270	0.04235	0.08943	0.02261	0.19267	*0.00316*	*0.00304*
7	0.00000+j15.25278	0.49494	0.52485	0.15723	0.24117	*0.04201*	*0.04278*
9	0.00000+j14.43775	0.08259	0.08946	0.13124	0.16108	*0.02953*	*0.03137*
11	0.00000+j14.37254	0.11481	0.10542	0.63001	16.91225	*0.14074*	*0.22645*
13	0.00000+j13.45432	0.34837	0.36741	0.20878	0.19601	*0.04972*	*0.05334*
15	0.00000+j12.99084	0.49887	0.47046	0.42204	0.43141	*0.17760*	*0.18173*
17	0.00000+j12.34916	0.12971	1.19046	0.29511	0.80224	*0.01482*	*0.04568*
19	0.00000+j11.82913	1.12338	0.90312	0.17334	0.54350	*0.37025*	*0.37248*
21	0.00000+j11.75325	0.01217	0.05211	0.08676	0.08818	*4.92157*	*4.87232*
23	0.00000+j1.90680	8.64018	9.51589	8.27400	2.27988	*2.70108*	*2.12310*
25	0.00000+j2.06527	23.77151	6.86408	22.82307	50.27121	*7.41509*	*10.30294*
27	0.00000+j2.83978	19.99069	19.58595	19.59527	10.92995	*6.13479*	*5.89574*
29	0.00000+j3.04833	10.03077	11.15233	9.93349	25.65649	*3.04360*	*3.67989*
31	0.00000+j3.71223	0.72570	2.53747	0.70019	2.16597	*0.19252*	*0.21098*
33	0.00000+j4.01148	1.14521	8.43531	1.23354	41.54592	*0.36183*	*5.06437*
35	0.00000+j4.82258	0.71130	2.88867	0.98803	6.67716	*0.23670*	*0.42886*
37	0.00000+j5.11321	1.44800	3.07695	1.49800	6.08685	*0.27001*	*2.26269*
39	0.00000+j5.28014	3.02598	5.60623	4.72609	18.47029	*0.96664*	*1.32367*
41	0.00000+j11.39522	0.05017	0.22778	0.02351	0.30172	*0.11067*	*0.08315*
43	0.00000+j6.16051	14.03252	16.30695	3.90162	13.21504	*3.53305*	*3.89862*
45	0.00000+j10.96258	1.01774	1.11843	0.86081	0.82258	*6.10465*	*6.03869*
47	0.00000+j11.00066	1.17819	1.33829	1.90720	1.54847	*11.85790*	*11.73749*
49	0.00000+j6.71479	7.85605	7.49505	4.52979	7.00338	*2.98229*	*2.81471*
51	0.00000+j10.72041	0.45979	1.80411	0.41735	1.08418	*0.84057*	*0.83499*
53	0.00000+j10.63721	0.60214	1.12444	0.06107	0.67638	*0.39193*	*0.41310*
55	0.00000+j10.60654	0.20493	0.23953	1.37234	2.87733	*1.45959*	*1.43362*
57	0.00000+j10.58130	1.22742	1.70792	0.67526	1.35111	*0.50094*	*0.51016*
59	0.00000+j10.47949	8.22297	8.05754	1.57119	1.32379	*2.92684*	*2.91872*
61	0.00000+j10.51298	4.50785	4.36884	0.02808	0.56786	*0.11704*	*0.12538*
63	0.00000+j10.01882	0.45924	0.24923	0.56300	0.86113	*0.34982*	*0.38072*
65	0.00000+j10.02873	2.46562	2.43303	0.43312	2.21385	*0.24423*	*0.22735*
67	0.00000+j9.66790	1.99806	1.95224	0.19857	0.36308	*0.05471*	*0.05430*
69	0.00000+j9.29818	0.21352	0.30426	1.38280	1.79119	*0.50310*	*0.55554*
71	0.00000+j9.11176	9.19339	8.87560	0.82713	2.82009	*0.30653*	*0.40366*
73	0.00000+j7.12654	2.22912	1.86067	2.80499	8.37811	*1.11803*	*1.29739*
75	0.00000+j7.39155	1.47876	0.07108	0.38823	1.74103	*1.39299*	*0.69589*
77	0.00000+j7.32055	0.27477	0.50626	1.33974	4.31891	*0.29680*	*0.26541*
79	0.00000+j7.16303	0.30693	0.73313	1.93592	4.48746	*0.07356*	*0.15173*
81	0.00000+j7.18538	4.32047	1.38029	2.48214	34.93801	*1.85610*	*2.44337*
83	0.00000+j8.69466	5.33951	5.12913	0.91276	2.92694	*0.24698*	*0.24861*
85	0.00000+j8.42575	0.77585	0.77295	0.04189	1.35156	*0.04151*	*0.03442*
87	0.00000+j8.36631	8.11091	7.97344	1.06236	1.45133	*0.04682*	*0.04295*
89	0.00000+j8.26946	12.25421	11.76283	3.01799	3.44791	*0.95127*	*0.93007*
91	0.00000+j7.85977	0.68901	0.63264	0.13708	2.66592	*0.04517*	*0.07605*
93	0.00000+j7.92387	2.08444	2.02208	0.47522	0.04472	*0.22789*	*0.23009*
95	0.00000+j8.02183	24.38815	23.87807	5.54267	2.68174	*1.51236*	*1.49638*
97	0.00000+j8.07065	7.86422	7.63426	0.22510	0.76302	*0.44966*	*0.44685*

* *The data in these columns may be inaccurate.*

Table 7.3 Single-eigenvalue-mode dominance measures for linear and second order, 1100 MW load level

		Fault at Bus 7		Fault at Bus 1		Fault at Bus 112	
k	Eigenvalue (rad/sec)	D_k	D_{2k}	D_k	D_{2k}	D_k	D_{2k}
1	0.00000+j18.04280	0.10169	0.08753	0.15108	0.14215	0.05002	0.04917
3	0.00000+j19.04213	0.31354	0.22052	0.20190	0.19813	0.02001	0.01866
5	0.00000+j15.88541	0.05725	0.06234	0.03983	0.03994	0.00893	0.00906
7	0.00000+j15.27463	0.55352	0.56134	0.24092	0.25268	0.05547	0.05690
9	0.00000+j14.47612	0.07929	0.07245	0.11369	0.10219	0.02788	0.02960
11	0.00000+j14.42804	0.06621	0.36865	0.41243	0.58369	0.11947	0.12428
13	0.00000+j13.44491	0.41625	0.42391	0.29177	0.28601	0.06376	0.06500
15	0.00000+j13.01702	0.49890	0.43388	0.46676	0.45018	0.17989	0.17957
17	0.00000+j12.31436	0.09556	0.14194	0.20332	0.18224	0.02259	0.07410
19	0.00000+j1.87957	19.93213	22.56206	20.02864	21.97030	6.15926	6.37795
21	0.00000+j2.01367	21.58592	5.51790	21.77203	5.33227	6.65041	3.11738
23	0.00000+j2.76257	21.16258	9.27982	22.03372	15.19581	6.37573	5.84874
25	0.00000+j3.01729	5.25068	3.80073	5.57269	5.49210	1.55984	1.59378
27	0.00000+j11.81480	1.37321	0.56214	0.45702	0.62093	0.33432	0.31718
29	0.00000+j11.77668	0.01396	0.02187	0.06414	0.06353	5.06017	5.02213
31	0.00000+j3.71108	0.65580	9.28436	0.70923	9.16943	0.17328	0.71900
33	0.00000+j4.01253	1.06357	7.56656	1.25243	7.13234	0.31832	2.75314
35	0.00000+j4.82883	0.76020	2.99180	1.17596	0.85071	0.22999	0.49488
37	0.00000+j5.10978	1.62461	2.62813	2.63278	3.26155	0.29892	0.38378
39	0.00000+j5.26884	3.42746	2.66472	6.52645	7.29099	0.93856	0.93133
41	0.00000+j11.39994	0.06189	0.18393	0.04647	0.01432	0.11638	0.13794
43	0.00000+j6.08005	11.59515	12.05266	12.04605	11.58493	3.23903	3.36857
45	0.00000+j11.01448	1.10051	26.13700	1.28828	22.36841	11.76092	12.92746
47	0.00000+j10.97086	0.83061	1.35735	0.40175	0.29067	5.09794	5.06223
49	0.00000+j10.72038	0.67022	2.64886	0.57665	1.17769	0.94924	0.91209
51	0.00000+j10.63350	0.55666	0.90906	0.02249	0.23644	0.43881	0.45573
53	0.00000+j10.60657	0.05229	0.14271	0.87596	1.17011	1.42625	1.42103
55	0.00000+j10.46807	8.43541	8.10980	0.88433	0.86012	2.53775	2.51422
57	0.00000+j10.58234	1.14651	6.60452	0.46001	1.24019	0.37568	0.41543
59	0.00000+j10.51326	3.59696	3.26880	0.21892	0.17010	0.73268	0.73793
61	0.00000+j10.01190	2.88940	2.56548	0.67027	0.60043	0.22154	0.23096
63	0.00000+j10.00886	1.47460	1.38786	0.19809	0.09157	0.43927	0.43759
65	0.00000+j9.30013	0.25774	0.31765	1.32292	1.20956	0.51001	0.50648
67	0.00000+j9.65714	2.18263	1.99958	0.35555	0.35863	0.04551	0.04282
69	0.00000+j6.70210	8.87603	3.44209	3.42571	1.28711	3.18347	2.82694
71	0.00000+j9.07255	9.30915	8.79873	0.58982	2.27143	0.26462	0.31434
73	0.00000+j7.10883	3.81339	3.72817	3.71663	3.67153	1.77949	1.84673
75	0.00000+j7.37801	0.63670	1.98847	0.32771	1.58639	1.41576	1.39319
77	0.00000+j7.15197	0.85458	0.92439	0.80272	0.59216	0.19523	0.20089
79	0.00000+j7.16726	4.51781	4.86937	1.51986	2.22449	1.77534	1.80175
81	0.00000+j7.31017	0.23606	1.10612	0.89887	1.26929	0.29031	0.29398
83	0.00000+j8.44006	0.47322	0.52591	0.08772	0.15158	0.04762	0.04823
85	0.00000+j8.70150	5.49776	3.27171	0.80692	0.43618	0.23625	0.21801
87	0.00000+j8.36173	6.54677	6.40969	0.73805	0.70251	0.05038	0.05328
89	0.00000+j8.25246	10.43155	14.43974	2.43845	8.23433	0.82582	1.52487
91	0.00000+j8.00468	25.80016	24.27237	3.95179	2.94323	1.50496	1.52172
93	0.00000+j8.09100	3.09895	3.01259	0.01438	0.06258	0.17249	0.17441
95	0.00000+j7.93037	1.58898	1.55210	0.25998	0.33598	0.18158	0.18133
97	0.00000+j7.92485	3.53157	3.55963	0.52893	0.43677	0.27285	0.28063

Table 7.4 Single-eigenvalue-mode dominance measures for linear and second order, 700 MW load level with damping

		Fault at Bus 7	
k	Eigenvalue (rad/sec)	D_k	D_{2k}
1	-0.10000 + j18.15318	0.19016	0.18783
3	-0.10000 + j19.05799	0.17493	0.17290
5	-0.10000 + j15.87920	0.03592	0.02843
7	-0.10000 + j15.24542	0.45090	0.39571
9	-0.10000 + j14.42336	0.08426	0.08498
11	-0.10000 + j14.34348	0.14629	0.22105
13	-0.10000 + j13.45821	0.30110	0.28712
15	-0.10000 + j12.97795	0.49759	0.45415
17	-0.10000 + j12.36983	0.15268	0.84883
19	-0.10000 + j11.83662	0.97861	0.99467
21	-0.10000 + j11.74382	0.01638	0.02705
23	-0.10000 + j1.91099	5.73236	5.30687
25	-0.10000 + j2.09163	22.37768	20.97248
27	-0.10000 + j11.39090	0.04439	0.23461
29	-0.10000 + j2.87433	17.50577	17.54298
31	-0.10000 + j3.07718	14.80076	14.20812
33	-0.10000 + j3.71044	0.78407	0.48348
35	-0.10000 + j4.00790	1.20252	7.24333
37	-0.10000 + j4.81602	0.68299	0.76447
39	-0.10000 + j5.10818	1.39524	1.73159
41	-0.10000 + j5.28110	2.67597	3.02471
43	-0.10000 + j10.95863	1.13274	1.15876
45	-0.10000 + j10.99474	1.23731	1.41410
47	-0.10000 + j6.18405	15.67044	14.20984
49	-0.10000 + j10.72124	0.37476	1.15682
51	-0.10000 + j10.63851	0.60537	0.67828
53	-0.10000 + j10.60705	0.28864	0.30405
55	-0.10000 + j10.58040	1.25509	1.13145
57	-0.10000 + j10.48225	7.64636	7.61602
59	-0.10000 + j10.51333	4.73339	4.62117
61	-0.10000 + j10.02896	0.51179	0.33973
63	-0.10000 + j10.03581	2.52941	2.14412
65	-0.10000 + j9.67241	1.89303	1.86736
67	-0.10000 + j9.29687	0.18079	0.19810
69	-0.10000 + j6.71624	7.17295	7.10411
71	-0.10000 + j9.13125	9.08872	8.15214
73	-0.10000 + j7.12982	1.61983	1.51034
75	-0.10000 + j7.17192	0.17476	0.35745
77	-0.10000 + j7.19367	4.04919	3.86936
79	-0.10000 + j7.32506	0.35937	0.30572
81	-0.10000 + j7.39823	2.03812	2.09672
83	-0.10000 + j8.68771	5.32751	5.14865
85	-0.10000 + j8.41257	1.19453	1.07539
87	-0.10000 + j8.36754	9.15839	8.95748
89	-0.10000 + j8.27688	13.25857	13.06262
91	-0.10000 + j7.81467	0.54084	0.47416
93	-0.10000 + j7.92103	1.77711	1.75963
95	-0.10000 + j8.02295	21.21749	20.97428
97	-0.10000 + j8.06530	12.44392	12.21592

The effect of damping on the dominance measures is also of interest. Tables 7.4 and 7.5 give linear and second-order dominance measures for the base-case fault at bus 7. The single-eigenvalue mode data (Table 7.4) is similar to that of Table 7.1 for the zero damping case, while the second-order two-eigenvalue data (compare Tables 7.5 and 7.6) are different. The dominant two-eigenvalue frequencies are not the same, and the dominance measures are generally larger for the case without damping (Table 7.6).

Table 7.5 Two-eigenvalue-mode dominance measures 700 MW load level, fault at bus 7 with damping (D/M = 0.2)

k	l	$\lambda_k + \lambda_l$ (rad/sec)	D_{22kl}
23	25	-0.20000 + j4.00262	4.50257
24	26	-0.20000 - j4.00262	4.50257

Table 7.6 Two-eigenvalue-mode dominance measures 700 MW load level

Fault at Bus 7				Fault at Bus 1				Fault at Bus 112			
k	l	$\lambda_k + \lambda_l$ (rad/sec)	D_{22kl}	k	l	$\lambda_k + \lambda_l$ (rad/sec)	D_{22kl}	k	l	$\lambda_k + \lambda_l$ (rad/sec)	D_{22kl}
7	18	0.0+j2.87552	5.4637	7	24	0.0+j12.3697	2.9938	1	46	0.0+j7.19436	0.8545
8	17	0.0-j2.87552	5.4637	8	23	0.0-j12.36967	2.9938	2	45	0.0-j7.19436	0.8545
17	44	0.0+j6.18538	10.523	17	44	0.0+j6.18538	2.5081	17	44	0.0+j6.18538	0.5950
18	43	0.0-j6.18538	10.523	18	43	0.0-j6.18538	2.5081	18	43	0.0-j6.18538	0.5950
21	30	0.0-j1.91515	3.5818	21	30	0.0-j1.91515	2.9027	19	21	0.0+j4.00764	0.2950
21	43	0.0+j8.27888	3.6092	21	43	0.0+j8.27888	2.1582	20	22	0.0-j4.00764	0.2950
21	90	0.0-j6.18346	4.8992	22	29	0.0+j1.91515	2.9027	21	30	0.0-j1.91515	0.9302
22	29	0.0+j1.91515	3.5818	22	44	0.0-j8.27888	2.1582	21	43	0.0+j8.27888	0.3048
22	44	0.0-j8.27888	3.6092	25	25	0.0+j6.15761	5.6267	22	29	0.0+j1.91515	0.9302
22	89	0.0+j6.18346	4.8992	26	26	0.0-j6.15761	5.6267	22	44	0.0-j8.27888	0.3049
25	25	0.0+j6.15761	6.2629	43	43	0.0+j12.3697	3.6791	25	25	0.0+j6.15761	0.4825
26	26	0.0-j6.15761	6.2629	44	44	0.0-j12.36970	3.6791	26	26	0.0-j6.15761	0.4825
43	43	0.0+j12.3697	4.9762					43	43	0.0+j12.3697	0.5970
43	90	0.0-j2.09263	5.3552					43	90	0.0-j2.09263	0.2803
44	44	0.0-j12.36970	4.9762					44	44	0.0-j12.3697	0.5970
44	89	0.0+j2.09263	5.3552					44	89	0.0+ j2.09263	0.2803

Table 7.7 Two-eigenvalue-mode dominance measures 900 MW load level

Fault at Bus 7				Fault at Bus 1				Fault at Bus 112*			
k	l	$\lambda_k + \lambda_l$ (rad/sec)	D_{22kl}	k	l	$\lambda_k + \lambda_l$ (rad/sec)	D_{22kl}	k	l	$\lambda_k + \lambda_l$ (rad/sec)	D_{22kl}
23	25	0.0+j3.97207	6.5290	11	82	0.0+j7.18715	19.506	*23*	*25*	*0.0+j3.97207*	*2.1865*
23	34	0.0-j2.10469	5.8274	12	81	0.0-j7.18715	19.506	*24*	*26*	*0.0-j3.97207*	*2.0595*
24	26	0.0-j3.97207	6.5290	25	29	0.0+j5.11359	27.482	*25*	*34*	*0.0-j1.94622*	*1.1125*
24	33	0.0+j2.10469	5.8274	25	34	0.0-j1.94622	46.421	*26*	*33*	*0.0+j1.94622*	*1.0734*
29	38	0.0-j2.06489	12.330	25	82	0.0-j5.12012	27.497	*29*	*38*	*0.0-j2.06489*	*3.2619*
30	37	0.0+j2.06489	12.330	26	30	0.0-j5.11359	27.482	*30*	*37*	*0.0+j2.06489*	*2.9970*
33	96	0.0-j4.01034	3.9217	26	33	0.0+j1.94622	46.421				
34	95	0.0+j4.01034	3.9217	26	81	0.0+j5.12012	27.497				
				29	38	0.0-j2.06489	56.115				
				30	37	0.0+j2.06489	56.115				
				39	82	0.0-j1.90524	20.886				
				40	81	0.0+j1.90524	20.886				

* *The data in these columns may be inaccurate.*

Table 7.8 Two-eigenvalue-mode dominance measures 1100 MW load level

Fault at Bus 7				Fault at Bus 1				Fault at Bus 112			
k	l	$\lambda_k + \lambda_l$ (rad/sec)	D_{22kl}	k	l	$\lambda_k + \lambda_l$ (rad/sec)	D_{22kl}	k	l	$\lambda_k + \lambda_l$ (rad/sec)	D_{22kl}
19	19	0.0+j3.75914	8.6505	19	19	0.0+j3.75914	8.2026	19	19	0.0+j3.75914	0.6913
19	21	0.0+j3.89324	4.2597	19	21	0.0+j3.89324	4.0084	19	21	0.0+j3.89324	0.6803
20	20	0.0-j3.75914	8.6505	20	20	0.0-j3.75914	8.2026	20	20	0.0-j3.75914	0.6913
20	22	0.0-j3.89324	4.2597	20	22	0.0-j3.89324	4.0084	20	22	0.0-j3.89324	0.6803
21	34	0.0-j1.99886	7.7543	21	34	0.0-j1.99886	7.0634	21	21	0.0+j4.02734	1.0821
22	33	0.0+j1.99886	7.7543	22	33	0.0+j1.99886	7.0634	21	34	0.0-j1.99886	1.5940
23	89	0.0+j11.0150	11.829	23	89	0.0+j11.0150	11.046	22	22	0.0-j4.02734	1.0821
24	90	0.0-j11.01503	11.829	24	90	0.0-j11.01503	11.046	22	33	0.0+j1.99886	1.5940
45	90	0.0+j2.76203	5.3583					23	46	0.0-j8.25191	0.6504
46	89	0.0-j2.76203	5.3583					23	89	0.0+j11.0150	0.7873
								24	45	0.0+j8.25191	0.6504
								24	90	0.0-j11.01503	0.7873

The italicized information in Tables 7.2 and 7.7 may not be accurate. Because of a convergence problem in the calculation of the inverse normal-form transformation for the initial conditions, the eigenvalue-pair dominance measures for this case were not equal (see the second-order data in Table 7.7). A similar problem was encountered for all fault cases at the 1300 MW plant A load level. The problem may be related to the size of the transformation coefficients, as well as the size of the elements of the initial condition vector.

7.2 Machine Perturbation

The perturbed machines are determined by taking the machines with angle $|O_i|$ greater than 0.3 times the maximum angle $|O_i|$. Tables 7.9-7.11 contain the linear perturbation factor data (magnitudes) for the 3 load levels (700, 900 and 1100 MW each at plant A). Three fault locations, at one load level, are presented in each table. The angle and speed $|O_i|$'s are given for each of the listed machines. As expected the unstable generator (number 27) has the largest O_i. for the plant mode cases. In the interarea mode cases, a large number of machines representing the unstable group have nearly the same sized perturbation factors.

For the second order, the perturbed machines are also determined by taking the machines with angle $|O_{2i}|$ greater than 0.3 times the maximum angle $|O_{2i}|$. Tables 7.12-7.14 contain the second-order perturbation factor data (magnitudes) for the 3 load levels (700, 900 and 1100 MW each at plant A). As in the linear case, three fault locations at each load level are presented in each table, and the angle and speed $|O_{2i}|$'s are given for each of the listed machines.

The single unstable generator (number 27) has the largest O_{2i} in the plant mode case, and the speed of machine 27 is much larger than those of the other perturbed machines. For the interarea fault at bus 7, only a few generators are included in the most perturbed groups (because of the large size of the perturbation factor for machine 43, which becomes unstable in the negative direction). The group still has similar-sized factors, but most of them are just below the cut-offs.

Table 7.9 Linear machine perturbation factors, 700 MW load level

Fault at Bus 7			Fault at Bus 1			Fault at Bus 112		
Gen	Angle $\lvert O_i \rvert$	Speed $\lvert O_i \rvert$	Gen	Angle $\lvert O_i \rvert$	Speed $\lvert O_i \rvert$	Gen	Angle $\lvert O_i \rvert$	Speed $\lvert O_i \rvert$
2	0.3431	0.4968	1	0.2462	0.6037	14	0.1944	0.6105
3	0.4173	0.9907	2	0.3156	0.5645	17	0.2469	1.2194
4	0.4042	0.8949	3	0.4367	1.3821	21	0.1893	0.5240
5	0.3790	0.5985	4	0.4221	1.2428	22	0.1881	0.5202
6	0.5296	1.1832	5	0.3820	0.8518	27	0.6261	5.7174
8	0.4353	0.9887	6	0.5532	1.6004			
9	0.3920	0.3804	7	0.2745	0.4641			
12	0.4937	1.0864	8	0.4457	1.5376			
13	0.3611	0.5637	9	0.5105	1.2121			
14	0.5584	1.4595	10	0.2200	0.2709			
15	0.4199	0.5480	12	0.5032	1.5038			
16	0.5037	1.0354	13	0.3260	0.5615			
17	0.5258	1.3333	14	0.5866	1.9859			
19	0.4682	0.7249	15	0.6042	2.0001			
20	1.0278	5.7270	16	0.5254	1.4848			
21	0.5031	0.9991	17	0.5381	1.9374			
22	0.4999	0.9839	19	0.4837	1.0172			
24	0.3578	0.4400	20	0.5466	1.8302			
25	0.3854	0.3663	21	0.5088	1.3064			
26	0.7223	3.0401	22	0.5060	1.2984			
27	0.5218	1.2891	23	0.2924	0.4762			
			24	0.3603	0.6246			
			25	0.4936	1.0791			
			26	0.4992	1.6121			
			27	0.5339	1.8845			
			33	0.1914	0.1783			
			34	0.1997	0.1853			
			35	0.2854	0.4551			

Table 7.10 Linear machine perturbation factors, 900 MW load level

Fault at Bus 7			Fault at Bus 1			Fault at Bus 112		
Gen.	Angle $\|O_i\|$	Speed $\|O_i\|$	Gen.	Angle $\|O_i\|$	Speed $\|O_i\|$	Gen.	Angle $\|O_i\|$	Speed $\|O_i\|$
2	0.3546	0.4522	1	0.2586	0.5389	12	0.1938	0.5986
3	0.4367	0.9630	2	0.3273	0.4931	14	0.2019	0.6125
4	0.4233	0.8678	3	0.4515	1.2760	17	0.2539	1.2200
5	0.3969	0.5787	4	0.4369	1.1450	21	0.1963	0.5243
6	0.5554	1.1906	5	0.3956	0.7638	22	0.1952	0.5209
8	0.4550	0.9585	6	0.5748	1.5358	27	0.6322	5.7159
9	0.4392	0.4807	7	0.2899	0.4364			
12	0.5175	1.0868	8	0.4583	1.3669			
13	0.3739	0.5292	9	0.6007	1.5762			
14	0.5850	1.4710	10	0.2337	0.2540			
15	0.4568	0.6053	12	0.5209	1.4044			
16	0.5296	1.0459	13	0.3392	0.5079			
17	0.5513	1.3457	14	0.6081	1.9093			
19	0.4935	0.7338	15	0.6499	2.0195			
20	1.0517	5.7237	16	0.5456	1.4005			
21	0.5279	1.0053	17	0.5549	1.7978			
22	0.5248	0.9906	19	0.5044	0.9581			
24	0.3751	0.4318	20	0.5653	1.7356			
25	0.4314	0.4603	21	0.5290	1.2415			
26	0.7401	2.9874	22	0.5260	1.2316			
27	0.5474	1.3029	23	0.3027	0.3946			
35	0.3156	0.3659	24	0.3727	0.5350			
			25	0.5764	1.3735			
			26	0.5160	1.5106			
			27	0.5509	1.7472			
			33	0.2007	0.1754			
			34	0.2104	0.1686			
			35	0.2960	0.3853			

Table 7.11 Linear machine perturbation factors, 1100 MW load level

Fault at Bus 7			Fault at Bus 1			Fault at Bus 112		
Gen.	Angle $\|O_i\|$	Speed $\|O_i\|$	Gen.	Angle $\|O_i\|$	Speed $\|O_i\|$	Gen.	Angle $\|O_i\|$	Speed $\|O_i\|$
2	0.3822	0.3883	1	0.2889	0.4378	6	0.1980	0.4435
3	0.4786	0.9176	2	0.3585	0.3863	12	0.2079	0.5957
4	0.4647	0.8263	3	0.4901	1.1078	14	0.2175	0.6172
5	0.4356	0.5473	4	0.4754	0.9916	16	0.1980	0.4706
6	0.6089	1.2007	5	0.4313	0.6275	17	0.2685	1.2227
8	0.4975	0.9129	6	0.6269	1.4353	20	0.1951	0.4954
9	0.5196	0.6217	7	0.3259	0.3919	21	0.2110	0.5265
12	0.5672	1.0858	8	0.4942	1.1057	22	0.2098	0.5230
13	0.4038	0.4767	9	0.7325	1.9377	27	0.6449	5.7152
14	0.6400	1.4881	10	0.2659	0.2295			
15	0.5293	0.6992	12	0.5660	1.2511			
16	0.5830	1.0616	13	0.3731	0.4264			
17	0.6039	1.3627	14	0.6607	1.7909			
19	0.5458	0.7480	15	0.7466	2.0807			
20	1.1031	5.7164	16	0.5954	1.2732			
21	0.5795	1.0150	17	0.5993	1.5849			
22	0.5763	1.0002	19	0.5547	0.8709			
23	0.3376	0.2814	20	0.6130	1.5905			
24	0.4130	0.4286	21	0.5784	1.1426			
25	0.5233	0.6557	22	0.5751	1.1293			
26	0.7808	2.9041	23	0.3312	0.2902			
27	0.5999	1.3201	24	0.4069	0.4303			
35	0.3414	0.3683	25	0.7498	1.9810			
			26	0.5599	1.3550			
			27	0.5952	1.5367			
			34	0.2370	0.1481			
			35	0.3250	0.3042			

Table 7.12 Second-order machine perturbation factors, 700 MW load level

Fault at Bus 7			Fault at Bus 1			Fault at Bus 112		
Gen.	Angle $\lvert O_{2i} \rvert$	Speed $\lvert O_{2i} \rvert$	Gen.	Angle $\lvert O_{2i} \rvert$	Speed $\lvert O_{2i} \rvert$	Gen.	Angle $\lvert O_{2i} \rvert$	Speed $\lvert O_{2i} \rvert$
20	0.7115	5.5374	3	0.3590	1.3463	17	0.2008	1.1994
25	0.3936	0.3607	4	0.3479	1.2177	27	0.6011	5.4819
26	0.4275	3.0583	5	0.3158	0.9282	43	0.3366	0.0387
43	1.2981	0.7814	6	0.4815	1.6127			
			8	0.3269	1.7001			
			9	0.4062	1.3250			
			12	0.3937	1.7683			
			14	0.4039	2.0153			
			15	0.5155	1.9678			
			16	0.3151	1.4697			
			17	0.3903	1.9126			
			19	0.3575	1.0477			
			20	0.3680	1.8151			
			21	0.3652	1.3706			
			22	0.3681	1.3666			
			25	0.3954	1.3323			
			26	0.3370	1.6444			
			27	0.3850	1.8607			
			43	0.9750	0.1407			

Table 7.13 Second-order machine perturbation factors, 900 MW load level

Fault at Bus 7			Fault at Bus 1			Fault at Bus 112		
Gen.	Angle $\|O_{2i}\|$	Speed $\|O_{2i}\|$	Gen.	Angle $\|O_{2i}\|$	Speed $\|O_{2i}\|$	*Gen.*	*Angle* $\|O_{2i}\|$	*Speed* $\|O_{2i}\|$
20	0.6248	5.3606	6	0.6906	8.0134	*6*	*0.2521*	*0.5033*
36	0.6240	0.0068	8	1.4682	23.2976	*12*	*0.2171*	*0.5955*
43	1.6838	0.6038	19	0.6501	8.6687	*14*	*0.2261*	*0.6088*
			25	0.6056	4.5139	*16*	*0.2399*	*0.5331*
			32	0.5007	2.8959	*17*	*0.2794*	*1.1309*
			37	0.5346	1.5265	*19*	*0.2674*	*0.6806*
			42	0.5154	1.1753	*20*	*0.2127*	*0.5068*
			43	0.6157	5.4090	*21*	*0.2174*	*0.5570*
			48	0.5633	4.1867	*22*	*0.2187*	*0.5513*
			49	0.4820	3.6066	*27*	*0.6684*	*5.3229*
						43	*0.2731*	*0.3727*

Table 7.14 Second-order machine perturbation factors, 1100 MW load level

Fault at Bus 7			Fault at Bus 1			Fault at Bus 112		
Gen.	Angle $\|O_{2i}\|$	Speed $\|O_{2i}\|$	Gen.	Angle $\|O_{2i}\|$	Speed $\|O_{2i}\|$	Gen.	Angle $\|O_{2i}\|$	Speed $\|O_{2i}\|$
20	0.7287	5.3583	43	1.8370	0.5159	17	0.2630	1.1427
43	1.7902	0.9117				27	0.6648	5.3128
						43	0.3915	0.0760

7.3 Contribution Factors

Contribution factors give the size of each modal oscillation in each machine state's solution. Thus there are m^2 linear contribution factors and $[m^2 + m^2(m+1)/2]$ second-order contribution factors. To illustrate the kind of information that can be obtained using contribution factors, base case data for the fault at bus 7 are presented in Tables 7.15-7.17.

Table 7.15 Linear-one-eigenvalue-mode contribution factors for fault at bus 7, base case

MC	$\lvert\sigma_{ij}\rvert$	j	$\lvert\sigma_{ij}\rvert$	j	$\lvert\sigma_{ij}\rvert$	j	$\lvert\sigma_{ij}\rvert$	j	$\lvert\sigma_{ij}\rvert$	j	$\lvert\sigma_{ij}\rvert$	j
2	0.088	21	0.058	23	0.040	43						
3	0.081	21	0.063	23	0.060	25						
4	0.080	21	0.062	23	0.060	25						
5	0.098	21	0.067	23	0.039	43	0.041	57	0.074	71	0.041	89
	0.052	95										
6	0.104	21	0.081	23	0.057	25	0.066	87	0.043	89	0.073	95
	0.031	97										
8	0.098	21	0.068	23	0.031	25	0.031	43				
9	0.108	21	0.086	23	0.058	25	0.048	43				
12	0.102	21	0.076	23	0.044	25	0.140	57	0.125	61		
13	0.091	21	0.061	23	0.046	43	0.051	71				
14	0.104	21	0.080	23	0.053	25	0.103	87	0.053	89		
15	0.108	21	0.085	23	0.226	95	0.234	97				
16	0.102	21	0.079	23	0.053	25	0.067	87	0.032	89		
17	0.100	21	0.075	23	0.046	25						
19	0.103	21	0.080	23	0.055	25	0.097	87	0.037	89		
20	0.100	21	0.075	23	0.047	25	0.048	89	0.078	95	0.040	97
21	0.105	21	0.080	23	0.051	25	0.042	43				
22	0.105	21	0.080	23	0.050	25	0.040	43	0.033	93	0.065	95
24	0.098	21	0.066	23	0.036	43	0.059	71	0.034	89	0.046	95
25	0.109	21	0.087	23	0.060	25	0.070	43	0.037	95		
26	0.097	21	0.071	23	0.042	25	0.030	43	0.032	89	0.055	95
27	0.100	21	0.075	23	0.046	25						
43	0.300	19	0.270	21								

Table 7.16 Second-order one-eigenvalue-mode contribution factors for fault at bus 7, base case

MC	$\lvert\sigma_{2ij}\rvert$	j	$\lvert\sigma_{2ij}\rvert$	j	$\lvert\sigma_{2ij}\rvert$	j	$\lvert\sigma_{2ij}\rvert$	j
20	0.123	21	0.053	25	0.077	95	0.040	97
25	0.134	21	0.068	25				
26	0.119	21	0.048	25	0.055	95		
43	0.333	21						

Table 7.17 Second-order one-eigenvalue-mode contribution factors for fault at bus 7, base case

MC	$\lvert\sigma_{22ijk}\rvert$	j, k	$\lvert\sigma_{22ijk}\rvert$	j, k	$\lvert\sigma_{22ijk}\rvert$	j, k	$\lvert\sigma_{22ijk}\rvert$	j, k
20	0.047	7,18	0.040	17,44	0.025	21,30	0.026	21,43
	0.018	21,90	0.023	25,25	0.048	43,90	0.024	95,96
25	0.054	7&18	0.095	17,44	0.044	21,90	0.059	25,25
	0.052	43,90						
26	0.045	7,18	0.041	17,44	0.025	21,30	0.018	21,43
	0.019	21,90	0.024	25,25	0.046	43,90	0.021	95,96
43	0.162	21,22	0.361	21,30	0.131	43,90		

Each table contains data for the most-perturbed machines as indicated by the machine perturbation factors (Table 7.9 and Table 7.12). For each machine the modes with the largest contribution factors (within 0.3 times maximum) are shown. In the linear case (Table 7.15) the dominant low frequency modes 21, 23 and 25 influence the group of machines. Some higher frequency modes, 89 and 95, also appear in a number of the perturbed machines. Although machine 43 is not picked up (by the linear machine perturbation factors) as being significantly perturbed, it is included in Table 7.15 to show it's link to mode 21. The contribution factors indicate that mode 19 and 21 influence machine 43, but their contributions cancel in the calculation of O_{43}.

The second-order, single-eigenvalue mode data (Table 7.16) shows results similar to the linear data. Machine 43's perturbation and mode 21's contribution to this perturbation are evident using this second-order analysis. The second-order, two-eigenvalue mode data (Table 7.17) shows the contributions of the

dominant second order modes to the perturbed machines. Machine 43 is primarily influenced by low frequency modes 21&30 and 43&90, whereas the machines of the group show these second-order low frequency modes (21&30, 7&18, and 43&90) as well as the second-order, 6.2 rad/sec modes (17&44, 25&25, and 21&90).

7.4 Summary

The following observations may be made concerning the results presented in this chapter:

7.4.1 Dominance Measures (*D*'s)

- The new dominance measures tell which frequencies dominate the system response in terms of the trajectories of the machine states.
- The size of the dominance measures in response to a given fault indicate the severity of that fault
- Comparing the size of the linear (D_k) and second-order (D_{2k} and D_{22kl}) dominance measures indicates the size of the second-order effects, thus indicating the degree of system stress. The second-order dominance measures are low for the plant mode (less stressed) cases and high for the interarea mode (stressed) cases.
- Including damping does not appear to change the size the of single-eigenvalue dominance measures (D_k and D_{2k}) significantly. The size of the two-eigenvalue modes measures is affected to a larger degree. This is one area for future work.

7.4.2 Machine Perturbation Factors (*O*'s)

- The machines with the largest O_i's agree well with the generators that become unstable in time simulations.

- The second order information (O_{2i}'s) more clearly indicate the role of machine 43 (which becomes unstable in the negative direction). The perturbation of the group is indicated by the fact that their O_{2i}'s are significant and similar in size.

7.4.3 Contributions Factors (σ's)

- The contribution factors quantify individual links between each machine state and each mode.

- The linear link between machine 43 and the group is evidenced in the contribution factors for mode 21. The second-order contribution factors indicate that modes 21&30 and 43&90 also participate in machine 43 and the group.

CHAPTER 8. MODE-MACHINE RELATIONSHIP RESULTS: FAULT-INDEPENDENT MEASURES

Before studying the mode-machine relationships, one needs to know which modes are dominant. Table 7.1 gives the linear and second-order single-eigenvalue mode dominance measures for the base case load level and for three different stub-fault locations. In the interarea-mode cases (faults at buses 1 and 7), the dominant modes are low frequency modes 21, 23, 25 and higher frequency mode 95 as indicated by the first-order dominance measures. In the plant mode case (fault at 112), the dominant modes are the high frequency modes 47 and 45.

The second-order, 700 MW-case data for the same faults is given in Table 7.6. In the interarea mode cases, the most dominant modes have a frequency around 6.2 rad/sec. Three modes, 17&44, 25&25, and 21&90, have approximately the same frequency and show up on the list of most dominant modes. There are also some dominant low frequency modes. Mode 21&30 has the lowest frequency, and modes 7&18 and 43&90 also have a low frequency. In the plant mode case, the dominance measures are quite small (compared to the corresponding linear dominance measures). A number of the second-order dominant modes are the same as those of the interarea mode cases. This indicates that these modes are still perturbed, but not enough to have a significant effect on the system response.

In this chapter, the relationships between the machine-states and the modes are investigated in three forms. First, the right eigenvector terms (both linear and second order) are presented to give a detailed picture of how the machines exhibit the oscillations of each mode. By examining the right eigenvector terms (u_{ij}'s and u_{2ijk}'s) for a mode, we can tell how that mode will be observed in the machine state oscillations. The magnitude of the element tells the size of the state oscillation, whereas the phase angle of the element tells the phase shift of the state oscillation. The second type of measure, the left eigenvectors, are utilized to determine which machines perturb which modes. By looking at modes individually, we can determine the machine-states that contribute the most to the perturbation of that mode by finding the largest left eigenvector terms (v_{ji}'s and v_{2jkl}'s) for that mode. The third type of link between modes and machine states is the participation factor. These measures are independent of

eigenvector scaling, but they combine the observability and controllability type information into a single measure of the link between each mode and each machine state.

8.1 Terms Associated with Right Eigenvectors

Tables 8.1-8.13 give linear eigenvector data. Machine states numbered 1-49 correspond with the relative machine angles, whereas states 50-98 correspond to the relative machine speeds. Thus, machine 43's angle is indicated by state number 43, while machine 43's speed is given by state number 92.

The right eigenvectors are related to observability and tell which modes are observed in which machine states. These tables give the largest (within a set of machine states) linear-eigenvector elements for selected modes. For example, Table 8.3 indicates that the largest right eigenvector element (u_{ij}) for mode 19 corresponds to machine state 92 (the speed of machine 43). The next largest state is number 43, the angle of machine 43. The other right eigenvector elements are much smaller for this mode. These observations indicate that the 1.91 rad/sec mode number 19 should be observed to a large degree in machine 43's oscillations but may not be significantly observed in the oscillations of the other machines.

Tables 8.14-8.19 give similar information for the second order modes. For example, Table 8.14 shows how the 6.185 rad/sec second-order mode 17&44 is observed in the machine states. Here the three largest states are the speeds of machines 9, 15, and 25 (the machines of plant A). Also note that these machines oscillate with a 180° phase shift with respect to the other machines in the list. This is determined by observing that the plant A machines have eigenvector element phase angles (second column of table) equal to 90°, whereas the other phase angles are -90°.

The magnitudes of the u_{ij}'s for linear mode 21 (Table 8.4) indicate that machine 43 and the group (the set of machines that becomes unstable in the positive direction for large disturbances as given in Table 3.1) both exhibit the oscillations of mode 21. Machine 43's speed oscillates in phase with the speeds of the group's machines as indicated by the second column of Table 8.4. Machine 43's angle is 180° out of phase with its speed, while the angles of the machines in

the group are 90° out of phase with their speeds in this mode. Machine 43's link is much stronger to this mode as indicated by the size of $|u_{ij}|$. The other dominant linear modes show machines of the group, but not machine 43.

The three dominant 6 rad/sec second-order modes (Tables 8.14-8.16) are linked to the machines of the group that becomes unstable in the positive direction. In each of these three modes, machines 9, 15, and 25 swing 180° out of phase with the others. These modes seem to represent oscillations within the severely perturbed group as it approaches instability. Low-frequency mode 7&18 shows up mostly in the group (all in phase), whereas low-frequency mode 43&90 shows up in machine 43 and the group (all in phase). Mode 21&30 (Table 8.19) has very nearly the same frequency as the single-eigenvalue mode 19 (strongly related to machine 43). In the right eigenvector data for mode 21&30, machine 43's speed swings with large amplitude, 180° out of phase with the speeds of the group (that also swing with sizable, nearly-equal amplitudes). The second-order information indicates that mode 21&30 causes machine 43 to swing against the group. The other links between the group and machine 43 (mode 21 and mode 43&90) cause machine 43 to swing with the group. These effects combine (depending on the dominance of the modes in question) to give the true system response.

8.2 Terms Associated with Left Eigenvectors

The left-eigenvector data of Tables 8.1-8.13 show how the modes get perturbed. The left eigenvector elements indicate which machines contribute (through being perturbed themselves) to the perturbation of a given mode. Again, the linear link between machine 43 and the group is evident in mode 21's data. In Table 8.4, the phase relationships within the group differ, but machine 43 is in phase with at least part of the group. The data for the other linear modes show how the group contributes to the perturbation of these modes.

The second-order data indicates those pairs of machines that contribute to the perturbation of a single mode. This data generally shows the contributions of the group to the mode perturbation. Machine 36 (also corresponding to state 85), appears in a large number of the machine interactions perturbing these second-order dominant modes. This machine is located at bus 128 and is not part of the

unstable group. Table 8.19 for mode 29 (29 and 30 are the same mode) shows how the interactions of machine 43 with itself, machine 36, and the members of the group perturb mode 29. Thus, machine 43, machine 36, and the group perturb mode 30, and in turn mode 21&30 perturbs the group and machine 43 (180° out of phase).

Table 8.1 Linear eigenvector elements for modal variable 7

$\|u_{ij}\|$	$\angle u_{ij}$	j	$\|vji\|$	$\angle vji$	j
0.778	0.0	51	6.875	-90.0	35
0.551	0.0	84	4.462	0.0	2
0.276	0.0	83	1.162	0.0	34
0.075	0.0	62	0.517	0.0	33
0.051	0.0	2	0.451	0.0	84
0.046	0.0	82	0.293	0.0	51
0.036	180.0	35	0.286	-90.0	39
0.023	0.0	88	0.164	-90.0	26
0.022	0.0	72	0.076	0.0	83
0.019	0.0	57	0.070	90.0	31
0.018	-90.0	34	0.065	90.0	23
0.018	0.0	75	0.063	0.0	20
0.014	0.0	66	0.048	0.0	13
0.014	0.0	76	0.037	-90.0	21

Table 8.2 Linear eigenvector elements for modal variable 17

$\|u_{ij}\|$	$\angle u_{ij}$	j	$\|vji\|$	$\angle vji$	j
0.742	0.0	72	6.825	-90.0	33
0.460	0.0	54	4.243	90.0	23
0.329	0.0	82	2.231	180.0	32
0.258	0.0	83	2.034	-90.0	34
0.203	0.0	57	1.202	90.0	37
0.088	0.0	61	0.552	0.0	82
0.060	90.0	23	0.343	0.0	72
0.051	0.0	81	0.280	180.0	38
0.039	0.0	73	0.270	-90.0	36
0.038	0.0	86	0.189	-90.0	2
0.037	0.0	5	0.180	0.0	81
0.027	0.0	33	0.170	0.0	5
0.026	0.0	66	0.167	90.0	46
0.024	0.0	76	0.164	0.0	83

Table 8.3 Linear eigenvector elements for modal variable 19

$\|u_{ij}\|$	$\angle u_{ij}$	j	$\|vji\|$	$\angle vji$	j
0.835	0.0	92	0.952	0.0	43
0.436	90.0	43	0.840	90.0	49
0.059	0.0	58	0.498	0.0	92
0.059	0.0	64	0.450	-90.0	44
0.059	0.0	74	0.439	0.0	98
0.058	0.0	70	0.400	-90.0	38
0.058	0.0	71	0.288	-90.0	36
0.057	0.0	55	0.248	90.0	42
0.057	0.0	63	0.235	0.0	93
0.057	0.0	68	0.227	180.0	45
0.056	0.0	61	0.209	0.0	87
0.056	0.0	65	0.162	-90.0	48
0.055	0.0	66	0.150	0.0	85
0.055	0.0	69	0.139	-180.0	25

Table 8.4 Linear eigenvector elements for modal variable 21

$\|u_{ij}\|$	$\angle u_{ij}$	j	$\|vji\|$	$\angle vji$	j
0.410	0.0	92	1.906	0.0	49
0.196	-180.0	43	1.288	-90.0	42
0.165	0.0	74	1.138	-90.0	44
0.164	0.0	58	0.910	0.0	98
0.163	0.0	64	0.663	-180.0	38
0.160	0.0	70	0.615	0.0	91
0.159	0.0	71	0.599	-90.0	36
0.158	0.0	55	0.543	0.0	93
0.157	0.0	63	0.436	-90.0	48
0.156	0.0	68	0.434	-180.0	43
0.155	0.0	61	0.316	0.0	87
0.155	0.0	65	0.311	-180.0	25
0.152	0.0	66	0.309	-90.0	9
0.152	0.0	69	0.286	0.0	85

Table 8.5 Linear eigenvector elements for modal variable 23

$\|u_{ij}\|$	$\angle u_{ij}$	j	$\|vji\|$	$\angle vji$	j
0.295	0.0	93	2.678	-90.0	44
0.210	0.0	74	2.400	-90.0	42
0.209	0.0	58	1.234	90.0	49
0.207	0.0	64	0.931	0.0	93
0.197	0.0	55	0.835	0.0	91
0.195	0.0	70	0.779	-180.0	38
0.194	0.0	63	0.691	-90.0	45
0.194	0.0	68	0.429	0.0	98
0.194	0.0	71	0.407	90.0	25
0.191	0.0	65	0.401	90.0	9
0.184	0.0	61	0.395	-180.0	41
0.183	0.0	69	0.368	180.0	47
0.182	0.0	66	0.346	177.1	40
0.182	0.0	76	0.292	0.0	21

Table 8.6 Linear eigenvector elements for modal variable 25

$\|u_{ij}\|$	$\angle u_{ij}$	j	$\|vji\|$	$\angle vji$	j
0.312	0.0	85	2.366	0.0	42
0.221	0.0	59	1.301	180.0	38
0.218	0.0	56	1.267	180.0	36
0.203	0.0	50	0.851	-180.0	44
0.199	0.0	81	0.768	0.0	91
0.192	0.0	60	0.452	-90.0	32
0.189	0.0	53	0.443	89.8	41
0.187	0.0	52	0.436	-180.0	47
0.186	0.0	74	0.426	179.9	45
0.183	0.0	58	0.423	0.0	87
0.181	0.0	64	0.412	0.0	85
0.179	0.0	86	0.376	0.0	25
0.177	0.0	55	0.369	-90.0	9
0.173	0.0	68	0.321	90.0	40

Table 8.7 Linear eigenvector elements for modal variable 29

$\|u_{ij}\|$	$\angle u_{ij}$	j	$\|vji\|$	$\angle vji$	j
0.418	0.0	85	2.727	-0.1	49
0.285	0.0	98	1.344	-90.0	44
0.275	0.0	89	0.914	0.0	40
0.270	0.0	97	0.820	-180.0	38
0.225	0.0	93	0.763	90.0	42
0.157	0.0	74	0.757	0.0	36
0.156	0.0	58	0.728	90.0	48
0.153	0.0	64	0.722	-180.0	45
0.148	0.0	72	0.680	0.0	98
0.147	0.0	54	0.335	0.0	93
0.147	0.0	82	0.301	179.9	47
0.146	0.0	70	0.228	0.0	89
0.145	0.0	71	0.204	0.0	87
0.145	0.0	73	0.190	0.0	91

Table 8.8 Linear eigenvector elements for modal variable 43

$\|u_{ij}\|$	$\angle u_{ij}$	j	$\|vji\|$	$\angle vji$	j
0.365	0.0	74	2.852	-180.0	25
0.263	0.0	64	2.020	180.0	9
0.249	0.0	58	1.038	90.0	35
0.240	0.0	62	1.026	0.0	21
0.217	0.0	70	0.754	180.0	45
0.208	0.0	51	0.732	90.0	33
0.208	0.0	71	0.676	90.0	20
0.207	0.0	83	0.655	-90.0	22
0.200	0.0	54	0.641	0.0	26
0.196	0.0	72	0.627	180.0	36
0.193	0.0	84	0.588	-90.0	42
0.188	0.0	73	0.529	0.0	2
0.173	0.0	61	0.522	-89.9	40
0.173	0.0	82	0.509	-90.0	47

Table 8.9 Linear eigenvector elements for modal variable 45

$\|u_{ij}\|$	$\angle u_{ij}$	j	$\|vji\|$	$\angle vji$	j
0.810	0.0	65	4.381	90.0	16
0.289	0.0	68	2.055	-90.0	27
0.223	0.0	76	1.963	90.0	17
0.220	0.0	53	1.659	0.0	19
0.213	0.0	66	1.559	-90.0	14
0.212	0.0	52	1.283	0.0	26
0.162	0.0	56	0.990	-31.5	3
0.144	0.0	63	0.795	0.0	21
0.084	0.0	54	0.583	-90.0	22
0.080	0.0	61	0.400	0.0	65
0.074	-90.0	16	0.304	-180.0	10
0.046	0.0	73	0.303	0.1	9
0.026	-90.0	19	0.277	-180.0	39
0.024	0.0	59	0.271	0.0	34

Table 8.10 Linear eigenvector elements for modal variable 47

$\|u_{ij}\|$	$\angle u_{ij}$	j	$\|vji\|$	$\angle vji$	j
0.589	0.0	76	3.798	0.0	27
0.559	0.0	66	3.618	0.0	17
0.478	0.0	65	1.970	-90.0	26
0.177	0.0	54	1.833	90.5	16
0.173	0.0	61	1.302	90.0	21
0.154	0.0	68	0.953	-180.0	22
0.095	0.0	73	0.628	-90.0	19
0.054	0.0	27	0.457	-90.0	34
0.051	0.0	17	0.440	90.0	39
0.047	0.0	63	0.439	-90.0	9
0.043	180.0	16	0.385	90.0	20
0.043	0.0	75	0.345	0.0	76
0.038	0.0	53	0.329	0.0	66
0.036	0.0	52	0.313	90.0	25

Table 8.11 Linear eigenvector elements for modal variable 89

$\|u_{ij}\|$	$\angle u_{ij}$	j	$\|vji\|$	$\angle vji$	j
0.370	0.0	63	5.735	0.0	45
0.331	0.0	69	5.196	-180.0	47
0.298	0.0	55	1.709	-90.0	46
0.288	0.0	72	1.692	0.0	38
0.283	0.0	54	1.369	90.0	20
0.259	0.0	68	1.294	-180.0	33
0.237	0.0	73	0.864	90.0	18
0.223	0.0	75	0.852	0.0	26
0.218	0.0	65	0.764	-90.0	39
0.202	0.0	95	0.753	0.0	40
0.200	0.0	82	0.693	0.0	94
0.193	0.0	96	0.628	0.0	96
0.171	0.0	67	0.540	90.0	36
0.162	0.0	88	0.518	-90.2	32

Table 8.12 Linear eigenvector elements for modal variable 95

$\|u_{ij}\|$	$\angle u_{ij}$	j	$\|vji\|$	$\angle vji$	j
0.751	0.0	64	4.318	-90.0	45
0.260	0.0	69	2.743	-90.0	47
0.243	0.0	55	2.654	-90.0	20
0.218	0.0	71	1.894	0.0	26
0.184	0.0	75	1.844	-90.0	46
0.174	0.0	72	1.612	0.0	15
0.172	0.0	54	1.361	180.0	25
0.152	0.0	73	1.290	-180.0	33
0.139	0.0	82	1.256	-90.0	38
0.123	0.0	74	1.184	90.0	22
0.113	0.0	95	1.071	-180.0	39
0.107	0.0	88	0.916	90.0	9
0.106	0.0	83	0.637	-90.0	18
0.097	0.0	57	0.620	180.0	48

Table 8.13 Linear eigenvector elements for modal variable 97

$\|u_{ij}\|$	$\angle u_{ij}$	j	$\|vji\|$	$\angle vji$	j
0.923	0.0	64	4.502	90.0	45
0.158	0.0	69	2.969	-118.7	47
0.124	0.0	55	2.762	-90.0	15
0.114	-90.0	15	2.368	-90.0	20
0.112	0.0	75	1.824	90.0	46
0.105	0.0	71	1.696	180.0	26
0.099	0.0	72	1.410	-90.0	25
0.097	0.0	54	1.046	90.0	33
0.086	0.0	73	1.031	-180.0	38
0.079	0.0	82	1.023	90.0	39
0.076	0.0	95	0.793	-90.0	22
0.070	0.0	88	0.674	-180.0	18
0.061	0.0	83	0.558	0.0	94
0.056	0.0	70	0.514	0.0	42

Table 8.14 Second-order eigenvector elements for modal variable 17&44

u_2's for modal variable 17&44 (6.185 rad/sec)			v_2's for modal variable 17 (12.370 rad/sec)			v_2's for modal variable 43 (6.185 rad/sec)		
$\lvert u_{2ijk} \rvert$	$\angle u_{2ijk}$	State	$\lvert v_{2ijk} \rvert$	$\angle v_{2ijk}$	States	$\lvert v_{2ijk} \rvert$	$\angle v_{2ijk}$	States
1.0471	90.0	74	1.4752	0.0	58&74	0.1492	0.0	85&85
0.7546	90.0	64	1.0419	0.0	74&74	0.0656	180.0	58&85
0.7152	90.0	58	0.7533	180.0	70&74	0.0641	180.0	74&85
0.6227	-90.0	70	0.5392	180.0	58&70	0.0531	0.0	58&69
0.5969	-90.0	71	0.5222	0.0	58&58	0.0494	180.0	70&85
0.4497	-90.0	75	0.4981	180.0	69&74	0.0423	180.0	69&85
0.4367	-90.0	69	0.4809	180.0	71&74	0.0370	0.0	74&75
0.4327	-90.0	55	0.4708	180.0	74&75	0.0368	0.0	58&75
0.3815	-90.0	63	0.4588	0.0	74&85	0.0358	180.0	75&85
0.3634	-90.0	65	0.3462	180.0	58&69	0.0335	0.0	70&75
0.3628	-90.0	76	0.3445	180.0	58&71	0.0332	180.0	71&85
0.3622	-90.0	66	0.3341	180.0	58&75	0.0262	0.0	69&75

Table 8.15 Second-order eigenvector elements for modal variable 25&25

u_2's for modal variable 25&25 (6.158 rad/sec)			v_2's for modal variable 25 (3.079 rad/sec)		
$\lvert u_{2ijk} \rvert$	$\angle u_{2ijk}$	State	$\lvert v_{2ijk} \rvert$	$\angle v_{2ijk}$	States
0.2896	-90.0	74	0.0228	0.0	58&74
0.2105	-90.0	64	0.0164	0.0	69&74
0.2012	-90.0	58	0.0163	0.0	70&74
0.1610	90.0	70	0.0118	0.0	69&70
0.1545	90.0	71	0.0108	0.0	71&74
0.1187	90.0	75	0.0099	180.0	85&85
0.1141	90.0	69	0.0088	180.0	70&70
0.1086	90.0	55	0.0079	0.0	74&85
0.0964	90.0	63	0.0076	180.0	66&71
0.0940	90.0	76	0.0075	0.0	58&85
0.0938	90.0	66	0.0068	180.0	69&69
0.0914	90.0	65	0.0067	180.0	69&75

Table 8.16 Second-order eigenvector elements for modal variable 21&90

u_2's for modal variable 21&90 (6.183 rad/sec)			v_2's for modal variable 21 (2.094 rad/sec)			v_2's for modal variable 89 (8.277 rad/sec)		
$\lvert u_{2ijk} \rvert$	$\angle u_{2ijk}$	State	$\lvert v_{2ijk} \rvert$	$\angle v_{2ijk}$	States	$\lvert v_{2ijk} \rvert$	$\angle v_{2ijk}$	States
0.2561	90.0	74	0.9290	0.0	74&85	0.0825	180.0	58&74
0.1840	90.0	64	0.8962	0.0	58&85	0.0636	180.0	70&74
0.1749	90.0	58	0.8944	0.0	85&85	0.0590	180.0	69&74
0.1529	-90.0	70	0.6120	0.0	70&85	0.0423	180.0	71&74
0.1468	-90.0	71	0.5830	0.0	69&85	0.0419	180.0	74&74
0.1096	-90.0	75	0.5344	0.0	75&85	0.0300	0.0	58&70
0.1092	-90.0	55	0.4091	0.0	71&85	0.0296	180.0	58&58
0.1052	-90.0	69	0.2139	0.0	58&69	0.0237	180.0	74&85
0.0906	-90.0	63	0.1848	0.0	74&75	0.0230	180.0	58&85
0.0893	-90.0	76	0.1683	0.0	55&85	0.0225	0.0	69&70
0.0891	-90.0	66	0.1403	0.0	64&85	0.0191	0.0	58&71
0.0879	-90.0	65	0.1380	0.0	58&75	0.0183	0.0	74&75

Table 8.17 Second-order eigenvector elements for modal variable 7&18

u_2's for modal variable 7&18 (2.876 rad/sec)			v_2's for modal variable 7 (15.246 rad/sec)			v_2's for modal variable 17 (12.370 rad/sec)		
$\lvert u_{2ijk} \rvert$	$\angle u_{2ijk}$	State	$\lvert v_{2ijk} \rvert$	$\angle v_{2ijk}$	States	$\lvert v_{2ijk} \rvert$	$\angle v_{2ijk}$	States
0.2260	90.0	74	0.0231	180.0	58&64	1.4752	0.0	58&74
0.2241	90.0	58	0.0169	0.0	58&69	1.0419	0.0	74&74
0.2222	90.0	64	0.0122	180.0	55&71	0.7533	180.0	70&74
0.2116	90.0	55	0.0118	0.0	58&75	0.5392	180.0	58&70
0.2100	90.0	70	0.0105	0.0	58&74	0.5222	0.0	58&58
0.2090	90.0	71	0.0097	0.0	55&70	0.4981	180.0	69&74
0.2089	90.0	63	0.0090	180.0	74&75	0.4809	180.0	71&74
0.2051	90.0	65	0.0064	180.0	70&74	0.4708	180.0	74&75
0.1966	90.0	69	0.0056	180.0	58&70	0.4588	0.0	74&85
0.1959	90.0	66	0.0053	180.0	58&71	0.3462	180.0	58&69
0.1959	90.0	76	0.0049	180.0	74&74	0.3445	180.0	58&71
0.1857	90.0	75	0.0045	180.0	71&74	0.3341	180.0	58&75

Table 8.18 Second-order eigenvector elements for modal variable 43&90

u_2's for modal variable 43&90 (2.093 rad/sec)			v_2's for modal variable 43 (6.185 rad/sec)			v_2's for modal variable 89 (8.277 rad/sec)		
$\lvert u_{2ijk} \rvert$	$\angle u_{2ijk}$	State	$\lvert v_{2ijk} \rvert$	$\angle v_{2ijk}$	States	$\lvert v_{2ijk} \rvert$	$\angle v_{2ijk}$	States
0.7008	90.0	92	0.1492	0.0	85&85	0.0825	180.0	58&74
0.2804	90.0	74	0.0656	180.0	58&85	0.0636	180.0	70&74
0.2794	90.0	58	0.0641	180.0	74&85	0.0590	180.0	69&74
0.2771	90.0	64	0.0531	0.0	58&69	0.0423	180.0	71&74
0.2707	90.0	70	0.0494	180.0	70&85	0.0419	180.0	74&74
0.2700	90.0	71	0.0423	180.0	69&85	0.0300	0.0	58&70
0.2682	90.0	55	0.0370	0.0	74&75	0.0296	180.0	58&58
0.2663	90.0	63	0.0368	0.0	58&75	0.0237	180.0	74&85
0.2623	90.0	65	0.0358	180.0	75&85	0.0230	180.0	58&85
0.2582	90.0	76	0.0335	0.0	70&75	0.0225	0.0	69&70
0.2582	90.0	66	0.0332	180.0	71&85	0.0191	0.0	58&71
0.2575	90.0	69	0.0262	0.0	69&75	0.0183	0.0	74&75

Table 8.19 Second-order eigenvector elements for modal variable 21&30

u_2's for modal variable 21&30 (1.915 rad/sec)			v_2's for modal variable 21 (2.094 rad/sec)			v_2's for modal variable 29 (4.009 rad/sec)		
$\lvert u_{2ijk} \rvert$	$\angle u_{2ijk}$	State	$\lvert v_{2ijk} \rvert$	$\angle v_{2ijk}$	States	$\lvert v_{2ijk} \rvert$	$\angle v_{2ijk}$	States
9.2812	-90.0	92	0.9290	0.0	74&85	5.1770	0.0	92&92
0.7046	90.0	74	0.8962	0.0	58&85	3.1462	180.0	85&92
0.7026	90.0	58	0.8944	0.0	85&85	2.1258	180.0	85&85
0.6979	90.0	64	0.6120	0.0	70&85	2.0540	180.0	74&85
0.6837	90.0	70	0.5830	0.0	69&85	2.0458	180.0	58&85
0.6818	90.0	71	0.5344	0.0	75&85	1.6024	180.0	70&85
0.6753	90.0	55	0.4091	0.0	71&85	1.5195	180.0	74&92
0.6740	90.0	63	0.2139	0.0	58&69	1.5134	180.0	58&92
0.6635	90.0	65	0.1848	0.0	74&75	1.5026	180.0	69&85
0.6538	90.0	76	0.1683	0.0	55&85	1.3797	180.0	75&85
0.6538	90.0	66	0.1403	0.0	64&85	1.1853	180.0	70&92
0.6535	90.0	69	0.1380	0.0	58&75	1.1116	180.0	69&92

Table 8.20 v_2's for modal variable 95

$\|v_{2ijk}\|$	$\angle v_{2ijk}$	States
0.0098	180.0	69&69
0.0071	180.0	85&85
0.0060	180.0	75&75
0.0059	180.0	69&75
0.0050	180.0	58&74
0.0049	0.0	69&71
0.0041	0.0	58&85
0.0038	180.0	70&74
0.0037	180.0	58&69
0.0037	0.0	70&85
0.0036	0.0	74&85
0.0031	180.0	64&64
0.0030	0.0	69&70
0.0030	0.0	71&71

8.3 Participation Factors

Tables 8.21-8.32 contain the largest participation factors for certain machines near plants A and B and for machine 43. The odd numbered tables give the single-eigenvalue-mode participation factors (linear and second order). The even numbered tables present the second-order participation factors for the two-eigenvalue modes. Looking at these factors for a single machine, one can see the modes that are most closely linked to that machine. It does not tell whether or not that mode is actually perturbed. The mode dominance measures are used to determine those modes that are of concern.

For the linear case, modes 21, 23, and 25 were seen to dominate in the interarea mode cases. In the participation factor tables, these modes show up in most of the machines given with factors in the range of 0.1-0.3. Note that machine 43 (corresponding to bus 137) participates strongly in mode 21. This is one indicator of a link between the unstable group and this machine that becomes unstable in the negative direction. The sign of the participation factors is the same, indicating that machine 43 should swing in phase with the group.

Table 8.21 Single-eigenvalue participation factors for generator 9

Linear Participation			Second Order Participation		
$\lvert p_{ij} \rvert$	$\angle p_{ij}$	Mode	$\lvert p_{2ij} \rvert$	$\angle p_{2ij}$	Mode
0.1753	0.0	75	0.1808	-0.9	75
0.1144	0.0	77	0.1146	-0.1	77
0.0814	0.0	43	0.0519	-1.9	43
0.0291	0.0	23	0.0271	-2.5	23
0.0243	0.0	21	0.0219	0.4	25
0.0219	0.0	25	0.0210	-0.9	73
0.0208	0.0	73	0.0201	-2.6	21
0.0120	0.0	39	0.0126	-3.9	39
0.0102	0.0	95	0.0102	0.8	95
0.0043	0.0	19	0.0089	-123.2	29
0.0022	0.0	49	0.0022	0.4	49
0.0021	0.0	29	0.0009	-8.2	35
0.0010	0.0	35	0.0006	-42.0	19
0.0006	0.0	81	0.0006	1.1	81
0.0005	0.0	79	0.0005	3.0	79

Table 8.22 Two-eigenvalue participation factors for generator 9

$\lvert p_{22ij} \rvert$	$\angle p_{22ij}$	Mode
0.0292	-3.2	17&44
0.0292	3.2	18&43
0.0099	45.4	19&21
0.0099	-45.4	20&22
0.0054	175.9	11&76
0.0054	-175.9	12&75
0.0049	30.6	21&30
0.0049	-30.6	22&29
0.0029	-8.8	19&30
0.0029	8.8	20&29
0.0029	90.8	25&25
0.0029	-90.8	26&26
0.0027	-93.8	39&78
0.0027	93.8	40&77
0.0021	-0.8	7&18

Table 8.23 Single-eigenvalue participation factors for generator 20

Linear Participation			Second Order Participation		
$\lvert p_{ij} \rvert$	$\angle p_{ij}$	Mode	$\lvert p_{2ij} \rvert$	$\angle p_{2ij}$	Mode
0.0860	0.0	95	0.0860	-1.7	95
0.0850	0.0	57	0.0850	-0.9	57
0.0710	0.0	61	0.0709	-1.5	61
0.0548	0.0	89	0.0542	0.3	89
0.0465	0.0	97	0.0465	-1.7	97
0.0285	0.0	71	0.0284	-1.5	71
0.0216	0.0	83	0.0216	-1.6	83
0.0168	0.0	23	0.0168	-3.0	23
0.0166	0.0	43	0.0164	-1.6	87
0.0164	0.0	87	0.0155	8.7	21
0.0162	0.0	21	0.0151	7.6	43
0.0111	0.0	25	0.0112	-4.8	25
0.0085	0.0	67	0.0085	-1.6	67
0.0043	0.0	65	0.0051	-85.1	29
0.0037	0.0	51	0.0044	-2.0	65

Table 8.24 Two-eigenvalue participation factors for generator 20

$\lvert p_{22ij} \rvert$	$\angle p_{22ij}$	Mode
0.0049	83.2	19&21
0.0049	-83.2	20&22
0.0027	3.8	21&30
0.0027	-3.8	22&29
0.0020	-73.7	21&43
0.0020	73.7	22&44
0.0020	2.3	17&44
0.0020	-2.3	18&43
0.0018	98.4	21&90
0.0018	-98.4	22&89
0.0014	-20.4	19&30
0.0014	20.4	20&29
0.0007	-88.7	25&79
0.0007	88.7	26&80
0.0007	-99.6	25&25

Table 8.25 Single-eigenvalue participation factors for generator 21

Linear Participation			Second Order Participation		
$\lvert p_{ij} \rvert$	$\angle p_{ij}$	Mode	$\lvert p_{2ij} \rvert$	$\angle p_{2ij}$	Mode
0.1880	0.0	93	0.1879	-1.4	93
0.1443	0.0	79	0.1441	-1.7	79
0.0360	0.0	43	0.0292	1.0	43
0.0199	0.0	23	0.0196	-4.6	23
0.0183	0.0	21	0.0172	-1.8	49
0.0172	0.0	49	0.0168	-2.7	77
0.0167	0.0	77	0.0163	-7.8	21
0.0157	0.0	73	0.0158	-1.8	73
0.0132	0.0	25	0.0134	-5.3	25
0.0046	0.0	95	0.0063	-98.9	29
0.0041	0.0	39	0.0046	-0.1	95
0.0038	0.0	71	0.0041	10.2	39
0.0033	0.0	19	0.0039	-1.7	71
0.0031	0.0	97	0.0033	-31.8	57
0.0031	0.0	47	0.0031	-0.2	97

Table 8.26 Two-eigenvalue participation factors for generator 21

$\lvert p_{22ij} \rvert$	$\angle p_{22ij}$	Mode
0.0070	-5.2	17&44
0.0070	5.2	18&43
0.0063	68.5	19&21
0.0063	-68.5	20&22
0.0030	1.1	21&30
0.0030	-1.1	22&29
0.0019	82.9	25&79
0.0019	-82.9	26&80
0.0017	-4.8	19&30
0.0017	4.8	20&29
0.0013	86.9	79&93
0.0013	-86.9	80&94
0.0012	-100.7	25&25
0.0012	100.7	26&26
0.0009	87.2	93&93

Table 8.27 Single-eigenvalue participation factors for generator 25

Linear Participation			Second Order Participation		
$\lvert p_{ij} \rvert$	$\angle p_{ij}$	Mode	$\lvert p_{2ij} \rvert$	$\angle p_{2ij}$	Mode
0.1683	0.0	43	0.0947	-0.4	75
0.0930	0.0	75	0.0917	-1.8	43
0.0661	0.0	77	0.0664	-1.2	77
0.0297	0.0	23	0.0255	-1.3	23
0.0245	0.0	21	0.0239	-0.3	49
0.0239	0.0	49	0.0227	1.2	25
0.0227	0.0	25	0.0210	-1.8	21
0.0209	0.0	95	0.0209	0.1	95
0.0194	0.0	73	0.0193	-0.8	73
0.0135	0.0	39	0.0136	1.7	39
0.0094	0.0	97	0.0094	-1.8	97
0.0043	0.0	19	0.0077	-72.8	29
0.0022	0.0	29	0.0010	-7.1	35
0.0010	0.0	35	0.0006	-111.7	89
0.0006	0.0	81	0.0006	-0.9	81

Table 8.28 Two-eigenvalue participation factors for generator 25

$\lvert p_{22ij} \rvert$	$\angle p_{22ij}$	Mode
0.0760	-2.2	17&44
0.0760	2.2	18&43
0.0072	91.5	19&21
0.0072	-91.5	20&22
0.0044	-19.0	21&30
0.0044	19.0	22&29
0.0043	92.4	25&25
0.0043	-92.4	26&26
0.0043	-5.3	7&18
0.0043	5.3	8&17
0.0018	175.6	11&76
0.0018	-175.6	12&75
0.0018	92.9	39&78
0.0018	-92.9	40&77
0.0018	-13.9	19&30

Table 8.29 Single-eigenvalue participation factors for generator 26

Linear Participation			Second Order Participation		
$\lvert p_{ij} \rvert$	$\angle p_{ij}$	Mode	$\lvert p_{2ij} \rvert$	$\angle p_{2ij}$	Mode
0.1547	0.0	61	0.1547	-1.1	61
0.1341	0.0	57	0.1339	-1.6	57
0.0434	0.0	95	0.0434	-1.4	95
0.0235	0.0	97	0.0236	-1.5	97
0.0229	0.0	89	0.0227	1.2	89
0.0193	0.0	51	0.0193	-1.0	51
0.0162	0.0	43	0.0148	4.4	43
0.0143	0.0	21	0.0140	-3.9	23
0.0141	0.0	23	0.0127	5.0	21
0.0088	0.0	25	0.0089	-3.0	25
0.0077	0.0	47	0.0077	-0.9	47
0.0076	0.0	87	0.0076	-1.1	87
0.0055	0.0	83	0.0055	-1.6	83
0.0047	0.0	31	0.0048	-88.1	29
0.0032	0.0	59	0.0047	-1.6	31

Table 8.30 Two-eigenvalue participation factors for generator 26

$\lvert p_{22ij} \rvert$	$\angle p_{22ij}$	Mode
0.0047	83.4	19&21
0.0047	-83.4	20&22
0.0024	93.2	43&90
0.0024	-93.2	44&89
0.0022	3.1	21&30
0.0022	-3.1	22&29
0.0017	1.3	17&44
0.0017	-1.3	18&43
0.0017	-13.4	19&30
0.0017	13.4	20&29
0.0011	-80.6	21&43
0.0011	80.6	22&44
0.0010	93.7	21&90
0.0010	-93.7	22&89
0.0010	79.8	25&79

Table 8.31 Single-eigenvalue participation factors for generator 43

Linear Participation			Second Order Participation		
$\lvert p_{ij} \rvert$	$\angle p_{ij}$	Mode	$\lvert p_{2ij} \rvert$	$\angle p_{2ij}$	Mode
0.4153	0.0	19	0.4105	5.6	19
0.0849	0.0	21	0.0036	99.6	27
0.0006	0.0	35	0.0014	-45.8	35
0.0003	180.0	23	0.0013	-170.9	21
0.0002	180.0	39	0.0007	137.6	39
0.0002	0.0	91	0.0004	-133.2	23
0.0001	180.0	37	0.0003	-156.1	49
0.0001	180.0	49	0.0003	111.4	29
0.0001	180.0	29	0.0003	136.8	37
0.0001	0.0	27	0.0002	-133.5	77
0.0001	-180.0	81	0.0002	1.3	91
0.0000	-180.0	77	0.0001	155.1	81
0.0000	-180.0	25	0.0000	-148.1	25
0.0000	-180.0	73	0.0000	-141.7	75
0.0000	180.0	43	0.0000	164.0	73

Table 8.32 Two-eigenvalue participation factors for generator 43

$\lvert p_{22ij} \rvert$	$\angle p_{22ij}$	Mode
0.0877	-15.7	19&30
0.0877	15.7	20&29
0.0381	-78.8	19&19
0.0381	78.8	20&20
0.0022	-4.0	19&28
0.0022	4.0	20&27
0.0018	104.7	19&21
0.0018	-104.7	20&22

Machine 43 very strongly participates in the lowest-frequency-mode (mode 19), which also has sizable dominance measures in Table 3.1. A number of the group of machines are seen to participate in the higher-frequency mode 95.

The second-order participation factors also show correlations between the perturbed group and the dominant, second-order modes. Generators 9 and 25 (the plant A machines) participate strongly in mode 17&44, which is one of the 6 rad/sec modes. Other machines of the group also participate in this mode but to a lesser extent. The other 6 rad/sec modes also show up in the group; mode 25&25 is stronger than mode 21&90. Machine 43 does not participate strongly in these 6 rad/sec modes. The 4.0 rad/sec mode (mode 19&21) shows up in the group as well as machine 43, but does not appear dominant in the interarea mode cases. The 1.9 rad/sec mode (mode 21&30) shows up in the group of machines, but is not in machine 43' s dominant list. The other dominant, low-frequency modes show up in some of the members of the group.

8.4 Summary

The following observations may be made concerning the results presented in this chapter:

8.4.1 Right Eigenvectors (u's)

- Right-eigenvector data shows the relationship (magnitude and phase) of each machine to each mode (independent of fault location).

- Second-order data shows that some of the dominant modes cause out-of-phase swings between the perturbed machines. The linear modes of the same frequency show in-phase relationships. In particular, low frequency mode 21&30 shows out-of-phase swings between machine 43 and the group of machines that becomes unstable in the positive direction. The linear mode of the same frequency is primarily linked to machine 43 alone. Three second-order 6.19 rad/sec modes show out-of-phase swings between plant A and the rest of the unstable group. The 6.19 rad/sec linear mode shows in-phase oscillations of the group.

8.4.2 Left Eigenvectors (v's)

- Left-eigenvector information shows which machines perturb which modes.
- The second-order data shows machine 43's perturbation of the modes that affect the unstable generators. Linear data indicates only a weak connection through mode 21.
- The second-order data also indicates that machine 36 contributes significantly to the oscillations of the "problem modes."

8.4.3 Participation Factors (p's)

- Participation factors provide a single link between the machines and modes. Both left and right-eigenvector information is imbedded in the participation factors.
- They show the strong links between mode 21&30 and the 6.19 rad/sec modes and the machines of the group.

CHAPTER 9. APPLICATION RESULTS: OVERVIEW OF APPLYING METHOD TO A POWER SYSTEM

9.1 System Characteristics

Through the application of this analysis to the 50-generator IEEE test system, the following summary of system characteristics can be made:

1. Dominant modes

   In the plant mode cases, two linear modes with frequencies of approximately 11.0 rad/sec dominate the system response (e.g., modes 47 and 45 of Table 7.1). Even for the stressed cases, the second-order dominance measures are quite small (last column of Table 7.8). Thus, for the plant modes cases, the second-order interactions do not significantly affect the response.

   In the interarea mode cases a number of low-frequency, first-order modes appear (e.g., modes 21, 23, and 25 of Table. 7.1). A couple of higher frequency linear modes (6.2 and 8.0 rad/sec) modes are also sizable. There are also a number of dominant, second-order, low-frequency modes with frequencies similar to those of the single-eigenvalue modes (see modes 21&30, 7&18 and 43&90 in Table 7.6). These second-order interactions produce dominant oscillation frequencies very close to the dominant linear frequencies. Three 6.2 rad/sec second-order modes also dominate the system response (modes 17&44, 21&90, and 25&25 in Table 7.6). These second-order interactions produce large oscillations at higher frequencies that also dominate the system response.

2. Severely affected machines.

   In the plant mode cases (faults at bus 112), the linear machine-state perturbation factors predict the perturbed machines well. The second-order factors change the analysis very little, but does eliminate a few less-severely affected machines (for example, compare the last three columns of Tables 7.9 and 7.12).

In the interarea mode cases, the linear perturbation factors also predict those machines that are a part of the large unstable group. Second-order factors pick out machine 43's perturbation, as well as indicating that there is a large group with nearly equal factors. This information predicts the type of mode by predicting how many machines are affected. The information is also useful in determining which machines to investigate further in order to attempt to control the dominant modes.

For both mode types the contribution factors give a clear picture of how the dominant modes, both linear and second order, influence the machine states for a given fault case (see Tables 7.14-7.16).

3. Mode-machine state relationships (independent of fault location).

The low-frequency modes, both the single-eigenvalue modes and the modes resulting from the sums of two eigenvalues, seem to be linked to oscillations of the group and machine 43. The single-eigenvalue modes and two of the low-frequency two-eigenvalue modes exhibit in phase oscillations of the group and machine 43. One two-eigenvalue low-frequency mode (1.91 rad/sec) indicates out-of-phase relationships between machine 43 and the group.

Machine 36, appears in a large number of the machine interactions perturbing the dominant modes resulting from sums of two eigenvalues. Machine 43, machine 36, and the group perturb mode 30, and in turn mode 21&30 perturbs the group and machine 43 (180° out of phase).

The higher-frequency single-eigenvalue modes are typically related to a single or small group of machines. Three 6.2 rad/sec two-eigenvalue modes indicate out-of-phase relationships between three machines of the unstable group and the rest of the machines of the group. Because they cause large angle differences between groups of machines, these out-of-phase swings indicate that large amounts of energy is transferred between the out-of-phase groups of machines.

9.2 Significance of Second-Order Effects

The significant second-order effects include:

- Time simulations indicate significantly increased accuracy because of including second-order terms.
- Time simulations also illustrate the link between system nonlinearity and stress due because of fault location.
- Large second-order dominance measures observed measure system stress as revealed by system nonlinearity.
- Right eigenvectors show out-of-phase relationships between machines. These relationships are not seen in the linear data.
- Second-order analysis shows stronger links between machine 43 and the group that becomes unstable in the positive direction.
- The participation factors show the strong links (related to both controllability and observability) between dominant modes resulting from sums of two eigenvalues and the machines of the group.

CHAPTER 10. CONCLUSIONS

In this research, the normal forms of vector fields are applied to characterize the transient response of stressed power systems. The significance of this work is that it includes second-order effects on system performance in a form similar to the linear concept of modal oscillations. Thus, in stressed system conditions, when system behavior is not explained using linear analysis, the existing linear methods of control design and placement can be adapted to account for second-order effects. In this manner, the range of usefulness of the existing methods has been extended by this analysis.

The original results of this research were reported in Chapters 6-9. The theory, analysis, data, and observations presented can be summarized as follows:

1. Significance of first, second and third-order terms: The simulation study illustrates the effects of including linear, second-order, and third-order terms in time simulations of a stressed system's response to a large disturbance. This study verifies the close relationship between stress and system nonlinearity. The linear system gives the basic modal picture, but becomes inaccurate for large disturbances and for interarea-type faults (stressed conditions). The second order system captures significantly more modal information than the linear system, and the third order system is more indicative of stability behavior. This dissertation focuses on utilizing the second-order information for system analysis because of the promise shown by the second-order system and because of the computational effort required to analyze the third-order system.

2. Second-order normal-form approximation: The second-order normal-form solutions have the same stability properties as the linear system (assuming no resonances occur). This is in contrast to observations made in some of the time simulation cases analyzed in the preliminary study. Some of the second-order terms present in the Taylor series expression are transformed into third-order and fourth-order terms in the second-order normal form system. When the higher-order terms of this normal form are neglected, some of the second-order Taylor series effects are lost. The significance of these higher-order normal-form terms is yet to be determined.

3. Measures of system stress: Near resonance of the system eigenvalues can cause wide variations in the size of the normal-form transformation coefficients

(h_{2ijk}'s). This variation does not appear to be linked to system stress. When uniform damping is included, the transformation coefficients become more uniform. The measures based on solutions are less sensitive to resonances because they depend on both the transformation and the inverse transformation. Comparing the relative size of the second-order and linear dominance measures indicates importance of the nonlinearities in the system as a whole. Thus the dominance measures provide a measure of system stress.

4. Near resonances: Although resonance does not appear to be directly related to stress, it is still unclear whether it represents a physical or a mathematical phenomenon. Near resonance conditions result in second-order oscillations that have nearly the same frequency as the linear modes. Thus, in a time simulation of the full system, an observed frequency may actually be caused by second-order interactions of modes. These second-order modes are transferred to the machine states in the same manner as the linear frequencies, but originate from the second-order interaction between the linear system modes.

5. Second-order modal analysis: The linear concept of modes is preserved in this analysis. Second-order analysis indicates that many more frequencies of oscillation may have a significant influence on the system response. These additional frequencies result from second-order interactions and have been referred to as second-order modes. By using the familiar concept of modal analysis, this work extends the linear theory and methods to include second-order information. Thus the results of the analysis are in a form that is readily adaptable to existing applications of power system design and control.

6. Solution-based measures of system performance: This work develops measures of system performance based on the actual system trajectories (solutions). The tool used for determining these solutions is the second-order normal-form transformation. The fault-dependent measures of system performance provide a means of quantifying the system's response to a given disturbance Because these measures are based on the solutions, they are independent of eigenvector scaling. For example, the new dominance measures indicate those modes that appear in the motions of the machines in the system. This is in contrast to the existing method that determines modal dominance based on the size to the mode's oscillations in the Jordan form of the system

(which depends on the scaling of the system eigenvectors). The dominance measures and machine perturbation factors are also used to "narrow down" the lists of important modes and machines, which may then be analyzed in detail using a reduced set of contribution factors.

7. Fault independent measures of system response: The fault-independent measures are introduced for use in the location and design of controls. The proposed second-order right and left eigenvectors can be used in a manner similar to their linear counterparts. The right-eigenvector elements give the size and phase relationship of each machine state to each mode. This information is useful in determining those states that should be used as control inputs when attempting to damp a given mode, because it indicates the state where the mode is most observable. The phase relationships indicated by the right eigenvectors may indicate the significance of a given mode by flagging out-of-phase system oscillations that can lead to energy exchanges between machines and groups of machines. Left-eigenvector elements tell how machine perturbations are translated into mode perturbation. This is useful in determining control outputs (i.e., which states should be controlled). The second-order participation factors provide a single measure of the connection between a mode and a machine in a manner similar to the widely used linear participation factors.

8. Generator groupings: Linear analysis gives a good indication of generator groupings for both plant and interarea modes. This linear analysis seems to provide a fairly good estimate of the most severely disturbed generators. However, linear analysis does not give information about how machine groups interact. Under stressed system conditions (interarea modes in particular) this interaction can dominate system dynamic behavior. The preliminary simulations and the introduced measures indicate that the second-order effects become dominant in the stressed cases.

CHAPTER 11. SUGGESTED FUTURE WORK

- Sensitivity analysis is needed to determine the effects of loading, system topology, etc. on the measures presented in this dissertation.
- The application of the eigenvector and participation factor information to control applications (design and location) should be tested.
- Third-order terms show potential for application to stability analysis.
- Optimization of the code used in these computations is needed to make the analysis more applicable.
- Limiting the analysis to certain modes of concern could also speed up the analysis.
- The solutions obtained using normal form analysis may also yield more information about the system through the use of energy analysis.

REFERENCES

[1] Klein, M., G. J. Rogers, and P. Kundur. "A Fundamental Study of Interarea Oscillations in Power Systems." *IEEE Transactions on PWRS* v. 6, (Aug. 1991): 914-21.

[2] Klein, M., G. J. Rogers, S. Moorty, and P. Kundur. "Analytical Investigation of Factors Influencing Power System Stabilizers Performance." Approved for IEEE-PES 1992 Winter Meeting. Paper No. 92 WM 016-6EC.

[3] Vittal, V., N. Bhatia, and A. A. Fouad. "Analysis of the Inter-Area Mode Phenomenon in Power Systems Following Large Disturbances." *IEEE Transactions on PWRS* v. 6, no. 4 (1991): 1515-1521.

[4] Berggren, B. L. "Transient Stability Behavior in a Stressed Power System." Master's Thesis, Iowa State University, Ames, Iowa, 1989.

[5] McCalley, J. "A Methodology for Determining the Effects of Non-Utility Generation on Interarea Oscillations in Electric Power Systems." Ph.D. Thesis, Georgia Institute Technology, Atlanta, Georgia, 1992.

[6] DeMello, F. P., P. F. Nolan, T. F. Laskowski, and J. M. Undrill. "Coordinated Application of Stabilizers in Multimachine Power Systems." *IEEE Transactions on PAS* v. 99, (May/June 1980): 892-901.

[7] Perez-Arriaga, I. J., G. C. Verghese, and F. C. Schweppe. "Selective Modal Analysis with Applications to Electric Power Systems. Part 1: Heuristic Introduction." *IEEE Transactions on PAS* v. 101, (Sept. 1982): 3117-3125.

[8] Pagola, F. Luis, Ignacio Perez-Arriaga, and George C. Verghese. "On Sensitivities, Residues and Participations: Applications to oscillatory stability analysis and control." *IEEE Transactions on PWRS* v. 4, (Feb. 1989): 278-85.

[9] Martins, Nelson and Leonardo T. G. Lima. "Determination of Suitable Locations for Power System Stabilizers and Static Var Compesators for Damping Electromechanical Oscillations in Large Scale Power Systems." *IEEE Transactions on PWRS* v. 5, (Nov. 1990): 1455-63.

[10] Treinen, R. "Application of the Transient Energy Function Method to the Northern States Power System." Master's Thesis, Iowa State University, Ames, Iowa, 1991.

[11] Fouad, A. A., and V. Vittal. *Power System Transient Stability Analysis Using the Transient Energy Function Method.* Prentice Hall Inc., Englewood Cliffs, New Jersey, 1992.

[12] Khorasani, K., M. A. Pai, and P. W. Sauer. "Modal-based Stability Analysis of Power Systems Using Energy Functions." *Electric Power and Energy Systems,* v. 8, n. 1, (January 1986): 11-16.

[13] Starrett, S. K., W. Kliemann, V. Vittal, and A. A. Fouad. "Power System Modal Behavior: Significance of second and third order nonlinear terms." Proceedings of the North American Power Symposium, Washington, D.C., 1993.

[14] Arrowsmith, D. K., and C. M. Place. *An Introduction to Dynamical Systems.* Cambridge University Press, Cambridge, 1990.

[15] Arnold, V. I. *Geometrical Methods in the Theory of Ordinary Differential Equations.* Springer-Verlag, New York, 1983.

[16] Kimbark, Edward Wilson. *Power System Stability Volume III Synchronous Machines* John Wiley and Sons, New York, 1956.

[17] Anderson, P. M., and A. A. Fouad. *Power System Control and Stability.* The Iowa State University Press, Ames, Iowa, 1977.

[18] Pai, M. A. *Power System Stability.* North-Holland Publishing Company, New York, 1981.

[19] Ajjarapu, V, and B. Lee. "Bifurcation Theory and Its Application to Nonlinear Dynamical Phenomena in an Electrical Power System." *IEEE Transactions on PWRS* v. 7, (Feb. 1992): 424-31.

[20] Chiang, Hsiao-Dong, Jianzhong Tong, and Karen Nan Miu. "Predicting Unstable Modes in Power Systems: Theory and Computations." *IEEE Transactions on PWRS* v. 8, n. 4, (Nov. 1993): 1429-37.

[21] Chen, C.-T. *Linear System Theory and Design* Holt, Rinehart and Winston, New York, 1970.

[22] Johnson, Johnny R., and David E. Johnson. *Linear Systems Analysis.* The Ronald Press Company, New York, 1975.

[23] Kundur, P., M. Klein, and Rogers, G. J. "Application of Power System Stabilizers for Enhancement of Overall System Stability." *IEEE Transactions on PWRS* v. 4, (May 1989): 614-21.

[24] Eigenanalysis and Frequency Domain Methods for System Dynamic Performance. IEEE Publication no. 90TH0292-3-PWR.

[25] Hauer, J. F. "Application of Prony Analysis to the Determination of Modal Content and Equivalent Models for Measured Power System Response." *IEEE Transactions on PWRS* v. 6, (Aug. 1991): p. 1062-8.

[26] *Extended Transients-Midterm Stability Package: Technical Guide for the Stability Program.* EPRI Publication # EPRI EL-2000-CCM Project 1208, (January 1987).

[27] Treinen, Roger, V. Vittal and A. A. Fouad. "Application of a Modal-Based Transient Energy Function to a Large-Scale Stressed Power System: Assessment of Transient Stability and Transient Voltage Dip." *International Journal of Electrical Power and Energy Systems*, 15, no. 2 (1993): 117-125.

[28] Ray, B. "Incorporation of the Modal Interactions in Stressed Power Systems Using the Transient Energy Function Method." Master's Thesis, Iowa State University, Ames, Iowa, 1991.

[29] Tamura, Y., and N. Yorino. "Possibility of auto-& hetero-parametric resonance in power systems and the Relationship to Long-term Dynamics." *IEEE Transactions of PWRS* v. 2, n. 4 (Nov. 1987): 890-897.

[30] Yorino, Y. H. Saski, Y. Tamura, and R. Yokoyama. "A Generalized Analysis Method of Auto-parametric Resonances in Power Systems." *IEEE Transactions on PWRS* v. 4, (Aug. 1989): 1057-1064.

[31] Yoo, Shin-Heng, Hironobu Morita, Yu Huang, and Yasuo Tamura. "On the Approximation of the Perturbation Method to Derive the Conditions of Auto-Parametric Resonance Likely Occur in Power Systems." 11th PSCC, Avignon France. (Sep. 1993) PSCC93-305.

[32] Ruelle, D. *Elements of Differentiable Dynamics and Bifurcation Theory.* Academic Press, Boston, 1988.

[33] Kang, Wei, and Arthur J. Krener. "Extended Quadratic Controller Normal Form and Dynamic State Feedback Linearization of Nonlinear Systems." *SIAM Journal on Control and Optimization,* v. 30, n. 6, (Nov. 1992): 1319-37.

[34] Lamarque, C.-H., J.-M. Malasoma, and V. Roberti. "Analysis of Mechanical Systems with Slowly Varying Parameters by Normal Form Method." *Journal of Sound and Vibration,* v. 160, n. 2, (Jan. 15, 1993): 364-8.

[35] Chua, Leon O., and H. Kokubu. "Normal Forms for Nonlinear Vector Fields--Part I: Theory and Algorithm." *IEEE Transactions on Circuits and Systems*, v. 35, n. 7, (July 1988).

[36] Chua, Leon O., and H. Kokubu. "Normal Forms for Nonlinear Vector Fields--Part II: Applications." *IEEE Transactions on Circuits and Systems*, v. 36, n. 1, (Jan. 1989).

[37] Rajagopalan, C., P. W. Sauer, and M. A. Pai. "Analysis of Voltage Control Systems Exhibiting Hopf Bifurcation." *Proceedings of the 28th IEEE Conference on Decision and Control*, Part 1, (Dec. 1989): 332-335.

[38] V. Vittal, W. Kliemann, S. K. Starrett, and A. A. Fouad "Analysis of Stressed Power Systems Using Normal Forms" Proceedings of the International Symposium on Circuits and Systems, San Diego, California, 1992.

[39] Starrett, S. K., V. Vittal, W. Kliemann, and A. A. Fouad. "Interarea Separation Via Nonlinear Modal Interaction Using Normal Forms of Vector Fields." Submitted to IEEE Power Engineering Society for review for the 1994 Summer Meeting, San Francisco, California, July 1994.

[40] Starrett, S. K., V. Vittal, W. Kliemann, and A. A. Fouad. "A Methodology for the Analysis of Nonlinear, Interarea Interactions Between Power System Natural Modes of Oscillation Utilizing Normal Forms of Vector Fields." Proceedings of the International Conference on Nonlinear Systems and Applications, Honolulu, Hawaii, December 1993.

[41] Starrett, S. K., V. Vittal, W. Kliemann, and A. A. Fouad. "Nonlinear Modal Interaction In A Stressed Power System: Identifying Critical Machines Using Normal Forms Of Vector Fields." Submitted to IEEE Power Engineering Society for review for the 1995 Winter Meeting, New York, New York, January 1995.

[42] Lin, Chih-Ming, V. Vittal, and A. A. Fouad. "Dynamic Modal Interaction in a Stressed Power System." Proceedings of the North American Power Symposium, Washington, D.C., 1993.

[43] J. F. Hauer. "Introduction to the 1989 IEEE/PES Symposium on Eigenanalysis and Frequency Domain Methods for System Dynamic Performance." *Proceedings of the 1989 IEEE/PES Symposium on Eigenanalysis and Frequency Domain Methods for System Dynamic Performance* 90TH0292-3-PWR (1989): 1-4.

[44] G. J. Rogers and P. Kundur. "Small Signal Stability of Power Systems." IEEE Publication *Eigenanalysis and Frequency Domain Methods for System Dynamic Performance* 90TH0292-3-PWR (1989): 5-16.

[45] Vidyasagar, M. *Nonlinear Systems Analysis.* Prentice-Hall, Englewood Cliffs, New Jersey, 1978.

[46] "Transient Stability Test Systems for Direct Stability Methods." *IEEE Transactions on PWRS* v. 7, (Feb. 1992): 37-42.

[47] Heydt, G. T. *Computer Analysis Methods for Power Systems.* Macmillan Publishing Company, New York, 1986.

[48] Zadeh, L. A., and C. A. Desoer *Linear System Theory the State Space Approach.* McGraw-Hill Book Company, New York, 1963.

ACKNOWLEDGMENTS

This work has been supported by the Electric Power Research Institute (Project RP8010-28), and by a fellowship from the National Science Foundation. The author also thanks Edison Electric Institute's Power Engineering Education Foundation for their support in the form of a forgivable loan award.

I would like to thank Dr. Fouad for the time, effort and advice that he generously provided during this research work. His concern for me and my work is greatly appreciated. He has taught me much more about research and professional life than I could ever get from a book.

I would also like to thank Dr. Vijay Vittal and Dr. Wolfgang Kliemann for their generous contributions of time and effort in progress of this research work and for serving on my graduate committee.

I greatly appreciate Dr. John Lamont's and Dr. Mustafa Khammash's helpful comments on this thesis as well as their other contributions as members of my committee.

I would also like to thank Dr. Horton and Dr. Geiger for giving me the opportunity to teach in the department, and I thank all of the professors who helped me through the experience with their helpful advice.

It has been a pleasure to get to know, work with, and be a part of the "laziest bunch of graduate students" Dr. Fouad has ever seen. I would also like to thank the secretaries of the Electrical Engineering and Computer Engineering Department for all of the help they have given me during my stay at Iowa State.

I am very thankful for the support and encouragement of all of my family during my entire (10 year) college career. I thank my wonderful husband Steve for his understanding, encouragement, support, household work, and roses.

APPENDIX A: DETAILS OF TAYLOR SERIES EXPANSION

Starting with the i^{th} original swing equations given by

$$M_i\ddot{\delta}_i = P_i - \sum_{\substack{j=1 \\ j\neq i}}^{n} |V_i||V_j||Y_{ij}|\cos(\theta_{ij} - \delta_i + \delta_j) \tag{A1}$$

the equations are re-written to include *sin* and *cos* terms containing the angle difference variables. The i^{th} equation becomes

$$M_i\ddot{\delta}_i = P_i - \sum_{\substack{j=1 \\ j\neq i}}^{n} D_{ij}\cos(\delta_i - \delta_j) - \sum_{\substack{j=1 \\ j\neq i}}^{n} C_{ij}\sin(\delta_i - \delta_j) \tag{A2}$$

where $D_{ij} = |V_i||V_j||Y_{ij}|\cos(\theta_{ij})$ and $C_{ij} = |V_i||V_j||Y_{ij}|\sin(\theta_{ij})$.

Now the equilibrium can be shifted to the origin by introducing the variable change, $\alpha_i = \delta_i - \delta_{ie}$ where δ_{ie} is $\delta(t=0)$, the i^{th} variable's value at the equilibrium. Applying this change of variable yields

$$\begin{aligned} M_i\ddot{\alpha}_i - M_i\ddot{\delta}_{ie} &= P_i - \sum_{\substack{j=1 \\ j\neq i}}^{n} D_{ij}\cos(\{\alpha_i - \alpha_j\} + \{\delta_{ie} - \delta_{je}\}) - \sum_{\substack{j=1 \\ j\neq i}}^{n} C_{ij}\sin(\{\alpha_i - \alpha_j\} + \{\delta_{ie} - \delta_{je}\}) \\ &= P_i - \sum_{\substack{j=1 \\ j\neq i}}^{n}\left[D_{ij}\cos(\delta_{ie} - \delta_{je}) + C_{ij}\sin(\delta_{ie} - \delta_{je})\right]\cos(\alpha_i - \alpha_j) \\ &\quad - \sum_{\substack{j=1 \\ j\neq i}}^{n}\left[-D_{ij}\sin(\delta_{ie} - \delta_{je}) + C_{ij}\cos(\delta_{ie} - \delta_{je})\right]\sin(\alpha_i - \alpha_j) \end{aligned} \tag{A3}$$

$$M_i\ddot{\alpha}_i = P_i - \sum_{\substack{j=1 \\ j\neq i}}^{n} E_{ij}\cos(\alpha_i - \alpha_j) - \sum_{\substack{j=1 \\ j\neq i}}^{n} F_{ij}\sin(\alpha_i - \alpha_j)$$

where $\ddot{\delta}_{ie}$ acceleration at the equilibrium and is equal to zero, and $E_{ij} = D_{ij}\cos(\delta_{ie} - \delta_{je}) + C_{ij}\sin(\delta_{ie} - \delta_{je})$ and $F_{ij} = -D_{ij}\sin(\delta_{ie} - \delta_{je}) + C_{ij}\cos(\delta_{ie} - \delta_{je})$.

The Taylor series expansions for the *cos* and *sin* functions are given in (A4).

$$\begin{aligned} \cos(x) &= 1 - \frac{x^2}{2!} + \frac{x^4}{4!} - \ldots \\ \sin(x) &= x - \frac{x^3}{3!} + \frac{x^5}{5!} - \ldots \end{aligned} \tag{A4}$$

So that the series expansion of (A3), including up to third-order terms, becomes

$$M_i\ddot{\alpha}_i = P_i - \sum_{\substack{j=1 \\ j\neq i}}^{n} E_{ij}\left[1 - \frac{(\alpha_i - \alpha_j)^2}{2}\right] - \sum_{\substack{j=1 \\ j\neq i}}^{n} F_{ij}\left[(\alpha_i - \alpha_j) - \frac{(\alpha_i - \alpha_j)^3}{6}\right] \tag{A5}$$

As stated above, the acceleration at the equilibrium must be equal to zero, thus substituting δ_{ie} into (A2) yields

$$0 = M_i \ddot{\delta}_{ie} = P_i - \sum_{\substack{j=1 \\ j \neq i}}^{n} D_{ij} \cos(\delta_{ie} - \delta_{je}) - \sum_{\substack{j=1 \\ j \neq i}}^{n} C_{ij} \sin(\delta_{ie} - \delta_{je}) \tag{A6}$$

so that

$$\begin{aligned} 0 &= P_i - \sum_{\substack{j=1 \\ j \neq i}}^{n} \left\{ D_{ij} \cos(\delta_{ie} - \delta_{je}) + C_{ij} \sin(\delta_{ie} - \delta_{je}) \right\} \\ &= P_i - \sum_{\substack{j=1 \\ j \neq i}}^{n} E_{ij} = 0 \end{aligned} \tag{A7}$$

Thus, the series expansion for the i^{th} equation, with the equilibrium shifted to the origin is

$$\ddot{\alpha}_i = -\frac{1}{M_i} \sum_{\substack{j=1 \\ j \neq i}}^{n} E_{ij} \left[\frac{(\alpha_i - \alpha_j)^2}{2} \right] - \frac{1}{M_i} \sum_{\substack{j=1 \\ j \neq i}}^{n} F_{ij} \left[(\alpha_i - \alpha_j) - \frac{(\alpha_i - \alpha_j)^3}{6} \right] \tag{A8}$$

This set of equations (for $i = 1$ *through* n) is not a linearly independent set. To obtain such a set, the n^{th} generator (without loss of generality) is chosen as a reference. Another change of variable is performed using $x_i = \alpha_i - \alpha_n$. The differences of the variables become $\alpha_i - \alpha_j = x_i + \alpha_n - (x_j + \alpha_n) = x_i - x_j$. By subtracting the n^{th} equation from each of the others, the left hand sides are also expressed in terms of the relative variables (i.e., $\ddot{\alpha}_i - \ddot{\alpha}_n = \ddot{x}_i$). At this point the equations are put in state space form, so that all of the equations are first-order differential equations. This is done by designating the speed variables as the last (n-1) "x" variables. The resulting equations are

$$\dot{x}_i = x_{i+(n-1)} \tag{A9}$$

for $i = 1$ *through* $(n-1)$ and

$$\begin{aligned} \dot{x}_i = &-\frac{1}{M_i} \sum_{\substack{j=1 \\ j \neq i}}^{n-1} E_{ij} \left[\frac{(x_i - x_j)^2}{2} \right] - \frac{1}{M_i} \sum_{\substack{j=1 \\ j \neq i}}^{n-1} F_{ij} \left[(x_i - x_j) - \frac{(x_i - x_j)^3}{6} \right] - \frac{E_{in}}{M_i} \frac{(x_i)^2}{2} - \frac{F_{in}}{M_i} \left[(x_i) - \frac{(x_i)^3}{6} \right] \\ &+ \frac{1}{M_n} \sum_{j=1}^{n-1} E_{nj} \left[\frac{(-x_j)^2}{2} \right] + \frac{1}{M_n} \sum_{j=1}^{n-1} F_{nj} \left[(-x_j) - \frac{(-x_j)^3}{6} \right] \end{aligned} \tag{A10}$$

for $i = n$ *through* $2(n-1)$. By multiplying and simplifying the above expressions, the desired form of equation (4.1) is obtained.

APPENDIX B: DETAILS OF TRANSFORMATION TO JORDAN FORM

This appendix starts with the Taylor series of the system, reduced to a linearly independent set and with the equilibrium shifted to the origin (see Appendix A).

$$\dot{x} = Ax + X_2(x) + X_3(x) + \ldots \tag{B1}$$

x is an m by 1 vector with $m = 2(n-1)$. The eigenvectors of the plant matrix A make up columns of the matrix U. U is used as the transformation matrix for obtaining the Jordan form (complex) of the system. The variable transformation $x = Uy$ is applied to the system of equations (B1) to obtain the Jordan form. y is the vector of Jordan form state variables.

Differentiating the transformation equation yields $\dot{x} = U\dot{y}$, and substituting into (B1) yields

$$U\dot{y} = AUy + X_2(Uy) + X_3(Uy) + \ldots \tag{B2}$$

The matrix with the left eigenvectors as rows, V, is the inverse of the right eigenvector matrix U. Pre-multiplying both sides of (B2) by $V = U^{-1}$ yields

$$\begin{aligned} \dot{y} &= VAUy + VX_2(Uy) + VX_3(Uy) + \ldots \\ &= Jy + Y_2(y) + Y_3(y) + \ldots \end{aligned} \tag{B3}$$

where $J = VAU$ is a diagonal matrix with the eigenvalues on the diagonal, and $Y_2(y) = VX_2(Uy)$, etc.

In order to program this, the equations need to be written for a single Jordan form variable (one row of (B3)). The linear terms are simply the eigenvalues and are assumed to be known (they can be recalculated as a check). The second and third order terms are much more complicated.

To ease computer computations, we start with the final equation of Appendix A, repeated below for convenience.

$$\dot{x}_i = x_{i+(n-1)} \qquad i = 1,2,\ldots\ n\text{-}1 \tag{B4}$$

$$\dot{x}_i = -\frac{1}{M_i}\sum_{\substack{j=1\\ j\neq i}}^{n-1} E_{ij}\left[\frac{(x_i - x_j)^2}{2}\right] - \frac{1}{M_i}\sum_{\substack{j=1\\ j\neq i}}^{n-1} F_{ij}\left[(x_i - x_j) - \frac{(x_i - x_j)^3}{6}\right] - \frac{E_{in}}{M_i}\frac{(x_i)^2}{2} - \frac{F_{in}}{M_i}\left[(x_i) - \frac{(x_i)^3}{6}\right]$$
$$+ \frac{1}{M_n}\sum_{j=1}^{n-1} E_{nj}\left[\frac{(-x_j)^2}{2}\right] + \frac{1}{M_n}\sum_{j=1}^{n-1} F_{nj}\left[(-x_j) - \frac{(-x_j)^3}{6}\right] \qquad \text{(B5)}$$

for $i = n, n+1, \ldots 2(n-1)$.

Note that the variable transformation $x = Uy$, can be written for the i^{th} state variable as

$$x_i = \sum_{j=1}^{m} u_{ij} y_j \qquad \text{(B6)}$$

so that the differences of (B5) become

$$x_i - x_j = \sum_{a=1}^{m}\left\{u_{ia}y_a - u_{ja}y_a\right\} = \sum_{a=1}^{m}\left\{u_{ia} - u_{ja}\right\}y_a \qquad \text{(B7)}$$

Equations for the squares of these terms are needed. For this work, only terms up to second-order are included, third-order terms could also be calculated, but with considerably more computational effort. Equations (B4) and (B5) need to be written in terms of the Jordan form variables (y's). In equation form, the squared difference terms become

$$\left(x_i - x_j\right)^2 = \left[\sum_{a=1}^{m}\left\{u_{ia} - u_{ja}\right\}y_a\right]\left[\sum_{a=1}^{m}\left\{u_{ia} - u_{ja}\right\}y_a\right] \qquad \text{(B8)}$$

and rearranging the summations yields

$$\left(x_i - x_j\right)^2 = \sum_{a=1}^{m-1}\sum_{b=a+1}^{m} 2\left(u_{ia} - u_{ja}\right)\left(u_{ib} - u_{jb}\right)y_a y_b + \sum_{a=1}^{m}\left(u_{ia} - u_{ja}\right)^2\left(y_a\right)^2 \qquad \text{(B9)}$$

Similarly the single variable terms are

$$\left(x_i\right)^2 = \sum_{a=1}^{m-1}\sum_{b=a+1}^{m} 2u_{ia}u_{ib}y_a y_b + \sum_{a=1}^{m}\left(u_{ia}\right)^2\left(y_a\right)^2 \qquad \text{(B10)}$$

Third-order terms could be found by multiplying the second-order terms by an additional $(x_i - x_j)$ term.

$$\left(x_i - x_j\right)^3 = \left(x_i - x_j\right)\left(x_i - x_j\right)^2$$
$$= \left[\sum_{a=1}^{m}(u_{ia} - u_{ja})y_a\right]\left[\sum_{a=1}^{m-1}\sum_{b=a+1}^{m} 2\left(u_{ia} - u_{ja}\right)\left(u_{ib} - u_{jb}\right)y_a y_b + \sum_{a=1}^{m}\left(u_{ia} - u_{ja}\right)^2\left(y_a\right)^2\right] \qquad \text{(B11)}$$

The system of equations (B5) can be written including up to second-order terms as

$$\dot{x}_i = -\sum_{\substack{j=1\\ j\neq i}}^{n-1}\frac{E_{ij}}{M_i}\left[\frac{\sum_{a=1}^{m-1}\sum_{b=a+1}^{m}2\left(u_{ia}-u_{ja}\right)\left(u_{ib}-u_{jb}\right)y_a y_b+\sum_{a=1}^{m}\left(u_{ia}-u_{ja}\right)^2\left(y_a\right)^2}{2}\right]-\sum_{\substack{j=1\\ j\neq i}}^{n-1}\frac{F_{ij}}{M_i}\left[\sum_{a=1}^{m}\left(u_{ia}-u_{ja}\right)y_a\right]$$

$$-\frac{E_{in}}{M_i}\left[\frac{\sum_{a=1}^{m-1}\sum_{b=a+1}^{m}2u_{ia}u_{ib}y_a y_b+\sum_{a=1}^{m}\left(u_{ia}\right)^2\left(y_a\right)^2}{2}\right]-\frac{F_{in}}{M_i}\left[\sum_{a=1}^{m}u_{ia}y_a\right]$$

$$+\sum_{j=1}^{n-1}\frac{E_{nj}}{M_n}\left[\frac{\sum_{a=1}^{m-1}\sum_{b=a+1}^{m}2u_{ja}u_{jb}y_a y_b+\sum_{a=1}^{m}\left(u_{ja}\right)^2\left(y_a\right)^2}{2}\right]-\sum_{j=1}^{n-1}\frac{F_{nj}}{M_n}\left[\sum_{a=1}^{m}u_{ja}y_a\right] \qquad \text{(B12)}$$

These summations can be reordered to give expressions for the linear and second-order coefficients in the equation above. The result is

$$\dot{x}_i = -\sum_{a=1}^{m-1}\sum_{b=a+1}^{m}\left[\sum_{\substack{j=1\\ j\neq i}}^{n-1}\frac{E_{ij}}{M_i}\left(u_{ia}-u_{ja}\right)\left(u_{ib}-u_{jb}\right)+\frac{E_{in}}{M_i}u_{ia}u_{ib}-\sum_{j=1}^{n-1}\frac{E_{nj}}{M_n}u_{ja}u_{jb}\right]y_a y_b$$

$$-\sum_{a=1}^{m}\left[\sum_{\substack{j=1\\ j\neq i}}^{n-1}\frac{E_{ij}}{2M_i}\left(u_{ia}-u_{ja}\right)^2-\sum_{j=1}^{n-1}\frac{E_{nj}}{2M_n}\left(u_{ja}\right)^2+\frac{E_{in}}{2M_i}\left(u_{ia}\right)^2\right]\left(y_a\right)^2 \qquad \text{(B13)}$$

$$-\sum_{a=1}^{m}\left[\sum_{\substack{j=1\\ j\neq i}}^{n-1}\frac{F_{ij}}{M_i}\left(u_{ia}-u_{ja}\right)+\frac{F_{in}}{M_i}u_{ia}+\sum_{j=1}^{n-1}\frac{F_{nj}}{M_n}u_{ja}\right]y_a$$

Because the terms in the [] brackets are constants, (B13) can be written in compact form as

$$\dot{x}_i = -\sum_{a=1}^{m-1}\sum_{b=a+1}^{m}\left[\Psi_{iab}\right]y_a y_b-\sum_{a=1}^{m}\left[\Psi_{iaa}\right]\left(y_a\right)^2-\sum_{a=1}^{m}\left[\Phi_{ia}\right]y_a \qquad \text{(B14)}$$

which is a form of (B2) including only up to second-order terms. Finally, the inverse transformation $y = Vx$ for the k^{th} Jordan form variable is

$$y_i = \sum_{b=1}^{m}v_{ib}x_b \qquad \text{(B15)}$$

so that the derivative is

$$\dot{y}_k = \sum_{b=1}^{m} v_{kb}\dot{x}_b \tag{B16}$$

Thus the equation in Jordan form, for the k^{th} Jordan variable is

$$\begin{aligned}\dot{y}_k &= \sum_{b=1}^{n-1} v_{kb}\left[x_{b+n-1}\right] + \sum_{b=n}^{m} v_{kb}\left[-\sum_{a=1}^{m-1}\sum_{b=a+1}^{m}\left[\Psi_{iab}\right]y_a y_b - \sum_{a=1}^{m}\left[\Psi_{iaa}\right](y_a)^2 - \sum_{a=1}^{m}\left[\Phi_{ia}\right]y_a\right] \\ &= \sum_{b=1}^{n-1} v_{kb}\left[\sum_{d=1}^{m} u_{b+n-1,d}y_d\right] + \sum_{b=n}^{m} v_{kb}\left[-\sum_{a=1}^{m-1}\sum_{b=a+1}^{m}\left[\Psi_{iab}\right]y_a y_b - \sum_{a=1}^{m}\left[\Psi_{iaa}\right](y_a)^2 - \sum_{a=1}^{m}\left[\Phi_{ia}\right]y_a\right]\end{aligned} \tag{B17}$$

again, the summations may be rearranged to yield

$$\dot{y}_k = -\sum_{a=1}^{m-1}\sum_{b=a+1}^{m}\sum_{b=n}^{m} v_{kb}\left[\Psi_{iab}\right]y_a y_b - \sum_{a=1}^{m}\sum_{b=n}^{m} v_{kb}\left[\Psi_{iaa}\right](y_a)^2 - \sum_{a=1}^{m}\left\{\sum_{b=n}^{m} v_{kb}\left[\Phi_{ia}\right] - \sum_{b=1}^{n-1} v_{kb}u_{b+n-1,a}\right\}y_a \tag{B18}$$

As mentioned earlier, the linear term (the last term) should simplify to $\lambda_k y_k$ and can be computed as a check. (B18) is fully transformed and is a form of (B3). (B3) in expanded form is given in (B19). By comparing coefficients the second-order terms Y_{2kab} can now be determined by back substitution.

$$\dot{y}_k = \lambda_k y_k + \sum_{a=1}^{m-1}\sum_{b=a+1}^{m} Y_{2kab}y_a y_b + \sum_{a=1}^{m} Y_{2kaa}(y_a)^2 \tag{B19}$$

APPENDIX C: 3-GENERATOR EXAMPLE

The 3-generator, 9-bus WSCC system from [17] is used to illustrate the measures described in this section. A 0.108 second fault is applied at Station 2, and the line from Station 2 to Station A is cleared. The base case loading is used, and the circuit is shown in Figure C1.

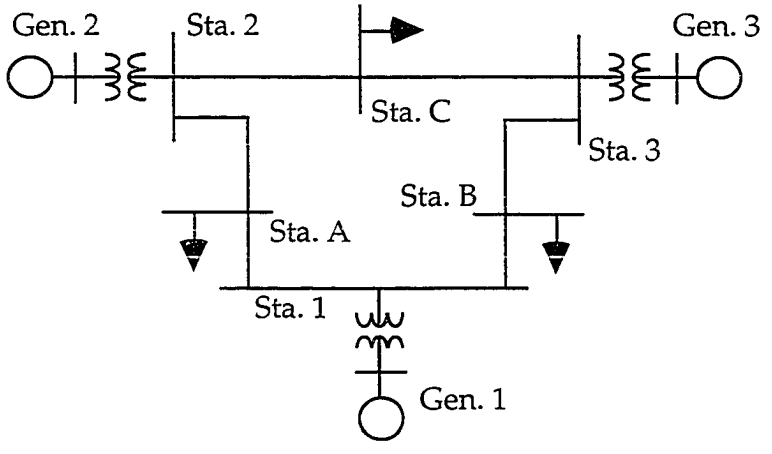

Figure C1 One-line diagram of 3-generator system

The eigenvalues for this system are $\lambda_1 = 0.000 + j12.902$ and $\lambda_2 = 0.000 + j6.090$. The linear solution for the first relative-angle, difference variable (for angle 1 relative to angle 3), is

$$x_1(t) = 2[0.0213\cos(12.902t - 75.8°) + 0.2833\cos(6.090t + 79.7°)]$$

Similarly the second, relative-angle difference variable is

$$x_2(t) = 2[0.0263\cos(12.902t - 75.8°) + 0.1335\cos(6.090t - 100.3°)]$$

The relative-speed difference variables are

$$x_3(t) = 2[0.2746\cos(12.902t + 14.2°) + 1.7256\cos(6.090t + 169.7°)]$$
$$x_4(t) = 2[0.3391\cos(12.902t + 14.2°) + 0.8131\cos(6.090t - 10.3°)]$$

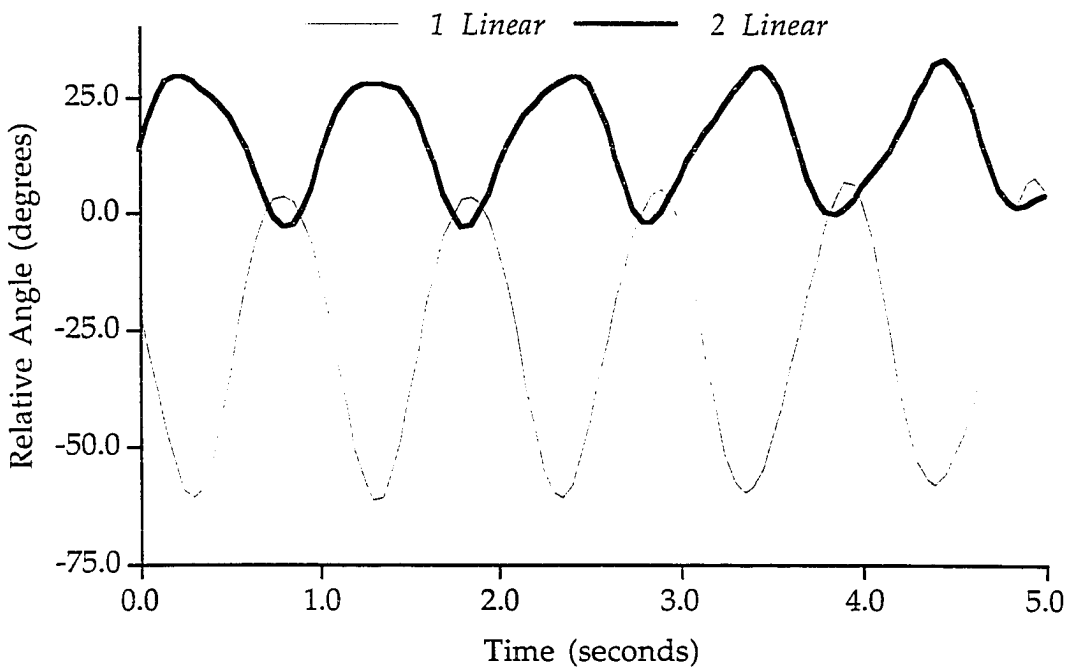

Figure C2 Linear, relative-angle plot for 3-generator system

Thus, the oscillations of machine state x_1 should have a dominant frequency of 6.090 rad/sec because of the relatively large magnitude of σ_{13} = 0.2833 rad, compared to the magnitude of σ_{11} = 0.0213 rad (σ_{13} = 13.3 σ_{11}). The pattern is similar for x_2, but the size difference is less pronounced (σ_{13} = 5.1σ_{21}). The contribution factors corresponding to mode 3 are also larger for the other states. Figure C2 is a plot of the relative-angle variables (x_1 and x_2 with the stable equilibrium point conditions added in) for the linear case. As expected, the curve related to x_1 appears nearly sinusoidal with a frequency of 6.09 rad/sec, whereas the curve related to x_2 also shows a frequency of around 6.09 rad/sec. Distortions from the higher frequency mode are more obvious in x_2.

The linear perturbation factors for the 3-generator system case are the following:

$$O_1 = 0.5282 \angle 77.8°$$
$$O_2 = 0.3156 \angle -96.3°$$
$$O_3 = 2.9602 \angle 165.3°$$
$$O_4 = 2.2609 \angle -3.1°$$

Figure C2 shows that the amplitude of the oscillation corresponding to x_1 is approximately 35° compared to O_1 = 30°. For x_2, the oscillation amplitude is roughly 17° compared to O_2 = 18°. Thus, the perturbation measures give good indications of machine state perturbation for this case.

The linear-mode dominance measures for this fault and load level are the following:

$$D_1 = 1.3225 = D_2$$
$$D_3 = 5.9111 = D_4$$

These dominance measures indicate that mode 3 is significantly more dominant than mode 1. This agrees with the observation made using the contribution factors and with the plots of Figure C2.

The second-order solution for the machine states will contain two terms corresponding to those found in the linear solution (one for each mode frequency) plus ten second-order terms (one for each second-order mode combination frequency). The second-order mode combinations are as follows:

$$\begin{aligned}
\lambda_1 + \lambda_1 &= 0.0000 + j\,25.8042 &&= -(\lambda_2 + \lambda_2)\\
\lambda_1 + \lambda_2 &= 0.0000 + j\,0.0000 &&= 0\\
\lambda_1 + \lambda_3 &= 0.0000 + j\,18.9922 &&= -(\lambda_2 + \lambda_4)\\
\lambda_1 + \lambda_4 &= 0.0000 + j\,6.8120 &&= -(\lambda_2 + \lambda_3)\\
\lambda_2 + \lambda_2 &= 0.0000 - j\,25.8042 &&= -(\lambda_1 + \lambda_1)\\
\lambda_2 + \lambda_3 &= 0.0000 - j\,6.8120 &&= -(\lambda_1 + \lambda_4)\\
\lambda_2 + \lambda_4 &= 0.0000 - j\,18.9922 &&= -(\lambda_1 + \lambda_3)\\
\lambda_3 + \lambda_3 &= 0.0000 + j\,12.1802 &&= -(\lambda_4 + \lambda_4)\\
\lambda_3 + \lambda_4 &= 0.0000 + j\,0.0000 &&= 0\\
\lambda_4 + \lambda_4 &= 0.0000 - j\,12.1802 &&= -(\lambda_3 + \lambda_3)
\end{aligned}$$

Note that eight of the combinations given above can be grouped into four complex-conjugate pairs. The other two are constant (zero frequency). Thus, the total number of second-order terms for each variable will be six (four oscillations and two constant shifts). For example, the second-order equation for the first relative-angle difference variable, is

$$
\begin{aligned}
x_1(t) = \; & 2\,[\,0.0125\cos(12.902t - 173.6°) \; + \; 0.2799\cos(6.090t + \; 68.9°) \\
& + \; 0.0000\cos(25.804t + 12.8°) \; + \; 0.0009\cos(18.992t - 104.7°) \\
& + \; 0.0020\cos(6.812t - 62.5°) \; + \; 0.0137\cos(12.180t - 42.2°)\,] \\
& - \; 0.0001 \; -0.0868
\end{aligned}
$$

Similarly, the second, relative-angle difference variable is

$$
\begin{aligned}
x_2(t) = \; & 2\,[\,0.0154\cos(12.902t - 173.6°) \; + \; 0.1319\cos(6.090t - 111.1°) \\
& + \; 0.0000\cos(25.804t + 12.8°) \; + \; 0.0011\cos(18.992t + -104.7°) \\
& + \; 0.0016\cos(6.812t - 62.5°) \; + \; 0.0399\cos(12.180t - 42.2°)\,] \\
& + \; 0.0000 \; +0.0308
\end{aligned}
$$

Thus, the oscillations of machine state x_1 are expected to again have a dominant frequency of 6.090 rad/sec because of the relatively large magnitude of the second-order contribution factor $\sigma_{2,13} = 0.2799$ rad, compared to the next largest magnitude of $\sigma_{22,133} = 0.0137$ rad ($\sigma_{2,13} = 20.4\sigma_{22,133}$). The pattern is similar for x_2, but the size difference is less pronounced ($\sigma_{2,23} = 3.3\sigma_{22,233}$). Figure C3 is a plot of the relative angle variables (x_1 and x_2 with the stable equilibrium point conditions added in) for this case. The linear and second-order plots are both included. As expected, both the linear and second-order curves related to x_1 appear nearly sinusoidal with a frequency of 6.09 rad/sec. The curves related to x_2 also show a frequency of around 6.09 rad/sec, but distortions from the other modes are more obvious. The second-order curve shows even more evidence of other modes than the linear case. This is expected because the ratio of the size of the largest second-order contribution factor to the others is not as large as in the linear case. The constant shift is also evident in the response of machine state 1.

The second-order perturbation factors for the 3-generator system case are the following:

$$
\begin{aligned}
O_{2,1} &= 0.5546 \angle 78.4° \\
O_{2,2} &= 0.1940 \angle -100.3° \\
O_{2,3} &= 2.9378 \angle 167.1° \\
O_{2,4} &= 2.8217 \angle -36.9°
\end{aligned}
$$

From Figure C3, the amplitude of the second-order oscillation corresponding to x_1 is approximately 32° compared to O_1 = 32°, and for x_2, the second-order oscillation amplitude is roughly 16° compared to O_2 = 11°. Thus, the perturbation measures also give good indications of machine state perturbation for this case.

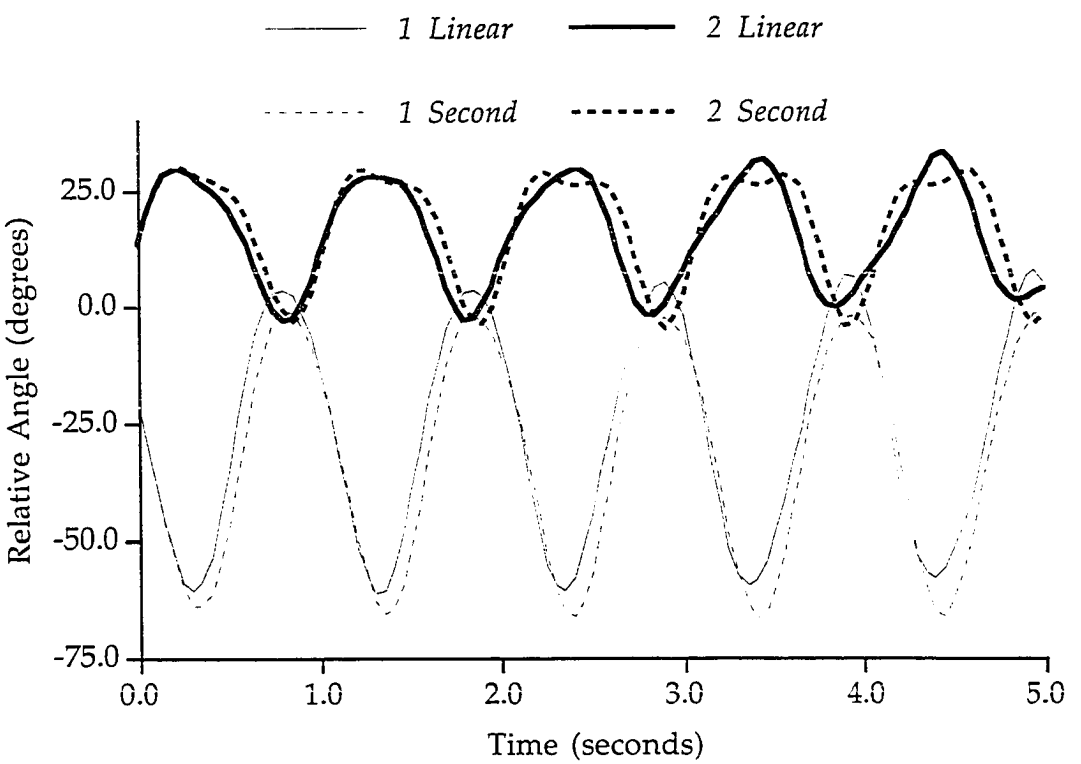

Figure C3 Second-order, relative-angle plot for 3-generator system

The second-order mode dominance measures for the 3-generator system case are the following:

$D_{2,1} = 0.7749 = D_{2,2}$	(12.902 rad/sec mode)
$D_{2,3} = 5.8398 = D_{2,4}$	(6.090 rad/sec mode)
$D_{22,11} = 0.0002 = D_{22,22}$	(25.804 rad/sec mode)
$D_{22,12} = 0.0001$	(0.000 rad/sec mode)

$D_{22,13} = 0.0408 = D_{22,24}$ (18.992 rad/sec mode)
$D_{22,14} = 0.0281 = D_{22,23}$ (6.812 rad/sec mode)
$D_{22,33} = 0.7067 = D_{22,44}$ (12.180 rad/sec mode)
$D_{22,34} = 0.1177$ (0.000 rad/sec mode)

The second-order dominance measures indicate that mode three is clearly the most dominant mode. Mode 1 and two-eigenvalue mode 3-3 have significant oscillations as well. These observations agree with the observation made using the contribution factors and with the plots of Figure C3.